RESEARCH TRENDS IN CHEMICAL AND MATERIAL SCIENCE

EDITORS:

DR. NEERAJ GUPTA

DR. SHAILENDRA KOLHE

DR. PRASENJIT TALUKDAR

DR. GAURAV PETHE

Bhumi Publishing

Research Trends in Chemical and Material Science

(ISBN: 978-93-48620-44-6)

Editors

Dr. Neeraj Gupta

Department of of Chemistry,

Govt P G College,

Guna, M. P.

Dr. Shailendra Kolhe

Department of Physics,

Shivaji Arts, Commerce and

Science College Kannad,

Dist-Chhatrapati Sambhajinagar

Dr. Prasenjit Talukdar

Department of Petroleum Engineering,

Dibrugarh University Institute of

Engineering and Technology (DUIET),

Dibrugarh University, Assam

Dr. Gaurav Pethe

Department of Chemistry,

Narayanrao Kale Smruti Model College,

Karanja Ghadge,

Dist.-Wardha, Maharashtra

Title: Research Trends in Chemical and Material Science

Editors: Dr. Neeraj Gupta, Dr. Shailendra Kolhe, Dr. Prasenjit Talukdar, Dr. Gaurav Pethe

First Edition: February 2025

ISBN: 978-93-48620-44-6

ISBN 978-93-48620-44-6

9 789348 620446

Published by:

Bhumi Publishing

BHUMI PUBLISHING

Nigave Khalasa, Tal – Karveer, Dist – Kolhapur, Maharashtra, INDIA 416 207

E-mail: bhumipublishing@gmail.com

Disclaimer: The views expressed in the book are of the authors and not necessarily of the publisher and editors. Authors themselves are responsible for any kind of plagiarism found in their chapters and any related issues found with the book.

PREFACE

Scientific progress in the fields of chemistry and material science has been instrumental in shaping modern technological advancements. These disciplines form the foundation for innovations in pharmaceuticals, energy storage, nanotechnology, environmental sustainability, and numerous other fields that impact our daily lives. As research in these areas continues to evolve, it is essential to explore emerging trends and their potential applications.

The book Research Trends in Chemical and Material Science presents a comprehensive collection of contemporary studies and advancements in these dynamic fields. This volume brings together contributions from researchers and experts, offering insights into the latest discoveries, experimental techniques, and theoretical developments. The chapters encompass diverse topics, including novel materials synthesis, chemical reactions, computational modeling, and their real-world applications in various industries.

A key focus of this book is to highlight interdisciplinary approaches, where chemistry and material science intersect with physics, biology, and engineering to address complex scientific challenges. The integration of sustainable practices, green chemistry principles, and eco-friendly materials is also emphasized, reflecting the growing need for responsible scientific research.

This book aims to serve as a valuable resource for researchers, academicians, and students who seek to stay updated on the latest trends in chemical and material science. It provides a platform for knowledge exchange and encourages further exploration in these ever-expanding fields.

We extend our gratitude to all the contributors whose dedicated research efforts have made this publication possible. We also appreciate the unwavering support of the scientific community in advancing knowledge for the benefit of society.

- Editors

TABLE OF CONTENT

CURRENT TRENDS IN VAPORIZING GAS DRIVE

Gaurav Gogoi, Anubhav Gogoi, Trishnav Bharadwaj,

Borsha Hazarika and Prasenjit Talukdar*

Department of Petroleum Engineering, DUIET,

Dibrugarh University, Assam-786004, India

*Corresponding author E-mail: prasenjit_duiet@dibru.ac.in

Abstract:

EOR techniques have transformed the petroleum industry by extracting oil beyond conventional methods. Among them, miscible gas injection, especially with CO_2, has been one of the most effective and widely used strategies. In addition to enhancing oil mobility through reduced viscosity and improved displacement efficiency, CO_2 injection provides the added advantage of carbon sequestration, which makes it an environmentally friendly option. Miscible gas injection involves one of the main mechanisms-Vaporizing Gas Drive, whereby the injected gas-CO_2 and hydrocarbon-rich gas-separately contacts and gradually mixes up with the reservoir oil. Intermediate hydrocarbons from the oil phase transfer to the gas, thereby enriching it, which makes it miscible. Reduced interfacial tension, swelling, and overall increased mobility are all positive factors in miscible gas injection. Experimental studies have shown that, despite the high Minimum Miscibility Pressure (MMP) of methane, ethane and CO_2 are much more effective in dissolving a broader range of hydrocarbons. Although CO_2 has been used as an EOR technique for decades, it is now being brought into the limelight due to the increased emphasis on CCUS. Because of the synergy between EOR and CCUS, injection of CO_2 will not only efficiently increase oil recovery but also be a feasible method to reduce greenhouse gas emission in the environment. In addition, optimizing the gas-injection technique is finding better EOR strategy for deep and unconventional reservoirs through MD and CFD simulations. In conclusion, Vaporizing Gas Drive, applied with CO_2 injection, presents one of the most efficient means of enhanced oil recovery. Other alternatives, like methane and nitrogen, have been considered; however, the most promising is CO_2 because of its excellent miscibility characteristics, environmental benefits, and its efficiency in tight and deep reservoirs. Continued research and innovation in this field will be essential to unlocking the full potential of EOR while addressing sustainability concerns in the energy sector.

Keywords: EOR; Miscible Gas Injection; CO_2 Injection; Minimum Miscibility Pressure (MMP); Carbon Capture Utilization and Storage (CCUS).

Introduction:

EOR is a group of innovative techniques designed to significantly increase oil output, going beyond the drawbacks of conventional primary and secondary recovery methods. Mature oil fields, where initial production rates decline due to decreased reservoir pressure and oil mobility, are the ideal candidates for EOR applications. These tactics aim to improve oil mobility and displacement efficiency by altering the properties of reservoir fluids such as infusing surfactants to alter the interfacial tension between water and oil or injecting compounds such as polymers to decrease the viscosity of oil and increase sweep efficiency. (Apostolos Kantzas *et al.*) (Abdurrahman *et al.*, 2025)

One well-known EOR method that uses the miscibility principle to improve oil recovery is miscible gas flooding. Miscibility between the resident oil and the injected gas is essential for effective displacement in the context of oil recovery. (Hamouda & Chughtai, 2018).

The oil in the reservoir interacts with the injected gas, which is usually a hydrocarbon gas or a mixture of gases. Miscibility develops as a result of a gradual change in the composition of both phases brought about by numerous interactions and mass transfer. This procedure can be intricate and affected by variables like temperature, oil composition, reservoir pressure, and the nature of injected gas. (Baharizade & Sedaee, 2022). Under particular reservoir circumstances, it is the lowest pressure at which miscibility between the injected gas and the reservoir oil can be attained. In order to maximize oil recovery and optimize injection tactics, the MMP must be determined. (Z. Chen *et al.*, 2025; Hawthorne & Miller, 2019) (Hawthorne *et al.*, 2016)

For a miscible gas flood to be successful, the right injection gas must be chosen. Because of its potential for carbon sequestration, high displacement efficiency, and comparatively low MMP, carbon dioxide (CO_2) is widely preferred. A widely accessible and reasonably priced alternative that is frequently combined with other gases. (Nobakht *et al.*, 2008)

Miscible gas flooding, especially when combined with CO_2, is a viable strategy to improve oil recovery from established reservoirs and possibly reduce greenhouse gas emissions. However, the effective application of these methods depends on thorough planning, reservoir characterization, and process optimization. (Bolouri *et al.*, 2013; Shen & Sheng, 2018; Zanganeh *et al.*, 2015)

In a vaporizing gas drive, the injected gas which is frequently rich in intermediate hydrocarbons is intended to evaporate into the reservoir oil. The dissolved gas components cause the oil phase's volume to rise noticeably, a process referred to as "oil swelling." Because the dissolved gas components are present, the oil's viscosity is greatly decreased, increasing its

mobility and ease of displacement. The combined effects of viscosity reduction and oil swelling improve the injected gas's capacity to move the oil more efficiently through the reservoir. (Apostolos Kantzas *et al.*)

CO_2 usage in EOR methods has been used for many decades, but it has seen a spike in interest due to the heated topics of Carbon Capture and Utilisation (CCU). Although new projects have not been as entertained as they should have been due to economic restraints. (Khan *et al.*, 2013) (Hawthorne & Miller, 2019)

Through experimentation it has been found that CO_2 is the most appropriate option. Methane tends to dissolve lighter hydrocarbons (upto C_{12}), CO_2 tends to dissolve light to mild hydrocarbons (upto C_{16}) while Ethane tends to dissolve nearly the whole range of hydrocarbons. It shows that CO_2 and Methane tend to be biased against the heavier hydrocarbons, while that is not the case with Ethane. (Derakhshan & Shariati, 2012; Hawthorne & Miller, 2019; Khan *et al.*, 2013)

Ethane can be used to yield higher overall recovery but it is best utilised when it is used along with CO_2 flooding or after, thereby reducing the deposition of paraffins and higher molecular weight hydrocarbons in the reservoir.

Though prior research has shown that adding methane to CO_2 increases MMP while adding ethane or other natural gas liquids (NGLs) to CO_2 decreases MMP, most experimental investigations on hydrocarbon behaviour under both miscible and immiscible conditions have concentrated on CO_2. Likewise, adding ethane or other NGLs to lean gas reduces MMP and can improve oil recovery when used for EOR. According to a recent study of experimentally determined MMPs for crude oil from a conventional reservoir undergoing CO_2 EOR, pure methane produced an MMP of 28.1 MPa (4076 psi), which was more than five times higher than the MMP with ethane of 5.27 MPa and nearly three times higher than the 9.68 MPa (1404 psi) MMP measured with CO_2.

Gas Injection

Gas Injection is considered an effective and widely used EOR method. Its effectiveness has been thoroughly studied and proved through numerous experiments, simulations and field projects. (Koyanbayev *et al.*, 2023). It can be estimated that about 60% of EOR projects are CO_2 based.

With the increasing demand for crude, we have started to shift from conventional reservoirs to deep reservoirs. In such reservoirs, water flooding starts to become ineffective. (Yan *et al.*, 2023) (Bahramian *et al.*, 2007) (M. Chen *et al.*, 2025; Ramadan & Shedid, 2018; Tang *et al.*, 2018)

The basic concept of CO_2 EOR is based upon the interrelation between carbon dioxide and crude oil existing under specific conditions of pressure and temperature that obtain in a geologic reservoir. CO_2 dissolves into the trapped oil, which occupies microscopic pore spaces in the reservoir rock. Thus, the crude oil dissolves into the porous spaces of the reservoir rock to the following advantages such as reduced viscosity, increased reservoir pressure, etc. It also helps to form an oil bank, such that the CO_2 sweeps through the reservoir. (Awan & Kirmani, 2024) (Khan *et al.*, 2013)

In normal procedure, the process of CO2 injection is carried out through specially drilled wells into the reservoir. Strategic injection well placement ensures that they are in optimal locations to achieve the maximum possible sweep efficiency of the injected CO2. The latter maximizes contact between CO2 and Reservoir Oil as much as possible. Mobilized oil is then pumped out through the producing wells towards the surface. (Baharizade & Sedaee, 2022) (Awan & Kirmani,2024)

For CO2 EOR to be successful, much infrastructure must provide and transport CO2 to oilfields. This is mainly through pipelines where carbon dioxide can be delivered over long distances from sources that include industrial plant sites, natural gas processing facilities, or CO2 producing wells. The pipeline systems facilitate continuous injection operation and thus ensure a steady supply of CO2. (Awan & Kirmani, 2024)

For periods, the sizeable drivers in the oil and gas assiduity have sought to establish the feasibility of Nitrogen gas injection for stronger oil recovery due to its excessive compressibility, idleness in chemical parcels, and pretty low cost of product (the source material is atmospheric air).

N_2 is carried out in better Oil recovery by 'miscible injection' or' miscible flooding', that is the technique that complements hydrocarbon mobility through a drop in interfacial stress between oil and water. (Tileuberdi *et al.*, 2023) The methane injection in EOR as detailed in the fractured reservoirs study mainly refers to the infusion of methane as a miscible or near-miscible gas to enhance oil recovery efficiency. (Baharizade & Sedaee, 2022)

Methodology

Determining MMP is essential to determine whether the Vaporising Gas Drive will be effective (Z. Chen *et al.*, 2025). To determine CO_2 MMP, we can conduct a number of experiments such as coreflood test, slim-tube test along with the use of models such as microfluidic models. Due to high computing requirements, empirical correlations along with computational simulations that use EOS equations are used. (Benelli *et al.*, 2025)

We can determine microscopic miscible mechanism and macroscopic flow characteristics of gas and crude by combining Molecular Dynamic (MD) simulation and Computational Fluid Dynamics (CFD) simulations. (Yan *et al.*, 2023)

We can combine theory and experimental data to find new empirical mass transfer correlations to better understand the Vaporising gas drive concept as it is important as condensates vaporize in porous media. (Mohamadi-Baghmolaei *et al.*, 2020) (Ramadan & Shedid, 2018)

To determine the pressure maintenance of CO_2 injection 3-D models are used which include five vertical and three horizontal wells. (Zheng *et al.*, 2013)

We can also take the help of Static Capacitance Resistance Model (SCRM), that uses time constant parameters, to better understand reservoir aquifer interactions and to enhance pressure maintenance. (Lesan *et al.*, 2023)

CO_2 can be sourced from the naturally sequestered emission sources of power plants and other industries that otherwise would have entered into the atmosphere. (Awan & Kirmani, 2024) In Nitrogen gas injection, N_2 of a suitable minimal Miscible strain (MMP) is equipped into a pressure to loosen up hydrocarbons trapped inside the conformation. (Tileuberdi *et al.*, 2023)

At veritably excessive pressures(psi), N_2 forms a miscible slug that sweeps oil and fuel from difficult-to-attain sections of the pressure and pools them collectively, after which they'll be pumped up the product well for collection. This procedure can recover as much as 60% of the authentic oil in place. (Tileuberdi *et al.*, 2023) (H. Zhao *et al.*, 2025)

1. Multiple Contact Miscibility Process in Vaporizing Gas Drive

Miscibility of the injected lean fuel and the reservoir oil starts taking place through successive contacts, which is called more than one touch miscibility (MCM) within the vaporizing fuel force process. The injected gasoline, wealthy in methane (C_1) or inert gases like nitrogen, is not to start with miscible with the reservoir oil. but, as the technique continues, the fuel turns into enriched with intermediate and heavier hydrocarbons from the oil and hence achieves miscibility beneath favourable conditions. (H. Zhao *et al.*, 2025)

The injected gasoline, point 'S' inside the pseudo ternary diagram, is basically wealthy in mild additives along with methane. The oil inside the reservoir, factor 'O', is intermediate and heavy hydrocarbons. The initial touch between the injected gasoline and the oil is a combination, M_1, which separates into two stages: Liquid phase, L_1 (Heavier hydrocarbons) Fuel section, V_1 (Injected gas rich in intermediate and heavy hydrocarbons).

2. Segment Mobility and Enrichment

The gas segment V_1 is extra cellular than the liquid segment L_1 and moves forward, and it encounters reservoir oil. On contact with oil, a brand-new combination M_2 is formed, which once more splits into gasoline section V_2 which is richer in intermediate hydrocarbons than V_1 and liquid phase L_2 contains heavier additives than L_1. Every successive gas section V_1, V_2, V_3. will become regularly enriched with intermediate hydrocarbons. This enrichment brings the gas composition closer to the critical factor composition.

3. Reaching Miscibility

After repeated contacts, the fuel section composition tactics the essential factor ('C') on the pseudo ternary diagram. At this point: The fuel and oil phases lose segment limitations. The tie line between the gasoline and liquid phases has zero distance, indicating miscibility. The miscible gasoline can then push out the reservoir oil in a non-stop, piston-like style without phase limitations within the transition sector. A transition sector develops at the main edge of the advancing fuel, wherein: The composition of the gas changes steadily from the injected lean gas to the important factor composition. Miscible displacement of the reservoir oil takes location easily inside this region, as there aren't any segment barriers.

4. Conditions for Miscibility

a) The reservoir pressure should be above the minimal miscibility pressure (MMP) for miscibility improvement. b) In the pseudo ternary diagram, the composition of oil needs to be on or to the right aspect of the crucial tie line; which means it has to have a good enough quantity of intermediate hydrocarbon composition. c) On the left aspect of the important tie line, the injected gasoline has to have a particularly wealthy composition of mild components along with methane. (Apostolos Kantzas *et al.*) (Cao & Gu, 2013b)
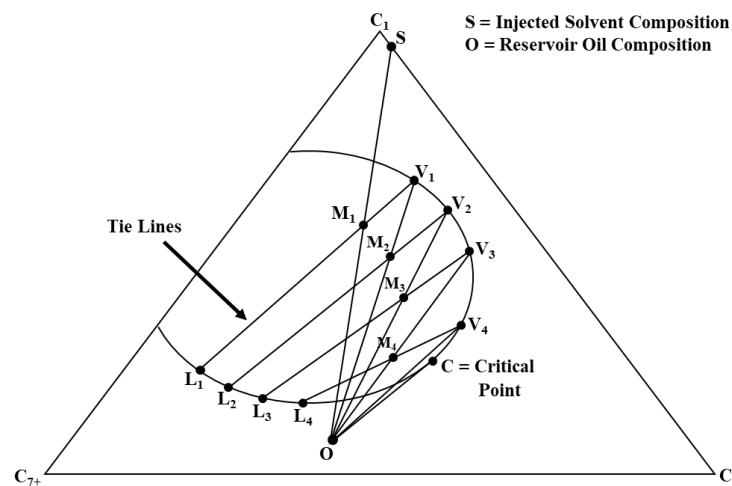

Figure 1: Pseudo Ternary Diagram (Apostolos Kantzas *et al.*)

Discussion:

Higher petroleum extraction can be done with the help of hydrocarbon gas injections. It is well known that hydrocarbon gas causes oil swelling, reduces viscosity and is fully miscible. Hence it is an important and beneficial EOR method (Yan *et al.*, 2023)

Injection mediums are crucial for EOR success, but owing to the complexity of a reservoir selection criteria may become cumbersome. Also, the characteristics of a deep reservoir to be of high temperature and pressure leads to further complications. Hence to tackle such problems, MD-CFD simulations need to be used. (Yan *et al.*, 2023)

Nitrogen fuel injection is any other one of the extra favoured EOR approaches since it is economically feasible and sustainable. One rail vehicle N_2 storehouse and shipping unit can hold as vital as 1.2 million (SCF) of liquid N_2. (Tileuberdi *et al.*, 2023)

Some other advantage of the use of Nitrogen gasoline injection for superior oil restoration is its inert chemical characteristics. N_2 can help down-hole combustion of ignitable feasts and has no sharp impact on channels, in contrast to CO_2. (Tileuberdi *et al.*, 2023)

Methane injection into the reservoir is for attaining the miscibility condition with the reservoir oil by reducing the interfacial tension and enhancing displacement efficiency. (Baharizade & Sedaee, 2022)

The MMP for methane was calculated as 465 atm, which is higher than the MMP of other gases like CO_2 and rich gas. This means it is that much harder to achieve miscibility. (Baharizade & Sedaee, 2022) (Derakhshan & Shariati, 2012)

Methane injection increased the recovery factor to 16.70% when it was 15.2% in the natural depletion scenario. Given that methane has evolved as an all-inferior EOR agent compared to CO_2 or rich gas, it is still able to accrue a marginal increase in ultimate oil recovery. (Baharizade & Sedaee, 2022)

With methane injection rates being very high, gas breakthrough may occur early, thus decreasing the net oil recovery. Optimization of the injection rate is imperative so that it balances the partial matching conditions avoiding a wastage of gas. (Baharizade & Sedaee, 2022) (Awan & Kirmani, 2024). SCRM method has shown acceptable accuracy of about 6% for homogeneous cases. (Lesan *et al.*, 2023)

For unconventional tight reservoirs such as Bakken reservoir, where oil recovery is difficult, use of miscible CO_2 flooding has proven to be effective. (Luo *et al.*, 2017) (C. Li *et al.*, 2020) (Hawthorne & Miller, 2020) (Bolouri *et al.*, 2013; Shen & Sheng, 2018; Zanganeh *et al.*, 2015) (Bolouri *et al.*, 2013; Cao & Gu, 2013a; S. Li & Luo, 2017; Shen & Sheng, 2018). Even

for shale reservoirs CO_2 is an attractive solution due to its low cost, high efficiency and environmentally friendly nature. (F. Chen *et al.*, 2024)

Use of techniques such as Polymer Inclusion Membranes can be used for metal removal from gas injections. (S. Zhao *et al.*, 2024) Plus nanoparticles can be used to enhance EOR. (Ahmadi *et al.*, 2024)

Conclusion:

Just like CO_2 and rich gas are more effective in reducing the interfacial tension with oil and thus achieve better miscibility, methane at large, was a disappointer in this regard. Methane tended to produce a higher gas/oil ratio in comparison to rich gas and CO_2 due to its lower oil solubility, thereby causing more gas-liquid drop-out at the surface. (Awan & Kirmani, 2024; Baharizade & Sedaee, 2022; Tileuberdi *et al.*, 2023).

Hydrocarbon gas should be studied in further detail to develop deep reservoirs (Yan *et al.*, 2023). Tight unconventional reservoirs are better suited to miscible CO_2 flooding. (Luo *et al.*, 2017) (Wang & Gu, 2011).

CO_2 shows favourable sequestration performance when shale reservoirs are concerned. (F. Chen *et al.*, 2024). It can also be used for CCUS. (Khan *et al.*, 2013) (Azzolina *et al.*, 2015; Gorecki *et al.*, 2015) (Azzolina *et al.*, 2015; Gorecki *et al.*, 2015; Nobakht *et al.*, 2008).

All in all, it can be concluded that CO_2 is a better option as compared to other gases for EOR methods.

Acknowledgement:

References:

1. Apostolos Kantzas, Jonathan Bryan, Saeed Taheri. *Fundamentals of Fluid Flow in Porous Media.* https://perminc.com/resources/fundamentals-of-fluid-flow-in-porous-media

2. Abdurrahman, A., Shuwa, S. M., Dabai, F. N., Orodu, O. D., Ogunkunle, F. T., Igbafe, A. I., & Jibril, B. Y. (2025). Chemical agents for enhanced oil recovery: A comparison of a switchable hydrophilic solvent and deep eutectic solvent. *Fuel Communications*, *22*, 100133. https://doi.org/10.1016/J.JFUECO.2025.100133

3. Ahmadi, Y., Hemmati, M., Vaferi, B., & Gandomkar, A. (2024). Applications of nanoparticles during chemical enhanced oil recovery: A review of mechanisms and

technical challenges. *Journal of Molecular Liquids*, *415*, 126287. https://doi.org/10.1016/J.MOLLIQ.2024.126287

4. Awan, M. M. A., & Kirmani, F. U. D. (2024). CO2 injection for enhanced oil recovery: Analyzing the effect of injection rate and bottom hole pressure. *Petroleum Research*. https://doi.org/10.1016/J.PTLRS.2024.08.006

5. Azzolina, N. A., Nakles, D. V., Gorecki, C. D., Peck, W. D., Ayash, S. C., Melzer, L. S., & Chatterjee, S. (2015). CO2 storage associated with CO2 enhanced oil recovery: A statistical analysis of historical operations. *International Journal of Greenhouse Gas Control*, *37*, 384–397. https://doi.org/10.1016/j.ijggc.2015.03.037

6. Baharizade, M. H., & Sedaee, B. (2022). Effect of gas type on miscible enhanced oil recovery at naturally fractured reservoirs: case study-Asmari. *SN Applied Sciences*, *4*(10). https://doi.org/10.1007/s42452-022-05148-z

7. Bahramian, A., Danesh, A., Gozalpour, F., Tohidi, B., & Todd, A. C. (2007). Vapour–liquid interfacial tension of water and hydrocarbon mixture at high pressure and high temperature conditions. *Fluid Phase Equilibria*, *252*(1–2), 66–73. https://doi.org/10.1016/J.FLUID.2006.12.013

8. Benelli, F. E., Pisoni, G. O., & Cismondi-Duarte, M. (2025). Complex phase behaviours related to gas injection in reservoir fluids. *The Journal of Supercritical Fluids*, *218*, 106475. https://doi.org/10.1016/J.SUPFLU.2024.106475

9. Bolouri, H., Schaffie, M., Kharrat, R., Ghazanfari, M. H., & Ghoodjani, E. (2013). An experimental and modeling study of asphaltene deposition due to CO 2 miscible injection. *Petroleum Science and Technology*, *31*(2), 129–141. https://doi.org/10.1080/10916466.2010.538787

10. Cao, M., & Gu, Y. (2013a). Oil recovery mechanisms and asphaltene precipitation phenomenon in immiscible and miscible CO2 flooding processes. *Fuel*, *109*, 157–166. https://doi.org/10.1016/j.fuel.2013.01.018

11. Cao, M., & Gu, Y. (2013b). Temperature effects on the phase behaviour, mutual interactions and oil recovery of a light crude oil-CO2 system. *Fluid Phase Equilibria*, *356*, 78–89. https://doi.org/10.1016/j.fluid.2013.07.006

12. Chen, F., Wang, Y., Bi, R., Pan, Y., & Wang, M. (2024). Molecular insights into CO2 enhanced hydrocarbon recovery and its sequestration in multiscale shale reservoirs. *Chemical Engineering Journal*, *498*, 155913. https://doi.org/10.1016/J.CEJ.2024.155913

13. Chen, M., Chen, X., Kang, Y., Cheng, Z., You, L., Xiong, G., Yang, D., & Qin, C. (2025). Investigation of water blocking mitigation in a normal-pressure shale gas reservoir by

high-temperature treatment: Insights from heat transfer range. *Fuel*, *382*, 133667. https://doi.org/10.1016/J.FUEL.2024.133667

14. Chen, Z., Chen, J., & Zhang, X. (2025). A comprehensive review of minimum miscibility pressure determination and reduction strategies between CO2 and crude oil in CCUS processes. *Fuel*, *384*, 134053. https://doi.org/10.1016/J.FUEL.2024.134053

15. Derakhshan, T., & Shariati, A. (2012). Prediction of wax precipitation temperature in petroleum reservoirs upon methane injection. *Journal of Petroleum Science and Engineering*, *98–99*, 1–10. https://doi.org/10.1016/J.PETROL.2012.08.012

16. Gorecki, C. D., Ayash, S. C., Liu, G., Braunberger, J. R., & Dotzenrod, N. W. (2015). A comparison of volumetric and dynamic CO2 storage resource and efficiency in deep saline formations. *International Journal of Greenhouse Gas Control*, *42*, 213–225. https://doi.org/10.1016/j.ijggc.2015.07.018

17. Hamouda, A. A., & Chughtai, S. (2018). Miscible CO2 flooding for EOR in the presence of natural gas components in displacing and displaced fluids. *Energies*, *11*(2). https://doi.org/10.3390/EN11020391

18. Hawthorne, S. B., & Miller, D. J. (2019). A comparison of crude oil hydrocarbon mobilization by vaporization gas drive into methane, ethane, and carbon dioxide at 15.6 MPa and 42 °C. *Fuel*, *249*, 392–399. https://doi.org/10.1016/j.fuel.2019.03.118

19. Hawthorne, S. B., & Miller, D. J. (2020). Comparison of CO2and Produced Gas Hydrocarbons to Dissolve and Mobilize Bakken Crude Oil at 10.3, 20.7, and 34.5 MPa and 110 °c. *Energy and Fuels*, *34*(9), 10882–10893. https://doi.org/10.1021/ACS.ENERGYFUELS.0C02112

20. Hawthorne, S. B., Miller, D. J., Jin, L., & Gorecki, C. D. (2016). Rapid and Simple Capillary-Rise/Vanishing Interfacial Tension Method to Determine Crude Oil Minimum Miscibility Pressure: Pure and Mixed CO2, Methane, and Ethane. *Energy and Fuels*, *30*(8), 6365–6372. https://doi.org/10.1021/ACS.ENERGYFUELS.6B01151

21. Khan, C., Amin, R., & Madden, G. (2013). Carbon dioxide injection for enhanced gas recovery and storage (reservoir simulation). *Egyptian Journal of Petroleum*, *22*(2), 225–240. https://doi.org/10.1016/J.EJPE.2013.06.002

22. Koyanbayev, M., Wang, L., Wang, Y., Hashmet, M. R., & Hazlett, R. D. (2023). Impact of gas composition and reservoir heterogeneity on miscible sour gas flooding — A simulation study. *Fuel*, *346*, 128267. https://doi.org/10.1016/J.FUEL.2023.128267

23. Lesan, A., Shams, R., Pourafshary, P., Bahrodi, A., & Rastkerdar, H. (2023). Application of the modified capacitance-resistance method to model reservoir pressure maintenance.

Results in Engineering, *19*, 101231. https://doi.org/10.1016/J.RINENG.2023.101231

24. Li, C., Pu, H., Zhong, X., Li, Y., & Zhao, J. X. (2020). Interfacial interactions between Bakken crude oil and injected gases at reservoir temperature: A molecular dynamics simulation study. *Fuel*, *276*. https://doi.org/10.1016/j.fuel.2020.118058

25. Li, S., & Luo, P. (2017). Experimental and simulation determination of minimum miscibility pressure for a Bakken tight oil and different injection gases. *Petroleum*, *3*(1), 79–86. https://doi.org/10.1016/j.petlm.2016.11.011

26. Luo, P., Luo, W., & Li, S. (2017). Effectiveness of miscible and immiscible gas flooding in recovering tight oil from Bakken reservoirs in Saskatchewan, Canada. *Fuel*, *208*, 626–636. https://doi.org/10.1016/J.FUEL.2017.07.044

27. Mohamadi-Baghmolaei, M., Azin, R., Osfouri, S., & Zendehboudi, S. (2020). Experimental and modeling investigation of non-equilibrium condensate vaporization in porous systems: Effective determination of mass transfer coefficient. *Fuel*, *262*, 116011. https://doi.org/10.1016/J.FUEL.2019.116011

28. Nobakht, M., Moghadam, S., & Gu, Y. (2008). Mutual interactions between crude oil and CO2 under different pressures. *Fluid Phase Equilibria*, *265*(1–2), 94–103. https://doi.org/10.1016/j.fluid.2007.12.009

29. Ramadan, A. H., & Shedid, S. A. (2018). Improved material balance equation (MBE) for gas-condensate reservoirs considering significant water vaporization. *Egyptian Journal of Petroleum*, *27*(4), 1209–1214. https://doi.org/10.1016/J.EJPE.2018.05.005

30. Shen, Z., & Sheng, J. J. (2018). Experimental and numerical study of permeability reduction caused by asphaltene precipitation and deposition during CO2 huff and puff injection in Eagle Ford shale. *Fuel*, *211*, 432–445. https://doi.org/10.1016/j.fuel.2017.09.047

31. Tang, Y., Yang, R., & Kang, X. (2018). Modeling the effect of water vaporization and salt precipitation on reservoir properties due to carbon dioxide sequestration in a depleted gas reservoir. *Petroleum*, *4*(4), 385–397. https://doi.org/10.1016/J.PETLM.2017.12.003

32. Tileuberdi, N., Mashrapova, M., & Toktarbay, Z. (2023). A Review on Nitrogen Flooding for Enhanced Oil Recovery. *ES Materials and Manufacturing*, *22*. https://doi.org/10.30919/esmm968

33. Wang, X., & Gu, Y. (2011). Oil Recovery and Permeability Reduction of a Tight Sandstone Reservoir in Immiscible and Miscible CO2 Flooding Processes. *Industrial and Engineering Chemistry Research*, *50*(4), 2388–2399. https://doi.org/10.1021/IE1016046

34. Yan, Z., Li, X., Zhu, X., Wang, P., Yu, S., Li, H., Wei, K., Li, Y., & Xue, Q. (2023). MD-

CFD simulation on the miscible displacement process of hydrocarbon gas flooding under deep reservoir conditions. *Energy*, *263*, 125730. https://doi.org/10.1016/J.ENERGY.2022.125730

35. Zanganeh, P., Dashti, H., & Ayatollahi, S. (2015). Visual investigation and modeling of asphaltene precipitation and deposition during CO2 miscible injection into oil reservoirs. *Fuel*, *160*, 132–139. https://doi.org/10.1016/j.fuel.2015.07.063

36. Zhao, H., Song, C., Wu, D., & An, C. (2025). Experimental Multiple-Contact miscibility and PVT properties with equation of state modeling for High-Pressure nitrogen injection into deep reservoirs with Tahe heavy and light crudes. *Fuel*, *385*, 134171. https://doi.org/10.1016/J.FUEL.2024.134171

37. Zhao, S., Samadi, A., Wang, Z., Pringle, J. M., Zhang, Y., & Kolev, S. D. (2024). Ionic liquid-based polymer inclusion membranes for metal ions extraction and recovery: Fundamentals, considerations, and prospects. *Chemical Engineering Journal*, *481*. https://doi.org/10.1016/j.cej.2024.148792

38. Zheng, S., Li, H., & Yang, D. (2013). Pressure maintenance and improving oil recovery with immiscible CO2 injection in thin heavy oil reservoirs. *Journal of Petroleum Science and Engineering*, *112*, 139–152. https://doi.org/10.1016/J.PETROL.2013.10.020

APPLICATION OF AI AND ML IN RESERVOIR ENGINEERING –
A COMPREHENSIVE REVIEW

Angshuman Baruah and Prasenjit Talukdar*

Department of Petroleum Engineering,

DUIET, Dibrugarh University, Assam-786004, India

*Corresponding author E-mail: prasenjit_duiet@dibru.ac.in

Abstract:

Artificial Intelligence (AI) and Machine Learning (ML) are increasingly making various several developments in the oil and gas industry, particularly in reservoir engineering. In this paper, a comprehensive review of the various applications of Artificial Intelligence and Machine Learning is given, highlighting on the need to enhance decision making, increasing efficiency, reducing costs and optimizing production. Important applications include prediction of permeability, estimating total production, differentiating between pores and microfractures, and optimizing field development through various machines learning techniques like Artificial Neural Networks (ANN), Support Vector Machines (SVM), and XGBoost. Moreover, AI plays an important role in automating subsurface analytics and provides accurate reservoir modeling without complex geological assumptions. Challenges of data integration, talent shortage, and AI scalability are addressed along with future scenarios suggesting a dynamic transformation in industrial practices and methods. This review emphasizes AI and ML's growing importance in tackling the complexities of modern reservoir management and focuses on effective, data-driven strategies.

Keywords: Artificial Intelligence, Machine Learning, ANN, SVM, Reservoir Engineering, Porosity, Permeability

Introduction:

Artificial Intelligence (AI) and Machine Learning (ML) play an important role in oil and gas industry, especially in the field of reservoir engineering. Earlier, reservoir engineering depended on labour-intensive, manual methods of gathering and analysing data, which require a significant amount of time and resources. But with the advancements in AI and ML, these processes have helped in achieving faster, accurate results in making predictions and optimizations. AI's capacities in analysing data from sources like seismic data, well logs, core analysis, etc., has changed the way of understanding and model the reservoir characteristics and predict performance. ML algorithms like Artificial Neural Networks (ANN), Genetic Algorithms and Support Vector Machines (SVM), have enhanced production forecasting, estimate

permeability and optimize oil recovery strategies. Also, AI is making significant improvements in tackling challenges of unconventional reservoirs, particularly shale formations, where hydrocarbon uncertainty is high and traditional methods often become cumbersome. This paper focuses in the prime applications of AI and ML in reservoir engineering, exploring their impact of efficiency, accuracy and decision making in reservoir management.

AI and ML Concepts

Artificial Intelligence (AI) and Machine Learning (ML) helps in making most jobs in the industries automation based. Similarly, oil industry has transformed and has similar advantages of AI and ML in improving reservoir development planning and operational accuracy through a number of automated systems. In field development, computerized static and dynamic simulation models are generated based on several petro-physical and geo-mechanical properties obtained from various earlier resources which are time-consuming and expensive. Using AI and ML, processes have become much easier, faster and economical using the learning through experiences from already explored reservoirs, rock properties and fluid flow behaviour under various conditions and predicts accordingly. E&P strategies in a reservoir depend mostly on the properties of reservoir rocks and geology of formations within the reservoir. But in an unconventional reservoir, particularly in shale formations, uncertainty in comparatively high. AI is making processes easier and accurate. Shale oil and gas are today the most significant producers of hydrocarbons in the United States from the unconventional reservoirs [1][2]. A few algorithms of AI and ML used commonly are: Artificial Neural Networks (ANN), Fuzzy rule-based systems, Genetic Algorithms (GA), Integrated Neural Networks, etc.

Usage in Reservoir Engineering

In reservoir engineering, topics like fluid flow through porous media, production forecasting and field optimization are included. Numerous simulations, models and experimentations are required for the preparation of subsurface property maps and PVT analysis [3]. Seismic data, well-log data, core analysis, past performance data of the reservoir are included into a single plan by machine learning algorithms. Complex pressure transient analysis and deconvolution of pressure data are performed by algorithms regarding Artificial Neural Networks, Genetic Algorithms, Response Surface Model (RSM), etc. Teixeira and Secchi (2019) used optimization algorithms to maximise total oil production by identifying optimum control [4]. The models are helpful in history matching of the reservoir. A huge amount of data is used to develop reservoir maps and need updates repetitively according to newer data updated. ANN can estimate permeability and porosity, but now it can be performed by other methods like K Nearest Neighbours (KNN), Support Vector Regression (SVR) to predict fluid properties in a reservoir. The synthetic reservoir model can be used for the numerical simulation of reservoir oil. The

parametric study can be carried out by comparing different machine learning techniques used to predict permeability, seismic attributes and wire-line data. Nwachukwu *et al.* (2018) selects five cases like homogenous reservoir water flood, channelized reservoir water flood, CO_2 flood in a heterogeneous reservoir with complex topography [5].

Permeability Prediction

Permeability is an important parameter in reservoir characterization and evaluation. Using traditional methods, we can determine permeability by core analysis along with other well test methods, which not only results in a heavy cost but also require huge amount of time. Numerous attempts have been undertaken due to these problems to employ artificial neural networks with the aim to find and present the relationship of all well log data and the measurements of core permeability recorded. More advancements have led to development of a better machine learning technique namely Support Vector Machine (SVM). Results obtained from SVM show a higher level of accuracy than ANN. Also, comparison of results of SVM with General Regression Neural Network (GNNN) showed SVM technique is more faster and precise than GNNN technique in predicting permeability of hydrocarbon reservoirs [5].

Prediction of Production

A P oilfield is an oilfield in a continental multilayer sandstone reservoir. It is very difficult to precisely determine productivity of oil well initially due to a long oil-bearing interval, difference in fluid properties. To predict initial productivity of oil wells, a deep neural network is built based on XGBoost, following by analysis of main controlling factors of productivity. A hundred oil wells were chosen. A period of 6 months with a certain productivity index is taken initially as target data along with various geological and reservoir parameters taken as input data, and formed a deep-learning based unconsolidated sandstone productivity forecast model was built for predicting initial productivity of oil wells. Mean square root error of predictive result was found to be less than 0.15, which was found similar to actual productivity. Machine learning has the advantages of effective forecasting of oil well productivity and the main controlling factors using multi-dimensional and big data hence saving costs and time for other useful processes [6].

Differentiating Pores and Micro-Fractures

Various petrographic observations are important for understanding geological structures and fluid storage capacities. However, current approaches to petrographic pore-typing heavily rely on manual techniques, yielding qualitative or semi-quantitative results that are difficult to integrate into a comprehensive subsurface analysis. Recent advancements in the field have seen attempts to automate pore classification through supervised machine learning (ML) and deep learning (DL). These methods focus on selecting basic morphological features of pores and

achieving impressive accuracy across diverse pore configurations. Nevertheless, concerns arise regarding the validity of findings from these studies, primarily due to conceptual and technical shortcomings in their methodologies leveraging these technologies. Firstly analysis of 18 carbonate thin sections sourced from different locations within the United States, quantifying them based on five key shape characteristics is done: compactness, aspect ratio, extent, solidity, and form factor. Utilizing a labeled dataset comprised of 400 samples each for pores and microfractures allowed to test nine widely recognized supervised models. The results were noteworthy; all tested models demonstrated high accuracy rates ranging from 89.58% to 90.42%. Interestingly, more complex non-linear models did not show substantial performance improvements over simpler linear alternatives. Among the evaluated features, compactness and aspect ratio emerged as particularly informative for classification purposes. Despite achieving high accuracy rates in our work—and across similar studies—the labeled datasets used do not encapsulate the entirety of data complexity typically found in natural carbonate systems. The excellent performance observed may stem from specific curated database constraints rather than an accurate reflection of variegated carbonate pore architectures. Thus, we conclude that relying solely on fundamental shape descriptors is inadequate for accurately classifying various carbonate pore types effectively. Carbonate pore-typing represents a pivotal challenge when it comes to rock type identification—petrographic techniques deployed via thin sections constitute one of the most sophisticated means available today for characterizing saline porosities at critical scales essential in geological assessments [7].

Subsurface Analytics

Subsurface analytics is a new technology that brings a revolution in the way of reservoir simulation and modeling. Instead of beginning with the development of mathematical equations that would describe the physics of the fluid flow through porous media and then alteration of the geological models to get the history match, Subsurface Analytics that is an entirely data-driven reservoir simulation and modeling technology is a completely different approach.

In data-driven reservoir modeling, field measurements form the foundation of the reservoir model. Using data-driven pattern recognition technologies, the physics of fluid flow through porous media is modeled through discovering the best, most appropriate relationships between all the measured data in a given reservoir. In this approach, to match the dynamic field measurements such as fluid (oil, gas, and water) productions, reservoir pressure, and water saturation, the interaction between all the field measurements such as reservoir characteristics, well placement and trajectory, completion details in space and time, operational constraints, etc. are modeled through discovery of the complex set of relationships and patterns between all the field measurements.

The essential characteristics of Subsurface Analytics are:

1. No Interpretations
2. No Assumptions
3. No Complex Initial Geological Model
4. No Upscaling.

In addition, it should be noted that the key series of dynamic variables, which are used to construct this model, are measured on the surface (flow line and wellhead pressure and temperature, choke setting, as well as oil, gas and water production) while other major static (well logs, cores, seismic, etc.) and sometimes even dynamic (completions) characteristics are based on subsurface measurements.

The Subsurface Analytics' "History Matching" process is fully automated, taking a tiny fraction of the time compared with the history matching of the traditional numerical simulation models.

Unlike history matching of the traditional numerical simulation models where local (well-based) modification of the model (measured reservoir characteristics, transmissibility, skin, etc.) plays a crucial role, especially for highly complex mature fields, the automatic history matching of Subsurface Analytics does not include any local modifications of the model.

Subsurface Analytics completely changes how mature fields are modeled. This Coupled Reservoir-Wellbore Simulation (CRWS) modeling technology, based on Artificial Intelligence and Machine Learning, has a very small computational footprint, which highly contributes to most of the post-modeling analyses such as single and multi-parameter sensitivity analysis, uncertainty quantifications, production and recovery optimizations, infill location optimization, injection optimization, and field development planning [8].

Relationship among Porosity, Permeability and Pore Throat Size

Finding an accurate method for estimating permeability other than from well logs has been a difficult task for many years. We can understand the relationship among porosity, permeability, and pore throat radii using three methods such as multiple regression analysis, artificial neural network (ANN), and adaptive neuro-fuzzy inference system (ANFIS) for application in transition zone permeability modeling. First, 228 core samples of carbonate from the transition zone were taken and subjected to a detailed MICP test. Multiple regression was then used on pore throat and porosity measurements to estimate the permeability. For ANN, a two-layer feed-forward neural network, sigmoid hidden neuron, and linear output neuron are used. It is a method that requires input/output data with training, validation, and testing. However, for the ANFIS method, a hybrid optimization consisting of least-square and back propagation gradient descent methods with a subtractive clustering technique was used. The

ANFIS combines both the artificial neural network and fuzzy logic inference system (FIS) for the training, validation, and testing of input/output data. The results indicate that the best correlation for the multiple regression technique is achieved for pore throat radii with 35% mercury saturation, which is referred to as R35. However, for both the ANN and ANFIS techniques, pore throat radii with 55% mercury saturation referred to as R55 give the best result. After their applications, it is realized that both the ANN and ANFIS are more effective and efficient, hence recommended to be used as compared to the multiple regression techniques that are normally practiced in the industry [9].

Trends, Challenges, and Scenarios for Future

It's quite evident that though artificial intelligence is an emerging trend in oil and gas, there are applications that have already added countable value [10]. Several examples of how artificial intelligence helps accelerate and minimize risk in many business processes associated with the exploration of hydrocarbon resources, development of oil and gas fields, and raw hydrocarbon production are visible.

There is an ongoing experiment on the scalability of artificial intelligence throughout the whole industry. Evaluation of the impact of education, organizational attitude and data availability on the speed and direction of penetration of artificial intelligence to oil and gas upstream will become a determining factor for the success of implementation of AI and/or ML. Based on this analysis, we draw three possible scenarios of the spread of artificial intelligence within oil and gas in the coming five to twenty years: People, Data and Open Collaboration [11]. The oil and gas industry is increasingly using AI and data-driven methodologies to improve decision-making and optimize drilling and production processes. The key applications of AI include seismic interpretation, well logging, reservoir engineering, and drilling optimization. Companies use machine learning and deep learning algorithms to analyze data from various sources to make more objective decisions, reduce risks, and realize cost savings. However, a lack of AI talent, poor data quality, and the need for cooperation hinder the fast adoption of AI technologies [12]. The role of the petroleum engineer has evolved to incorporate skills in data science, and three potential scenarios for the integration of AI in the industry highlight the range of possible outcomes-from significant cost reductions to decreased profit margins. Strategic leadership and organizational change underpin successful digital transformation.

AI and ML practises help in accelerating processes, improving decision-making, transforming the oil and gas sector through AI. Further, seismic interpretation, well logging, and drilling optimization through AI are some other advantages. The machine learning algorithm provides an objective analysis of data from a source. But the shortage of talent and quality of

data create challenges to speed up AI. Also, role of the petroleum engineer changes to data science competencies integration with application of these practises.

The integration of AI into the oil and gas sector is symbolic of a new paradigm that embodies better decision-making processes and higher operational efficiencies. AI helps bridge the gap from traditional, largely subjective methods towards more structured data-driven approaches for both exploration and production workflows. The recent trends in the industry show that AI tools are increasingly being used to not only speed up processes but also mitigate risks associated with upstream operations through predictive insights and real-time analytics. Upstream operations are highly uncertain due to the volatile nature of oil and gas markets, geological complexities, and shifting regulatory landscapes. The need for AI in oil and gas in today's world can be as following:

Increasing Complexity: The growing shift towards "difficult-to-recover" reserves and difficulty in extraction of hydrocarbons that are beyond recoverable by conventional techniques. Decision-making Uncertainties: Traditional decision-making processes are often ruined by expert biases and dependence on previous experiences. Consequently, AI emerges as a critical enabler that gives objective assessments, more effective investment strategies and operational decisions.

Case Studies: The practical application of AI across various upstream activities, as evidenced by the authors' experiences, includes successful projects encompassing geological assessments, reservoir simulations, and production optimization, demonstrating AI's versatility in enhancing operational outcomes.

Some key challenges in AI use are:

- Talent shortage: With AI technologies developing at such a sharp pace in the oil sector, it requires recruitment and retention of talent to effectively fill the gap between traditional petroleum engineering practices and modern-day data science methods.
- Educational Reforms: In response, universities are increasingly developing interdisciplinary programs that merge petroleum engineering with data science curriculums, ensuring that the next generation of engineers is equipped with essential skills to thrive in this evolving industry.
- Data Integration Challenges: The existing corporate structures of oil and gas companies frequently hinder effective data sharing and collaborative efforts, which are critical for meaningful AI development and deployment.
- The Need for Centralized Data Storage: Organizations are thus motivated to change their data management approach and adopt comprehensive data-sharing agreements among all stakeholders to ease access to the data and promote the application of AI technologies.

- Some future scenarios for AI in oil and gas are described as follows:
- Positive Scenario: A future characterized by widespread acceptance of AI technologies leads to the establishment of robust infrastructure for data sharing, resulting in significant cost savings and enhanced decision-making processes, underpinned by advanced AI tools.
- Realistic Scenario: In a more tempered scenario, while some advancements occur, the pace of AI integration remains restrained due to ongoing data-sharing challenges and lingering scepticism regarding the reliability of AI outputs.
- Negative Scenario: In the least favourable scenario, poor data sharing practices and distrust in AI technologies stifle innovation and limit practical applications, resulting in marginal improvements within the oil and gas margins.

Conclusion:

In conclusion, AI and ML are proving to be transformative tools in reservoir engineering, offering innovative solutions to some of the industry's most complex challenges. From predicting permeability and production rates to automating subsurface analytics, these technologies are improving the speed and accuracy of decision-making in reservoir development. Machine learning algorithms have significantly reduced the time and cost associated with traditional reservoir modeling, enabling engineers to focus on more strategic tasks. Despite the clear advantages, challenges such as talent shortages, data integration, and AI scalability remain barriers to widespread adoption. However, as data quality improves and collaboration between engineers, data scientists, and management increases, the future of AI in the oil and gas industry looks promising. With continued investment in AI technologies and education, the oil and gas sector will be better equipped to handle the complexities of modern reservoir engineering and maximize resource management for years to come.

References:

1. F. I. Syed, A. AlShamsi, A. K. Dahaghi, and S. Neghabhan, "Application of ML & AI to model petrophysical and geomechanical properties of shale reservoirs – A systematic literature review," *Petroleum*, vol. 8, no. 2, pp. 158–166, 2022, doi: 10.1016/j.petlm.2020.12.001.

2. M. Anemangely, A. Ramezanzadeh, H. Amiri, and S. A. Hoseinpour, "Machine learning technique for the prediction of shear wave velocity using petrophysical logs," *J. Pet. Sci. Eng.*, vol. 174, no. November 2018, pp. 306–327, 2019, doi: 10.1016/j.petrol.2018.11.032.

3. A. Sircar, K. Yadav, K. Rayavarapu, N. Bist, and H. Oza, "Application of machine learning and artificial intelligence in oil and gas industry," *Pet. Res.*, vol. 6, no. 4, pp. 379–391, 2021, doi: 10.1016/j.ptlrs.2021.05.009.

4.   A. F. Teixeira and A. R. Secchi, "Machine learning models to support reservoir production optimization," *IFAC-PapersOnLine*, vol. 52, no. 1, pp. 498–501, 2019, doi: 10.1016/j.ifacol.2019.06.111.

5.   A. Nwachukwu, H. Jeong, M. Pyrcz, and L. W. Lake, "Fast evaluation of well placements in heterogeneous reservoir models using machine learning," *J. Pet. Sci. Eng.*, vol. 163, no. December 2017, pp. 463–475, 2018, doi: 10.1016/j.petrol.2018.01.019.

6.   Z. Wang *et al.*, "Production prediction and main controlling factors in a highly heterogeneous sandstone reservoir: Analysis on the basis of machine learning," *Energy Sci. Eng.*, vol. 10, no. 12, pp. 4674–4693, 2022, doi: 10.1002/ese3.1297.

7.   I. S. A. J. Jayachandran *et al.*, "An Object-Based Approach to Differentiate Pores and Microfractures in Petrographic Analysis Using Explainable, Supervised Machine Learning," *Earth Sp. Sci.*, vol. 11, no. 2, pp. 1–25, 2024, doi: 10.1029/2023EA003291.

8.   S. D. Mohaghegh, "Subsurface analytics: Contribution of artificial intelligence and machine learning to reservoir engineering, reservoir modeling, and reservoir management," *Pet. Explor. Dev.*, vol. 47, no. 2, pp. 225–228, 2020, doi: 10.1016/S1876-3804(20)60041-6.

9.   J. O. Adegbite, H. Belhaj, and A. Bera, "Investigations on the relationship among the porosity, permeability and pore throat size of transition zone samples in carbonate reservoirs using multiple regression analysis, artificial neural network and adaptive neuro-fuzzy interface system," *Pet. Res.*, vol. 6, no. 4, pp. 321–332, 2021, doi: 10.1016/j.ptlrs.2021.05.005.

10. J. Bughin, J. Seong, J. Manyika, M. Chui, and R. Joshi, "Notes From the Ai Frontier: Modeling the Impact of Ai on the World Economy," *Model. Glob. Econ. impact AI | McKinsey*, no. September, pp. 1–61, 2018, [Online]. Available: https://www.mckinsey.com/featured-insights/artificial-intelligence/notes-from-the-ai-frontier-modeling-the-impact-of-ai-on-the-world-economy [Accessed 03 April 2021]

11. D. Koroteev and Z. Tekic, "Artificial intelligence in oil and gas upstream: Trends, challenges, and scenarios for the future," *Energy AI*, vol. 3, p. 100041, 2021, doi: 10.1016/j.egyai.2020.100041.

12. A. Ng, "and Can ' t Do Right Now," *Hbr*, pp. 9–12, 2016.

PAPER-BASED SENSORS FOR CARBON DIOXIDE DETECTION

Manasa Chandramouli

Department of Chemistry, Vidyavardhaka College of Engineering,

Visvesvaraya Technological University, Mysuru-570 002, Karnataka, India

Corresponding author E-mail: manasac@vvce.ac.in

Abstract:

Paper-based sensors have emerged as a promising technological advancement in the development of analytical devices that are cost-effective, portable, and disposable. These sensors have gained significant attention across various fields, including clinical diagnostics, food quality control, and environmental monitoring. Their widespread applicability is primarily attributed to the inherent properties of paper, such as its ability to facilitate passive liquid transport and its compatibility with various chemical and biochemical reactions.

Despite these advantages, the practical application of paper-based sensors is often constrained by limitations related to accuracy and sensitivity. These challenges hinder their broader adoption in analytical applications requiring precise measurements. However, continuous advancements in fabrication techniques and analytical methodologies are expected to enhance the performance of these sensors. Future developments in this field may lead to the creation of highly sensitive, selective, and multifunctional paper-based sensors that align with the growing demand for economical and portable sensing solutions.

This chapter provides a comprehensive review of paper-based sensors specifically designed for carbon dioxide detection. By examining their working principles, fabrication techniques, and recent advancements, the discussion aims to highlight the potential of these sensors in real-world applications while addressing existing limitations and future research directions.

Keywords: Paper-Based Sensors, Carbon Dioxide Detection, Applications in Food Packaging.

Introduction:

Paper-based sensors have emerged as a promising low-cost, portable, and eco-friendly alternative for carbon dioxide (CO_2) detection. These sensors utilize the unique properties of cellulose, such as high porosity, flexibility, and biodegradability, making them suitable for sensitive and selective detection platforms. The detection mechanisms employed in these sensors typically include colorimetric detection, fluorometric detection, and electrochemical detection. The development of paper-based CO_2 sensors holds significant implications for various applications, including air quality monitoring, food packaging, and biomedical applications.

They can be deployed in urban environments to monitor air quality effectively and affordably, integrate into food packaging to monitor spoilage, and facilitate point-of-care testing in medical diagnostics. Their affordability and ease of use make them particularly suitable for resource-limited settings and enable real-time monitoring and data collection in smart buildings and other facilities where continuous monitoring is vital.

Recent advancements in paper-based sensor technology focus on improving sensitivity, response time, and mass production capabilities. Researchers are exploring various designs and materials to optimize performance while maintaining low production costs. As research continues to enhance their capabilities, these sensors could play a crucial role in addressing global challenges related to environmental monitoring and public health.

1. Role of carbon dioxide sensors in food packaging

The growing consumer demand for food safety and quality has driven technological advancements in food packaging. To meet these expectations, researchers and industries have developed novel and innovative packaging technologies that ensure food integrity throughout the supply chain (Zhou *et al.*, 2020). Among these, intelligent or smart packaging has emerged as a cost-efficient and reliable alternative to traditional analytical techniques used for food quality assessment (Kuswandi *et al.*, 2011). Smart packaging enables continuous monitoring of food quality by transmitting critical information at different stages of the distribution chain, ensuring that consumers receive products that meet safety standards (Yam *et al.*, 2005).

One of the key indicators of food spoilage is the production and accumulation of byproducts during storage, which can significantly affect food quality under normal atmospheric conditions (Mills *et al.*, 2012**).** Apart from byproducts, factors such as pH variations, temperature fluctuations, and pressure changes within the packaging environment can also contribute to food deterioration (Pereira *et al.*, 2021). However, these indicators pose challenges in practical applications. Heat levels vary unpredictably during spoilage, pH changes differ across food types, and pressure fluctuations are difficult to standardize, making them unreliable for real-time food quality assessment (Fang *et al.*, 2019).

2. Carbon dioxide as a prime indicator of food spoilage

Given these limitations, carbon dioxide (CO_2) has emerged as a critical marker for food spoilage detection**.** Modified Atmosphere Packaging (MAP) relies on maintaining optimal CO_2 levels to preserve food freshness (Rodrigues *et al.*, 2020). A deviation from these levels can indicate microbial activity and product degradation, making CO_2 sensors a direct and effective tool for food quality monitoring (Mangaraj *et al.*, 2018).

Despite advancements in CO_2 sensor technology, their widespread application in food packaging has been hindered by several factors, including high energy consumption, bulky

designs, high production costs, and potential safety concerns (Gupta *et al.*, 2022). Current CO_2 sensors lack versatility, limiting their adaptability across various food types and packaging conditions (Escobedo *et al.*, 2010). Consequently, there is an urgent need for a highly efficient, cost-effective, and user-friendly CO_2 sensor that can overcome these limitations while ensuring accurate real-time monitoring of gas levels (Lee *et al.*, 2019).

3. Future perspectives of CO_2 sensors in the food industry

In recent years, CO_2 sensors have gained significant attention in the food and agricultural sectors as a reliable tool for assessing food quality and safety (Zhang *et al.*, 2021). The ability to monitor CO_2 levels in packaged food provides critical insights into product freshness and storage conditions. The development of affordable and highly sensitive CO_2 sensors has become a priority, as consumer preferences increasingly focus on food safety and quality assurance (Wang *et al.*, 2017).

Moreover, real-time data collection and analysis are essential for designing effective food packaging systems. Sensor technology plays a pivotal role in decision-making, ensuring that food safety measures align with industrial standards (Chen *et al.*, 2020). An ideal CO_2 sensor should exhibit high sensitivity, reliability, and ease of interpretation, allowing for seamless integration across diverse food products. Since CO_2 plays a crucial role in MAP, a decline in its concentration can serve as a definitive indication of food spoilage. This underscores the importance of CO_2 sensors as an indispensable tool in the modern food packaging industry (Ali *et al.*, 2022).

Emerging trends in carbon dioxide sensors for food packaging

1. Advancements in CO_2 sensor technology

Recent years have witnessed remarkable progress in the development of various CO_2 sensors, including optical sensors, polymer opal films, polymer hydrogels, and paper-based sensors. These innovations are highly relevant in applications such as food packaging, where monitoring gas levels is critical for maintaining product quality (Smith *et al.*, 2019). The introduction of paper-based assay technology has garnered widespread recognition due to its cost-effectiveness, simplicity, and rapid analytical capabilities (Lee *et al.*, 2021).

Paper-based sensors (PADs) have become increasingly popular in both research and academic settings, offering an economical alternative for large-scale and small-scale applications (Khan *et al.*, 2020). These sensors are valued for their ease of fabrication (Chen *et al.*, 2018), high-speed analysis (Zhao *et al.*, 2020), and adaptability across diverse applications (Mei *et al.*, 2017). Moreover, their portability and suitability for point-of-care (POC) diagnostics make them a versatile tool for field and clinical use (Gupta & Verma, 2019).

The inherent properties of paper, such as its lightweight nature (Brown & Taylor, 2015)**,** varying thicknesses (Singh *et al.*, 2016), and biodegradability (Jones *et al.*, 2020), contribute to its environmental compatibility (Patel & Roy, 2022). These attributes enable the integration of microfluidic channels, biomolecules, and chemical reagents, transforming paper into an affordable and efficient diagnostic tool (Nguyen *et al.*, 2018).

2. Microfluidic Paper-Based Analytical Devices (µPADs)

The emergence of Microfluidic Paper-Based Analytical Devices (µPADs) marks a new era in analytical chemistry. These devices, which diagnose conditions with high sensitivity, have seen a surge in fabrication to meet market demands and diverse application needs (Liu *et al.*, 2019). However, developing integrated devices that encompass all analytical stages remains a critical challenge. Enhancing the versatility and production efficiency of µPADs could lead to broader adoption and commercialization (Kim & Park, 2020).

3. Innovations in sensor technology

Recent innovations in CO_2 sensor technology include devices with amino-functionalized silica nanoparticles, offering reproducible and selective CO_2 detection through rapid acid-base reactions (Zhang *et al.*, 2021). Similarly, polyaniline-based sensors demonstrate high efficiency in agricultural applications, detecting CO_2 concentrations ranging from 102 to 104 ppm (Chen *et al.*, 2022).

Another advancement is the use of hydrophobic silicone water-repellent sprays for creating paper-based sensors capable of differentiating CO_2 and ammonia using RGB readouts and MATLAB analysis (Wang *et al.*, 2020). Additionally, fluorescent paper sensors infused with P4VB offer quick response times and low-cost operation, suitable for continuous CO_2 monitoring (Li & Zhao, 2021). The incorporation of luminescence pH-sensitive dyes in copolymer films further enhances CO_2 detection accuracy without interference from other gases (Feng *et al.*, 2019).

4. Future prospects of paper-based CO_2 sensors

Advancements in paper-based CO_2 sensors indicate a promising future for these technologies. The integration of functional materials and novel fabrication techniques is crucial for developing stable, sensitive, and multi-analyte devices (Xu *et al.*, 2022). By maintaining the inherent advantages of paper-based sensors, researchers can create economical and efficient diagnostic tools for a wide range of applications.

Future Perspectives:

Before commercializing paper-based sensors, it is essential to address existing limitations, particularly concerning sensitivity and accuracy (Patel & Kumar, 2021). By overcoming these challenges, paper-based sensors could become invaluable in medical

diagnostics, offering precise prognostic capabilities. Simplifying the manufacturing process is also vital for scaling up production and reducing costs (Singh *et al.*, 2021).

Despite current limitations, point-of-care devices have proven indispensable in food quality monitoring, agricultural applications, and biomedical research. They have demonstrated effectiveness in detecting biomarkers for liver and kidney disorders, diabetes, and environmental toxins (Ramirez *et al.*, 2020). As research progresses, paper-based sensors are expected to evolve into key technologies for diverse analytical needs.

Conclusions:

Paper-based sensors offer a cost-effective and versatile solution for various analytical applications. With advancements in fabrication techniques, these sensors have the potential to provide rapid, colorimetric responses under different environmental conditions, rivaling commercial electronic sensors (Liu *et al.*, 2020). Continued innovation in this field could lead to portable, reliable, and user-friendly diagnostic tools that address the needs of modern industries and consumers alike.

References:

1. Zhou, L., Zhao, Y., Khan, I. M., & Ling, Z. (2020). Advances in intelligent packaging technologies for food applications. *Trends in Food Science & Technology, 102*, 29-39.

2. Kuswandi, B., Wicaksono, Y., Jayus, A., Abdullah, A., Heng, L. Y., & Ahmad, M. (2011). Smart packaging: Sensors for monitoring food quality and safety. *Sensing and Instrumentation for Food Quality and Safety, 5*(3-4), 81-91.

3. Yam, K. L., Takhistov, P. T., & Miltz, J. (2005). Intelligent packaging: Concepts and applications. *Journal of Food Science, 70*(1), R1-R10.

4. Mills, A., Wang, J., & McGrath, S. (2012). A CO_2-sensitive colorimetric plastic film for packaging applications. *Analytical Chemistry, 84*(6), 2870-2875.

5. Pereira, M. C., Marques, A. T., & Morais, S. (2021). Recent advances in food packaging sensing technologies. *Sensors and Actuators B: Chemical, 330*, 129353.

6. Fang, Z., Zhao, Y., Warner, R. D., & Johnson, S. K. (2019). Active and intelligent packaging in meat industry. *Trends in Food Science & Technology, 86*, 51-58.

7. Rodrigues, C., Felício, B. C., de Oliveira, A. C., & Conti-Silva, A. C. (2020). Shelf-life estimation of ready-to-eat food using smart packaging technologies. *Food Packaging and Shelf Life, 23*, 100447.

8. Mangaraj, S., Goswami, T. K., & Mahajan, P. V. (2018). Modified atmospheric packaging—Principles and applications in food. *Critical Reviews in Food Science and Nutrition, 58*(10), 1577-1590.

9. Gupta, S., Nayak, S. K., & Rath, P. (2022). Current trends and future prospects of CO_2 sensors for food packaging applications. *Sensors and Actuators B: Chemical, 355*, 131249.

10. Escobedo, P., Fernández-Ramos, M. D., & Martínez-Máñez, R. (2010). Optical CO_2 sensors for food packaging applications. *Journal of Sensors, 2010*, 1-11.

11. Lee, D. S., Cheigh, C. I., & Kang, S. J. (2019). Real-time gas sensors for food packaging applications. *Food Science and Biotechnology, 28*(6), 1619-1630.

12. Zhang, Z., Zhu, X., & Zhang, H. (2021). CO_2-responsive intelligent packaging for food safety monitoring. *Trends in Food Science & Technology, 115*, 78-91.

13. Wang, X., Liu, W., & Zhang, X. (2017). Development of advanced CO_2 sensors for real-time food packaging applications. *Biosensors and Bioelectronics, 94*, 61-69.

14. Chen, H., Wang, X., & Sun, Y. (2020). Nanomaterial-based CO_2 sensors for smart packaging applications. *Advanced Materials Interfaces, 7*(14), 2000731.

15. Ali, A., Siddiqui, M. W., & Rahman, M. S. (2022). Future perspectives of CO_2 sensors in food packaging: Challenges and opportunities. *Food Chemistry, 389*, 132988.

16. Smith, A., *et al.* (2019). Innovations in CO_2 sensing technology for food packaging. *Journal of Food Engineering, 245*, 62-74.

17. Lee, H., *et al.* (2021). Paper-based sensors in food quality control. *Analytical Chemistry, 93*(2), 654-667.

18. Khan, M., *et al.* (2020). Applications of paper-based analytical devices. *Sensors, 20*(9), 2501.

19. Chen, J., *et al.* (2018). Advances in paper-based microfluidics. *Lab on a Chip, 18*(4), 571-580.

20. Zhao, W., *et al.* (2020). Rapid analysis using paper-based devices. *Biosensors and Bioelectronics, 150*, 111849.

21. Gupta, N., & Verma, A. (2019). Point-of-care diagnostics using paper-based sensors. *Current Analytical Chemistry, 15*(4), 345-355.

22. Patel, R., & Roy, S. (2022). Environmental benefits of biodegradable paper sensors. *Environmental Science & Technology, 56*(3), 1498-1507.

23. Xu, L., *et al.* (2022). Future directions in paper-based sensor technology. *Sensors and Actuators B: Chemical, 370*, 132859.

SEMICONDUCTORS

Jyothi Budida*[1] and Kamala Srinivasan[2]

[1]Department of Physics, Aditya University, Surampalem, India

[2]Department of Physics, S. V. University, Tirupati

*Corresponding author E-mail: budidajyothi2012@gmail.com

What are semiconductors?

A semiconductor material has an electrical conductivity value falling between that of a conductor, such as metallic copper, and an insulator, such as glass. Its resistivity falls as its temperature rises; metals behave in the opposite way. Its conducting properties may be altered in useful ways by introducing impurities ("doping") into the crystal structure. When two differently-doped regions exist in the same crystal, a semiconductor junction is created. The behaviour of charge carriers, which include electrons, ions and electron holes, at these junctions is the basis of diodes, transistors and most modern electronics. Some examples of semiconductors are silicon, germanium, gallium arsenide, and elements near the so-called "metalloid staircase" on the periodic table. After silicon, gallium arsenide is the second most common semiconductor and is used in laser diodes, solar cells, microwave-frequency integrated circuits, and others. Silicon is a critical element for fabricating most electronic circuits.

Semiconductor devices can display a range of useful properties, such as passing current more easily in one direction than the other, showing variable resistance, and sensitivity to light or heat. Because the electrical properties of a semiconductor material can be modified by doping, or by the application of electrical fields or light, devices made from semiconductors can be used for amplification, switching, and energy conversion. By adding impurity to conductor generally conductivity decreases, but in semiconductor conductivity increases. In semiconductors both electrons and holes will conduct current.

Introduction:

Semiconductors are materials whose electronic properties are intermediate between those of good conductors and insulators.

- The resistivity of semiconductors varies from 10^{-5} to 10^{+4} ohm-m,
- The band gap of semiconductors varies from 0.2 to 2.5 eV.
- These intermediate properties are determined by crystal Structure, bonding characteristics, electronic Energy bands.
- The interesting feature about semiconductors is that they are bipolar and current is carried by two charge carriers of opposite sign (electrons and holes).

- Semiconductors have negative temperature co-efficient of resistance.
- Silicon and Germanium are elemental semiconductors which belong to the group IV elements in periodic table.
- Besides these, there are certain compound semiconductors such as GaAs, InP, CdS etc.,

Variable Electrical Conductivity

Semiconductors in their natural state are poor conductors because a current requires the flow of electrons, and semiconductors have their valence bands filled, preventing the entire flow of new electrons. Several developed techniques allow semiconducting materials to behave like conducting materials, such as doping or gating. These modifications have two outcomes: n-type and p-type. These refer to the excess or shortage of electrons, respectively. An unbalanced number of electrons would cause a current to flow through the material.

Heterojunctions

Heterojunctions occur when two differently doped semiconducting materials are joined together. For example, a configuration could consist of p-doped and n-doped germanium. This results in an exchange of electrons and holes between the differently doped semiconducting materials. The n-doped germanium would have an excess of electrons, and the p-doped germanium would have an excess of holes. The transfer occurs until an equilibrium is reached by a process called recombination, which causes the migrating electrons from the n-type to come in contact with the migrating holes from the p-type. The result of this process is a narrow strip of immobile ions, which causes an electric field across the junction.

Excited Electrons

A difference in electric potential on a semiconducting material would cause it to leave thermal equilibrium and create a non-equilibrium situation. This introduces electrons and holes to the system, which interact via a process called ambipolar diffusion. Whenever thermal equilibrium is disturbed in a semiconducting material, the number of holes and electrons changes. Such disruptions can occur as a result of a temperature difference or photons, which can enter the system and create electrons and holes. The process that creates and annihilates electrons and holes are called generation and recombination, respectively.

Light Emission

In certain semiconductors, excited electrons can relax by emitting light instead of producing heat. These semiconductors are used in the construction of light-emitting diodes and fluorescent quantum dots.

High Thermal Conductivity

Semiconductors with high thermal conductivity can be used for heat dissipation and improving thermal management of electronics.

Thermal Energy Conversion

Semiconductors have large thermoelectric power factors making them useful in thermoelectric generators, as well as high thermoelectric figures of merit making them useful in thermoelectric coolers.

Types of Semiconductors

Semiconductors are mainly two types

1. Intrinsic (Pure) Semiconductors   2. Extrinsic (Impure) Semiconductors

Intrinsic Semiconductor

A Semiconductor which does not have any kind of impurities, behaves as an Insulator at 0k and behaves as a Conductor at higher temperature is known as Intrinsic Semiconductor or Pure Semiconductors. Germanium and Silicon (4 th group elements) are the best examples of intrinsic semiconductors and they possess diamond cubic crystalline structure.
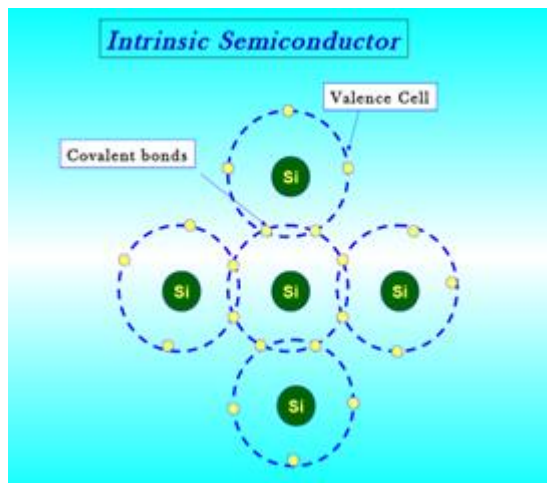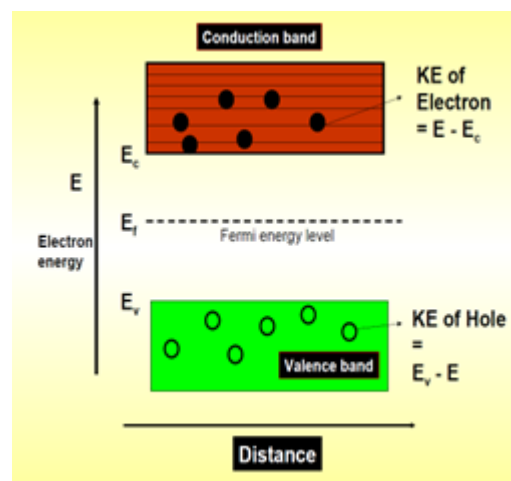

Figure 1: Bond structure   **Figure 2: Energy band diagram**

Charge Carrier in Intrinsic Semiconductor

When a suitable form of Energy is supplied to a Semiconductor then a few covalent bonds are broken. So one electron becomes free and leaves a empty space in the atom, it is known as hole. The hole acts as a positively charged particle having equal charge and opposite sign. If the hole is filled by an electron from neighbouring atom then the hole is now shifted to new place.

Hence a free electron in Conduction band and simultaneously free hole in Valence band is formed. This phenomenon is known as Electron - Hole pair generation. In Intrinsic Semiconductor the Number of Conduction electrons will be equal to the Number of Vacant sites or holes in the valence band.
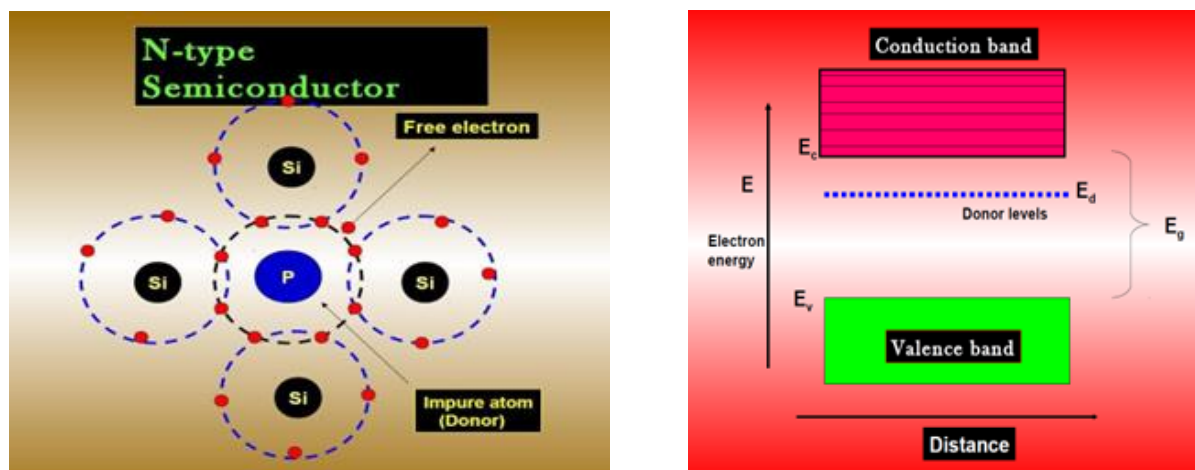
Extrinsic Semiconductor

The Extrinsic Semiconductors are those in which impurities of large quantity are present. Usually, the impurities can be either 3rd group elements or 5th group elements. Based on the impurities present in the Extrinsic Semiconductors, they are classified into two categories.

1. N-type semiconductors

2. P-type semiconductors

N – type Semiconductors

When any pentavalent element such as Phosphorous, Arsenic or Antimony is added to the intrinsic Semiconductor, four electrons are involved in covalent bonding with four neighboring pure Semiconductor atoms. The fifth electron is weakly bound to the parent atom. And even for lesser thermal energy it is released Leaving the parent atom positively ionized**.**


Figure 3: The Intrinsic Semiconductors doped with pentavalent impurities are called N-type Semiconductors

The energy level of fifth electron is called donor level. The donor level is close to the bottom of the conduction band most of the donor level electrons are excited in to theconduction band at room temperature and become the Majority charge carriers. Hence in N-type Semiconductors electrons are Majority carriers and holes are Minority carriers.

P – type Semiconductors

When a trivalent elements such as Al, Ga or Indium are added to the Intrinsic Semiconductor all the three electrons of these are involved in Covalent bonding with the three neighboring Si atoms.

There is deficiency of one electron to complete the fourth bond. This deficiency is called hole and acts like positively charged particle.
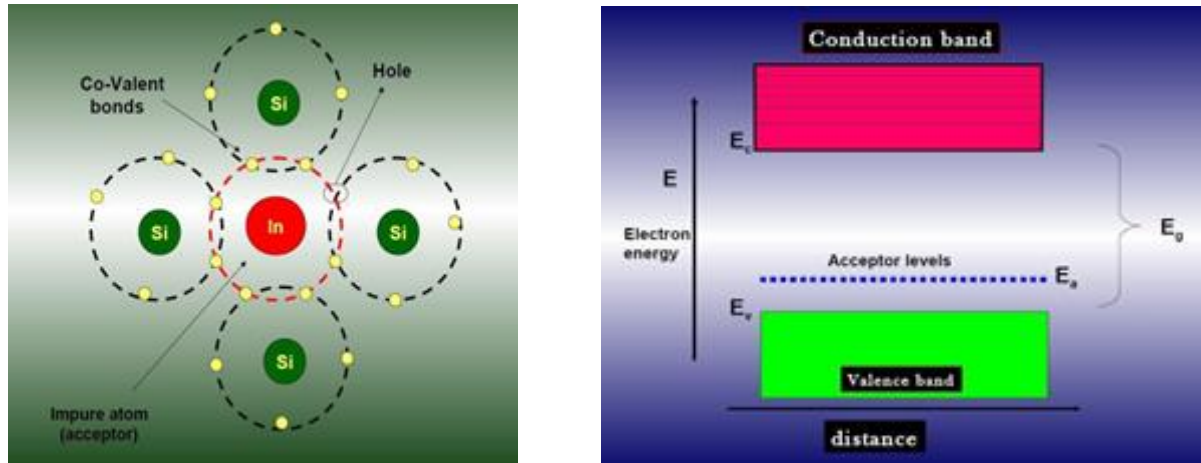
Figure 4: Semiconductors doped with the acceptor impurities are called P-type Semiconductors

These like compound accepts one extra electron, the impurity atom is called acceptor impurity. the energy level of this impurity atom is called Acceptor level and this acceptor level lies just above the valence band. Thus, holes are more in number than electrons and hence holes are majority carriers and electros are minority carriers in P-type semiconductors.

References:

1. Feynman, R. (1963). *Feynman lectures on physics.* Basic Books.
2. The "hot-probe" experiment. (n.d.). *ecee.colorado.edu*.
3. Shockley, W. (1950). *Electrons and holes in semiconductors: With applications to transistor electronics.* R. E. Krieger Pub. Co. ISBN 978-0-88275-382-9.
4. Neamen, D. (n.d.). *Semiconductor physics and devices* [PDF]. Elizabeth A. Jones.
5. Al-Azzawi, A. (2007, March 4). *Light and optics: Principles and practices.*
6. Kang, J. S., Li, M., Wu, H., Nguyen, H., & Hu, Y. (2018). Experimental observation of high thermal conductivity in boron arsenide. *Science, 361*(6402), 575–578. https://doi.org/10.1126/science.aat5522
7. How do thermoelectric coolers (TECs) work? (n.d.). *marlow.com*.
8. Yacobi, B. G. (2003). *Semiconductor materials: An introduction to basic principles.* Springer. ISBN 0-306-47361-5.
9. Yu, P. (2010). *Fundamentals of semiconductors.* Springer-Verlag. ISBN 978-3-642-00709-5.
10. Cutler, M., & Mott, N. (1969). Observation of Anderson localization in an electron gas. *Physical Review, 181*(3), 1336. https://doi.org/10.1103/PhysRev.181.1336
11. Kittel, C. (1995). *Introduction to solid state physics* (7th ed.). Wiley. ISBN 0-471-11181-3.
12. Allen, J. W. (1960). Gallium arsenide as a semi-insulator. *Nature, 187*(4735), 403–405. https://doi.org/10.1038/187403b0

RICE HUSKS IN DIGITAL FABRICATION:
UNLOCKING SUSTAINABLE MATERIAL POTENTIAL

Indrajit Chakraborty

Department of Chemistry,

Malda College, Malda, 732101, West Bengal, India

Corresponding author E-mail: indraji2001@gmail.com

Abstract:

Effective use of biological resources, to the extent that they are renewable, is crucial to the creation of a sustainable society. A valuable biomass resource, rice husk is produced in large quantities across different regions. It is crucial to broaden the fields in which they are utilized in order to encourage their use even more. In light of the growing popularity of 3D printers and Computer Numerical Control (CNC) machines in recent years, this study examines the research on materials derived from rice husks that can be utilized in digital fabrication. The authors first described the features of each machining technique before reviewing and evaluating the prior studies on particleboard used in digital fabrication machines for 2D machining and rice-husk-based materials for 3D printers. In order to increase the use of materials derived from rice husks, this review highlights problems and suggests fixes. It also suggests that more research is required on a number of topics, including the equipment's maintainability and workability.

Keywords: Green Materials; Rice Husk; Agricultural Byproduct; 3D Printing; Digital Fabrication; Particle Board

Introduction:

A growing body of research has explored design strategies for sustainability, focusing on models such as "Design for resource conservation," outlined by Moreno *et al.*[1] Additionally, the butterfly system diagram from the Ellen MacArthur Foundation illustrates the circular economy principles, emphasizing the need to keep products and materials in use at their highest value.[2] This approach underscores the importance of effective utilization and renewal of biological resources in achieving sustainability.

Rice husks from rice cultivation are one example of an agricultural residue that can be regarded as a significant biological resource. A significant agricultural waste product, rice husks are a valuable by-product of the rice milling process. The Food and Agriculture Organization of the United Nations (FAO) released statistical data on rice paddy production worldwide, which is displayed in Table 1.[3]

Table 1: Annual production quantity of rice paddies in 2010 and 2020 (FAOSTAT)

Region	Production Quantity [$\times 10^6$ton]	
	2010	**2020**
World	694.5	756.7
Africa	26.0	37.9
Americas	36.5	38.1
Asia	627.5	676.6
Europe	4.3	4.1
Oceania	0.2	0.1

Table 2: Number of review articles published on rice husks (ScienceDirect). A keyword search for "rice husk" was performed in ScienceDirect, and the results were sorted by checking the "Review Article" checkbox. The results for 2013–2022 are listed and categorized into those where the research content and application methods were analyzed broadly and those where a more detailed review was conducted by narrowing down the application cases.

Research Target	2013	2014	2015	2016	2017	2018	2019	2020	2021	2022	Total
Rice husk	0	0	1	0	0	0	0	1	0	1	3
General Rice husk ash	0	1	0	1	0	0	1	0	0	0	3
Rice husk derived silica	0	0	0	0	1	0	0	0	0	0	1
Cement/concrete	1	0	0	0	2	2	1	3	4	2	15
Adsorbents, soil Application conditioners, fertilizers	0	0	0	0	0	1	2	0	2	0	5
Energy	0	0	1	2	1	0	0	0	0	2	6
Fiber-reinforced polymer composites	0	0	0	0	0	0	0	0	1	0	1
Application to metal matrix	0	0	0	0	0	0	0	0	0	1	1
Application to alkali activated materials	0	0	0	0	0	0	0	0	0	1	1
Total	1	1	2	3	4	3	4	4	7	7	36

Around 756 million tons of rice were produced worldwide in 2020; this amount has increased since 2010, particularly in Asia and Africa. Rice husks are valuable materials with mechanical qualities as well as the ability to extract and use their primary constituents, cellulose, lignin, and silica, as functional materials. As a result, research on reusing rice husks has been extensive for a long time. The quantity of review article submissions since 2013 is compiled in Table 2. According to these findings, there is a growing interest in using rice husks, as evidenced by the rising number of submissions.

For continued advancement in the future, it's crucial not just to enhance technology in existing fields of application, but additionally to broaden usage in emerging sectors. One such emerging sector is the application of materials in digital fabrication. This is significant due to the contemporary advancements in digital fabrication technologies, like 3D printers and laser cutters, and the historical focus of rice husk utilization materials in sectors such as architecture and product design, where these technologies are prominently employed. Generally speaking, in this domain, rice husk is often combined with concrete and cement materials. However, further research has been published on various other materials that can be utilized in construction and product development, as demonstrated in Table 3.

Based on the aforementioned, it is anticipated that additional research on rice husk materials suitable for digital fabrication will encourage their application in the fields of product design and architecture while further optimizing the use of waste materials. Indeed, in 2020 and later, studies on the application of rice husks as a material for 3D printers have already been published. This material's potential applications will only increase if it can be utilized by other digital fabrication tools like CNC machines and laser cutters. A thorough review of original research on the application of particleboard as a practical material for digital fabrication and rice-husk-based materials for 3D printers is thus provided by this study. This study attempts to further the field's development by highlighting current research trends, outlining research gaps, and offering suggestions for resolving these issues.

Table 3 shows the number of studies published from 2013 to 2022 on the use of rice husks in product and construction industries, found on ScienceDirect and Springer platforms. After searching for "rice husk" in titles, ScienceDirect provided 1243 results, and Springer 535. Relevant articles were then selected and categorized based on their application described in Table 3.

Table 3: The number of studies published from 2013 to 2022 on the use of rice husks in product and construction industries

Application	2013	2014	2015	2016	2017	2018	2019	2020	2021	2022	Total
Polymer composite	2	5	3	5	8	5	10	16	21	14	89
Metal matrix composite	3	1	2	0	1	3	2	2	1	4	19
Rubber composite	1	0	0	1	0	1	1	2	4	2	12
Glass	1	0	2	0	1	0	3	1	0	2	10
Particleboard	1	0	0	0	1	2	0	2	0	3	9
Building materials	0	0	0	1	0	1	1	3	1	0	7
3D printing materials	0	0	0	0	0	0	0	1	1	1	3
Others	1	0	1	1	0	0	0	1	1	6	11
	9	6	8	8	11	12	17	28	29	32	160

2. The Physical Properties of Rice Husks

Rice husk makes up about 20% of paddy rice's weight pre-milling[4] and comprises cellulose (25–35%), hemicellulose (18–21%), lignin (26–31%), silica (15–17%), soluble matter (2–5%), and moisture (~7.5%).[5] Notably, rice husks are rich in silica and ash,[6] and their products show higher hydrophobicity due to elevated lignin levels compared to those from wood.[7] The combustion of husks produces rice husk ash, making up 20–25% of the husks' weight,[8] mostly consisting of 85–95% amorphous silica. However, characteristics of the ash vary with combustion and processing techniques.[9] Materials derived from the ash are porous and used as adsorbents and fillers.

3. Targeted Digital Fabrication Machines

Figure 1: Extrusion printing and deposition modeling were combined to create a 3D printer

Machines that process materials using computer-designed data are referred to as digital fabrication machines; the 3D printer is a common example. Three-dimensional (3D) printing technology, sometimes referred to as additive manufacturing, is a technique for layering materials

using information produced by a 3D scanner or 3D computer-aided design (3D CAD). There are several different ways to apply layers of thermally melted resin or paste, curing liquid resins with UV light, and sintering powdered materials. Figure 1 depicts two common types of machines.

Digital fabrication comprises not only 3D printers but also devices like computer numerical control (CNC) machines and laser cutters that can cut flat materials like board using 2D data generated by CAD or Graphic Soft. With the use of an end mill and 2D data, a CNC milling machine is a device that cuts materials. The apparatus can be seen in Figure 2.

Figure 2:. Computer numerical control (CNC) machine

This tool supports 3D cutting by leveraging 3D data and operates through "subtractive manufacturing" by eliminating excess material. Utilizing a laser beam, a laser cutter engraves or cuts objects, different from traditional end mill tools. These technologies may be applied in architecture and product design fields. Research introduced in this section covers materials for 3D printers using rice husks and suitable board materials for 2D processing, as detailed in Figure 3.
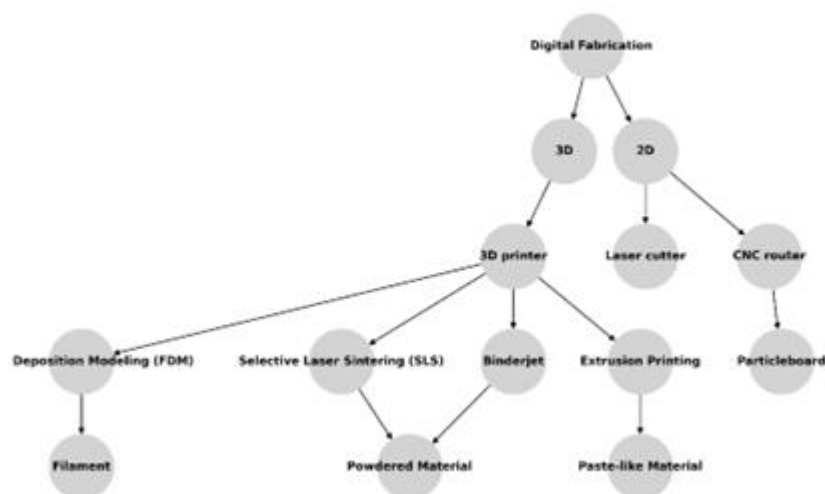
Figure 3: The target machines and materials

4. Articles on Materials for 3D Printer Utilizing Agricultural Wastes Including Rice Husks

4.1 *Method*

Our literature search on the utilization of rice husk as material for 3D printers was initially conducted on ScienceDirect and Springer, yielding one review and three research articles. To broaden our search, we subsequently utilized Google Scholar with the keyword "rice husk 3D printer," focusing on articles from 2013 to 2022. After reviewing titles and abstracts, we selected articles that specifically discussed rice husks as a raw material for 3D printing. We categorized the selected articles into review and original articles, offering an overview and highlighting key issues.

4.2 *Review Articles on Materials for 3D Printer Utilizing Agricultural Wastes Including Rice Husks*

Fused deposition modeling (FDM) is a prevalent 3D printing technique that utilizes thermoplastic filaments, typically polylactic acid (PLA) or acrylonitrile butadiene styrene (ABS), melted and layered to create objects. There has been substantial research into enhancing these filaments with natural fibers to create composite materials. Several reviews have been conducted in this domain; for instance, Rajendran *et al.* examined the use of natural-fiber-reinforced polymer composites for 3D printing filaments, focusing on fiber treatment methods and filament production techniques.[10] Ahmed *et al.* discussed the impact of natural fiber additives on polymer properties in 3D printing filaments, noting a lack of detailed fiber structure information in many studies.[11] Mazzanti *et al.* explored the potential of other semi-crystalline polymers like polyethylene (PE) and polypropylene (PP) beyond the commonly used materials in FDM,[12] while also analyzing PLA as a matrix for PLA-based bio-composites in FDM applications.[13] Lastly, Seker *et al.* proposed using these composites in manufacturing acoustic panels, highlighting their sound absorption benefits due to voids formed between deposition lines.[14] While these reviews focus extensively on FDM, this paper extends the study to other 3D printing technologies using rice husks as potential materials.

4.3 Original Articles on 3D Printer Materials Using Rice Husks

Table 4 provides examples of research articles on materials made from rice husks for 3D printers. The method, matrix, and filler or binder materials are given for every article.

Table 4: Original articles on materials for 3D printers using rice husks

	Matrix	Filler or Binder	Authors	Year
FDM	PLA	Rice husk	Charles *et al.* [15]	2019
FDM	PLA	Rice husk	Wu *et al.* [16]	2019
FDM	PLA	Rice husk/wood	Guen *et al.* [17]	2019
FDM	Recycled polypropylene	Rice husk	Morelos *et al.* [18]	2021
FDM	ABS	Rice husk ash	Philip *et al.* [19]	2021
SLS	Co-polyamide	Rice husk	Lim *et al.* [20]	2022
Material Extrusion	Cement	Rice husk ash	Kumar *et al.* [21]	2022
Material Extrusion	Cement	Rice husk ash	Palermo [22]	2020
Material Extrusion	Soil	Rice husk and lime	Ferrero *et al.* [23]	2022
Material Extrusion	Rice husk	Guar gum (as a binder)	Nina *et al.* [24]	2021
Material Extrusion	Al_2O_3-SiO_2 ink (includes rice-husk-derived silica)	PVA solution, glycerol, and dispersant (as a binder)	Husein *et al.* [25]	2022
Binder Jetting	Miscanthus particles, wood flour, seashell powder, fruit stone flour, rice husk (only mentioned)	Lignin sulfonate/sodium silicate/polyvinyl alcohol (as a binder)	Zeidler *et al.* [26]	2018

4.3.1. *Fused Deposition Modeling*

The primary method for incorporating natural resources into 3D printing involves blending them with polymers to create composite filaments. Examples include filaments combined with wood, bamboo, and rice husks. Tsou *et al.* enhanced the performance of rice husk composites by using methylene diphenyl diisocyanate, which improved tensile strength and impact resistance while facilitating porosity.[15] Wu *et al.* used acrylic acid-grafted PLA and treated rice husks to boost tensile strength and water resistance of their bio-composites.[16] Le Guen *et al.* analyzed wood and rice husk-blended PLA filaments, citing differences in visual

quality and processing stability due to variations in particle size and silica content.[17] Morales *et al.* experimented with rice husks in recycled polypropylene filaments, noting issues like increased water absorption but reduced warpage, making it suitable for certain applications.[18] Furthermore, research on rice husk ash blended with ABS indicated its potential in manufacturing optical components due to improved refractive indices and reduced absorption coefficients.[19]

Filament mixed with wood flour   Filament mixed with bamboo flour
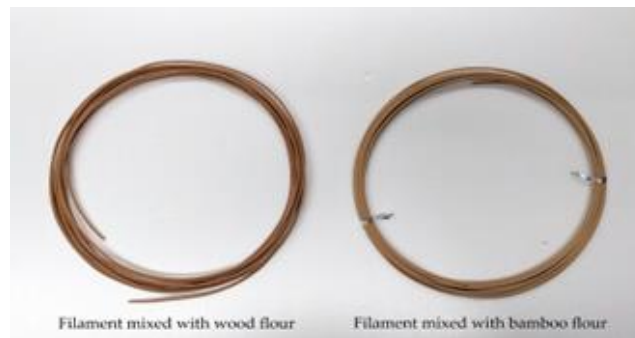
Figure 4: Filaments mixed with natural fiber materials

4.3.2. *Selective Laser Sintering* (SLS)

Selective Laser Sintering (SLS) SLS is a 3D printing technology that selectively scans a powder bed with a laser, creating precise models with minimal material loss. Common materials include polycarbonate and polystyrene powders. While rice husks are rarely used in SLS, a method incorporating rice husk powder into CO-polyamide powder for composite fabrication has been proposed.[20] This study examined the impact of rice husk content on mechanical properties, dimensional accuracy, residual ash, and sintering properties, optimizing SLS for investment casting applications.

4.3.3 *Extrusion Printing*

Extrusion Printing Extrusion printing injects a paste-like material through a nozzle using air pressure or a screw. It is widely used in construction and food 3D printing. Research on cement 3D printing with rice husk ash has increased. Muthukrishnan used a screw-type extruder to fabricate structures with rice husk ash, showing improved shape stability and curing properties.[21] Palaniappan *et al.* explored waste-based 3D printing materials, including rice husk ash and GGBS, for construction.[22] WASP developed a soil-based 3D printer incorporating rice husks and lime, enhancing stiffness through Si-O-Si bonding.[23] Nida *et al.* investigated guar gum-modified ground rice hulls for food packaging applications.[24] Another study examined the development of in situ mullite ($3Al_2O_3-2SiO_2$) foam using silica extracted from rice husk ash for high-performance applications.[25]

4.3.4 *Binder Jetting*

Binder Jetting Binder jetting forms 3D objects by layering powder and binding it with liquid. While material loss is minimal, post-processing is often required due to low strength. Zeidler *et al.* studied different binders for biomass-based components, finding that Miscanthus/PVA provided optimal results but lacked the mechanical strength of polymer-based materials. They suggested applications in food packaging but did not include rice husks, highlighting their potential for future research.[26]

5. **Articles on Materials for Particleboard Using Rice Husks**

Table 5: Original article on particleboard utilizing rice husks

Matrix	Binder	Treatment	Authors	Year
Rice husks/sawdust	Synthetic adhesives Fevicol/Ponal/Woodfix	-	Otieno *et al.* [27]	
Mixture of groundnut shell and rice husk particles	Cassava starch blended with urea-formaldehyde	-	Akin *et al.* [28]	2022
Mixture of insect rearing residue and rice particles	Citric acid/tapioca starch	-	Battistoni *et al.* [29]	2022
Rice husk particles/hemp fibers	Cornstarch	-	Huang *et al.* [30]	2018
Rice husk particles/hemp fibers	Cornstarch	Add ammonium dihydrogen phosphate to the binder	Battistoni *et al.* [31]	2018
Rice husk particles	Soy protein concentrate	Impregnate the board with tung oil	Nikolas *et al.* [32]	2020
Rice husk particles	Soy protein concentrate	Add two jute fabric layers to the board	Charapa *et al.* [33]	2020
Rice husk particles	Phenol-formaldehyde resin	Sandwiched between two wood strand layers	Jin *et al.* [34]	2013
Rice husk particles	Branched polyethylene imine and poly acrylic acid	Layer by Layer coating on rice husks	Battistoni *et al.* [35]	2017

Articles on Materials for Particleboard Using Rice Husks Particleboard is produced by hot-pressing wood chips with adhesives. However, deforestation and urea-formaldehyde's harmful effects raise concerns. Rice husks offer a sustainable alternative. Research articles on rice husk-based particleboards were reviewed using ScienceDirect and Springer, with all keywords included in the title. Table 5 summarizes the extracted studies by material, binder, and treatment.

Research on rice husk-based particleboards explores various material-binder combinations to enhance mechanical strength, water, and heat resistance. Olupot *et al.* found that adding sawdust improved low-density particleboards, using synthetic adhesives instead of traditional urea- or phenol-formaldehyde binders.[27] Akinyemi *et al.* combined agricultural waste, including peanut shells and rice husks, with cassava starch-urea-formaldehyde adhesive to create eco-friendly interior panels.[28] Huang *et al.* used insect breeding residues and rice husks with citric acid/tapioca starch binders, identifying ratios that met Japanese Industrial Standards (JIS).[29]

Studies on fiberboard and particleboard using rice husks and hemp fibers employed cornstarch as a binder. Hot-pressed fiberboard showed higher stiffness and load capacity, making it suitable for interiors.[30] Adding ammonium dihydrogen phosphate enhanced fire resistance, meeting flame-retardant standards.[31] However, rice husk boards often struggle with strength and performance, especially with natural adhesives.

To improve functionality, Nicolao *et al.* used soy protein binders and impregnated boards with tung oil for better water resistance.[32] Chalapud *et al.* reinforced boards with jute cloth layers, enhancing mechanical strength.[33] Kwon *et al.* adopted a wood strand sandwich structure, demonstrating a viable alternative to wood strand boards.[34] A unique layer-by-layer method, studied by Battegazzore *et al.*, applied vapor-deposited binders followed by hot pressing, achieving strong electrostatic bonding and sustainable performance using water-based solvents.[35]

Discussion:

Compared to common wood particleboards, and the focus is on how to reduce performance loss and maintain this within the standard. These studies have focused on improving properties such as mechanical strength and have not mentioned the workability of the material. In particular, there is no research on the machinability of CNC or laser cutters for these materials. Therefore, to promote the use of rice-husk-derived particleboard as a material for digital fabrication, it is necessary to evaluate its workability.

This research paper comprehensively reviews existing literature on the application of rice husks, particularly in architecture and product design domains. The survey results indicated a

prevalent focus on the incineration of rice husks to create ash utilized as a concrete filler, reflecting substantial interest since 2017 with an upward trend in research. This points to the method's potential for sustainable ash utilization. Moreover, it was recognized that rice husks could be transformed into various forms. Commonly, they serve as base materials or fillers, where valuable components such as silica and lignin are extracted for use. The choice of utilization method largely depends on the material performance, economic factors, regional yield, and the proportion needed for each application. Future research must address the volume of processed rice husks and evaluate the economic implications of each method.

Utilizing rice husk in 3D printing predominantly involves its integration as a filler in filaments for FDM printers—the most accessible types of 3D printers. Polylactic Acid (PLA) was frequently used as the primary polymer mixed with rice husk. Typically, adding natural fiber fillers has been observed to diminish the material's mechanical strength and durability. To mitigate these challenges, additives were introduced, although this impacts the overall cost. Future considerations must focus on material purpose versus cost, coupled with establishing uniform methods to measure and report filler particle size for better understanding material behavior.

Rice husks show promise as an addition to materials in cement extrusion printing, facilitating shape retention in mold-free 3D printing—an area still under development but expected to grow alongside 3D printing in construction. For Selective Laser Sintering (SLS), rice husks have potential; yet, challenges include the handling and environmental impact due to easily scattered powder materials. Comparing physical properties like particle size and specific gravity with those of conventional materials will be crucial for practical applications.

Extrusion printing techniques offer diverse applications but introduce issues such as material separation and changes state over time, influenced by the rheological properties of binders. Organic material integration can lead to contamination in the form of mold or corrosion, although using ash can mitigate these risks. Therefore, enhancing understanding of material aging, physical property deterioration before solidification, and designing easy-to-clean equipment will be vital for broadening the use of rice husks via this method.

Despite the digital fabrication trends, rice husks have been explored for use in particleboards, which generally show reduced mechanical properties compared to wood particleboards. The challenge revolves around minimizing performance degradation while maintaining standards. Research has primarily focused on enhancing mechanical strengths, yet fails to address the workability of these materials with tools like CNC or laser cutters. Thus,

deepening the investigation into the machinability of rice-husk-derived particleboards could promote their application in digital fabrication practices.

Conclusions:

The utilization of rice husks as materials for digital fabrication involves certain challenges and potential solutions, as summarized below.

Tailoring Applications to Material Properties

The integration of rice husk fibers with other pristine materials, such as polymer composites, often results in decreased performance. Although adding supplementary materials or treatments can enhance functionality, this may also raise costs. Thus, it's crucial to select applications that naturally align with the inherent properties of rice husks to optimize both functionality and cost-efficiency.

Assessing Long-term Performance and Equipment Maintenance

The consistency of the paste used in material extrusion can alter over time, potentially impacting the printing process due to residual materials in syringes or nozzle tips. Previous studies typically overlook the material's aging or operational issues, thus future research should focus on the longevity of material properties and equipment upkeep.

Machinability of Board Materials

When cutting rice-husk-based particleboard with CNC machines, the silica content of the material can reduce the lifespan of cutting tools and lead to surface peeling. This issue might be mitigated by minimizing the particle size or enhancing the adhesive properties, though significant reduction of silica content is not feasible. When using CNC machines, slower speeds or metal-specific end mills may be more effective. Additionally, processing with laser cutters requires examining the interaction between the rice husk components and laser beams. Investigating and optimizing processing conditions is vital for the broader application of these materials.

Despite these challenges, utilizing rice husks in building and industrial products represents a promising strategy for material recycling that helps manage agricultural waste and enable long-term carbon storage.

This analysis reflects current research trends concerning the digital fabrication use of rice husks, highlights potential applications, and outlines both the challenges and viable solutions. Advancing material research in digital fabrication will promote the further efficient use of agricultural waste, facilitating its broader adoption in architectural and product design sectors. This review aims to enrich the understanding and usage of rice husks within these fields.

References:

1. Morelli, M., Rios, C. D., Rowan, Z., & Charney, F. (2016). A framework for circular design theory. *Environmental Sustainability, 8*, 940.

2. Circular Economy and Materials Association, Ellen MacArthur Programme. (n.d.). Retrieved May 29, 2023, from https://www.ellenmacarthurprogramme.org/circle-economy-materials

3. United Nations Department of Agriculture and Food. (n.d.). Crop and livestock statistics, "UNAStats." Retrieved May 30, 2023, from https://www.una.org/unastats/en/#data/QCL

4. Nasir, N. N. A., Hossein, M. Z., Noor, A. M., Zainal, S. A., Rahim, D., Jamal, K. R., & Azizi, S. A. (2021). Mechanical properties of rice husk and coco peat in polymer composites. *Composite Materials, 13*, 1150.

5. Ludovic, L., Facio, D., Alvarado, V. A., & Stefano, P. M. (2011). Extraction of nanocellulose from rice husks by alkali methods. *BioMatter, 6*(4).

6. Shukla, S., Chavda, R., Apparao, S., Bahadurdeen, A., & Bala, K. V. R. (2022). Eco-friendly methods for rice husk utilization. *Journal of Green Chemical Engineering, 10*, 106870.

7. Karanja, S. W., Wanjiru, J., Kirira, M., & Muriithi, G. (2020). Utilizing crop residues in lignocellulose particleboard production. *Ecovisions, 6*, e04930.

8. Hashim, S. K., Abeed, A., Khalid, C. R., Maruf, S. M., & Layla, N. (2022). Review on the beneficial applications of rice husk ash in building materials. *Construction and Building Research, 345*, 127340.

9. Samadi, A., Monir, M. A. A., Alhaj, R., & Hossein, M. (2021). Comprehensive review on rice husk ash as a cement enhancement. *Journal of Structural University Engineering, 33*, 300–312.

10. Reynold, R. N., Lee, J. S., Chang, W. N., Tan, J. R., & Samson, Z. B. S. (2021). Challenges in using natural fiber composites in 3D printing. *Polymers in Printing, 13*, 2290.

11. Ashraf, W., Anwar, F., Zaidi, E., Al-Mansouri, A. H., Gomashe, M., & Sharif, S. (2020). Strategies for using natural fibers in 3D printing for sustainable materials. *Material Innovations, 13*, 4070.

12. Massimo, V., Lucio, M., & Fabrizio, M. (2019). A comprehensive overview of FDM 3D printing with natural polymer composites. *Composite Polymers, 11*, 1097.

13. Balaji, S., Krishna, K., Raj, A., Satler, A., Juraj, D., & Rinaldo, L. (2021). Challenges in 3D printing of eco-friendly biocomposites. *Advanced Material Applications, 24*, 101090.

14. Suresh, V., Fouladi, M. H., Namasivayam, S., & Sivaneshan, S. (2019). Development of acoustic panels using additive manufacturing with enhanced properties. *Journal of Mechanical Engineering, 2019*, 4546888.

15. Charles, T., Wendell, H. Y., Claire, W. C., & Wu, C. S. (2019). Renewable composite materials for 3D printing applications. *Research on Polymers, 26*, 230.

16. Wu, C. S., & Thomas, C. (2019). Investigations on biocomposites with PLA and rice husk for green applications. *Research on Polymers, 26*, 46.

17. Guen, M. L., Stefan, H., & Dave, S. (2019). Exploring biomass properties for 3D printing filaments. *Chemistry Frontiers, 7*, 740.

18. Morelos, M. A., Atencia, M. C. L., Marques, A., & Cortes, H. (2021). Composite filaments for 3D printing from rice husk and recycled polymers. *Polymers in Development, 13*, 1077.

19. Philip, H. Y., Chen, C., Wilson, Y., & Yuen, R. (2021). Terahertz properties of ABS composites with rice husk for 3D printing. *Optical Material Technologies, 11*, 2780.

20. Lim, H., Yijun, G., Song, S., & Jiang, L. (2022). Selective laser sintering of biocomposite materials. *Journal of Thermoplastic Composite Materials, 36*, 2300.

21. Kumar, M., Kuan, H. W., Yulian, L., & Charles, J. K. H. (2020). Properties of 3D printing materials containing rice husk ash. *Journal of Civil Materials, 32*, 04020199.

22. Palermo, M. (2022). Enhanced concrete strength through waste materials and 3D printing possibilities. In S. Singh, C. Prakash, & R. Kumar (Eds.), *Sustainable Innovations in 3D Printing* (pp. 150–160). Springer.

23. Ferrero, E., Moretti, M., Chieregato, A., Naldi, L., & Fabrizio, D. (2022). Long-term effects of rice husk on earthen mixtures for 3D printing. *Materials Engineering, 15*, 750.

24. Nina, S., Taniya, A., & Moses, J. A. (2021). 3D printing from milled rice husk fractions. *Waste Valorisation Journal, 12*, 95–105.

25. Husein, S. S., Baek, I. W., & Son, H. J. (2022). 3D printing of mullite ceramics from rice husk ash. *Journal of European Ceramic Society, 42*, 2400.

26. Zeidler, H., & Klemm, D. (2018). 3D printing using biodegradable and renewable materials. *Procedia in Manufacturing, 21*, 120–127.

27. Otieno, P. W., & Menge, E. (2022). Particleboard properties enhanced by sawdust and adhesive variations using rice husk. *Results in Engineering, 16*, 100780.

28. Akin, B. A., Kolawole, T. E., & Ademola, O. (2022). Particleboard manufacturing using blended adhesive with agricultural waste. *Clean Technology and Environmental Policy, 24*, 1660.

29. Battistoni, D., Alongi, J., & Duracci, D. (2018). High-density bio-based composite boards from agricultural residues. *Journal of Polymer Environmental Science, 26*, 1655.

30. Huang, H. K., Hsu, C. H., & Pai, K. H. (2022). Insect residue and rice husk particleboards using natural binders. *Bioresource Conversion and Refinement, 12*, 640.

31. Battistoni, D., Alongi, J., & Duracci, D. (2018). Reuse of hemp fibers and rice husks for fire-resistant boards. *Journal of Polymer Environmental Science, 26*, 3740.

32. Nikolas, E. S., Levi, P., & Chalapud, M. C. (2020). Mechanical properties of biobased particleboards. *Journal of Building Engineering, 30*, 101265.

33. Charapa, M. C., Helm, M., & Nikolaos, E. S. (2020). Rice husk based biobased particleboards and their oil impregnation effects. *Construction and Building Materials, 230*, 116999.

34. Jin, K., Ayrilmis, N., & Han, T. H. (2013). Improved mechanical properties of rice husk boards with wood strand layers. *Composites Part B: Engineering, 44*, 730.

35. Battistoni, D., Alongi, J., & Frache, A. (2017). Functionalized rice husk particles for sustainable particleboard production. *Materials Today Communications, 13*, 95.

CHARACTERIZATION OF Pr³⁺DOPED CdS NANOMATERIAL

Jitendra Pal Singh*[1], Sudha Pal[2], B. K. Singh[3], Vipin Kumar[3],

L. Anandaraj[4], Shujaat Ullah Khan[1] and Deepak Sharma[3]

[1]Department of Physics, School of Sciences, IFTM University, Moradabad-244102, India

[2]Department of Physics, Govt. P.G. College, Sitarganj, US Nagar Uttrakhand-262405, India

[3]Department of Mathematics & School of Sciences, IFTM University, Moradabad-244102,

[4]PG and Research Department of Physics,

Sacred Heart College (Autonomous), Tirupattur-635601, India

*Corresponding author E-mail: paljitendra124@gmail.com

Abstract:

Cadmium sulfide (CdS) Nanoparticles doped with praseodymium ion (Pr^{3+}) were synthesized by simple chemical precipitation method. The prepared $CdS:Pr^{3+}$ nanomaterial have been characterized by powder X-ray diffraction studies (XRD),(TEM),EDAX, and FTIR at room temperature. The $CdS:Pr^{3+}$nanomaterial exhibits spherical shape.

Keywords: $CdS:Pr^{3+}$ Nanomaterial, XRD, SEM, EDAX

Introduction:

The most common working definition of nanoscience and nanotechnology as given by the Royal society and Royal academy of engineering UK are as the following. "Nanoscience is the study of phenomena and manipulation of materials at atomic, molecular and macromolecular scales, where properties different significantly from those at a larger scale and nanotechnologies characterization production and application of structures devices and systems by controlling shape and size at nanometer scale"[2]. This intense interest in the science of the nanomaterials, which confined within the atomic scales, stems from the fact that this nonmaterial exhibit fundamentally interesting unique properties with great potentials of next generation technologies in CdS nanoparticles are known for their extensive applications dual semiconducting and luminescence properties and show a great promise in medical imaging and treatment of disease. Nano size particles of semiconductor materials have gained much more interest in recent years due to their desirable properties and applications in different areas such as catalysts [1], sensors [2], photoelectron devices [3, 4], electronics, computing, optics, biotechnology medical imaging, medicine drug delivery, structural materials, aerospace, energy etc. Semiconductor nanoparticles II-VI semiconductor are thus a type of compound semiconductors composed of group II and VI elements. Which have wide and direct band gap structures, are very important in many field, due

to their tunable electrical and optical properties[5,6]. In present research chapter, the Cadmium sulfide nanoparticles (CdS) doped with 0.1mol% praseodymium (Pr^{3+})ion were synthesized by chemical precipitation synthesis method and characterized by XRD, TEM, EDAX,FTIR.

Experimental Details

The CdS:Pr^{3+}nanomaterial were synthesized by simple chemical precipitation synthesis method.All the chemicals were of analytical gradeand were used without further purification. Cadmium nitrate tetrahydrate [Cd (NO3)2.4H2O], sodium sulphide [Na2S], diethylene glycol [DEG], ethanol [C2H5OH], praseodymium chloride [PrCl3] and distilled water were used as a source material.0.1M of Cd (NO3)2.4H2O (50ml) was taken in conical flask. Around 20 ml of diethylene glycol (DEG) was added to cadmium Nitrate tetrahydrate solution under constant stirring. After 15 minutes, 50 ml Sodium sulphide solution and (0.1 mol %) praseodymium chloride were added drop wise under constant stirring, reaction was kept 4hrs(at60^{0}C)at constant stirring and yellow precipitate of CdS formed,washed with ethanol and distill water, dried at room temperature[7,8]. The prepared samples were characterized by XRD, TEM, EDAX, and FTIR at room temperature. Characterization of CdS:Pr^{3+} nanomaterial have been done by courtesy of Indian Institute of Technology, Roorkee, India.

Figure 1: CdS doped Pr^{+3} Powder

Result and Discussion:

The CdS: Pr^{3+} nanomaterial have been synthesized by chemical precipitation synthesis method and characterized by XRD, TEM, EDAX Particle.

XRD patterns of nanoparticles were obtained using X-Pert Pro XRD spectrometer (P analytical B.V. Holland) from 10 to 80 degree (2Ө) value using Cu K-α radiation wavelength- 0.15418nm[9,10]. The XRD spectrum of CdS:Pr^{3+} nanomaterial doped with 0.1 mol % Pr^{3+} ion is shown in Fig 2. The synthesized particles produce highly intense X- ray reflections in their corresponding XRD pattern indicating that all the materials are crystalline in nature. Fig.2 is suggesting that incorporation of Pr^{3+}ion in the sample not introduce appreciable changes in

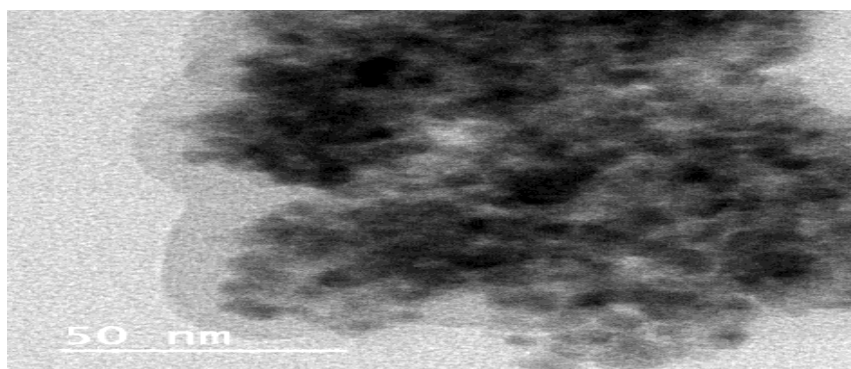**XDR Spectra**
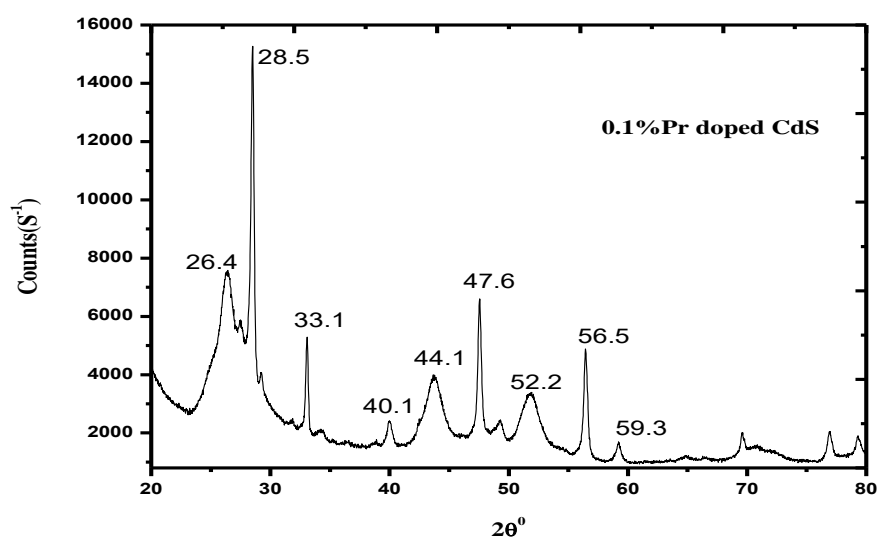

Figure 2: XDR Spectra Pr³⁺ doped CdS nanomaterial

TEM Micrograph

The crystal structure of CdS.TEM images of the CdS nanoparticles are shown in Fig .3.Nearly Spherical shapes for the dark spots in the images indicate that the CdS nanoparticles are almost spherical[11,12]. The estimated average particles size is 50nm.

**Figure 3: TEM micrograph CdS nanomaterial with of Pr³⁺ion**

EDAX spectrum
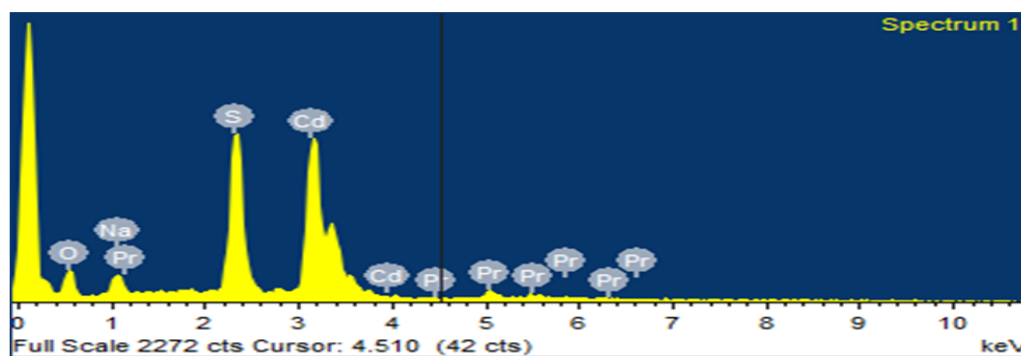
Figure 4: EDAX spectrum of CdS nanomaterial with Pr³⁺ ion

The EDAX spectrum of CdS:Pr^{3+} nanomaterial doped with0.1mol% praseodymium ion is shown in fig. 4. These spectra reveal that all the elements are present in the final composition which is take initially.

FTIR spectra

Infrared spectrum is formed as a consequence of the absorption of the absorption of the electromagnetic radiation at frequency that vibration of specific sets of chemical bonds within a molecules. The experimental in formed pattern is show in range of 4000cm^{-1}, show in fig.5.
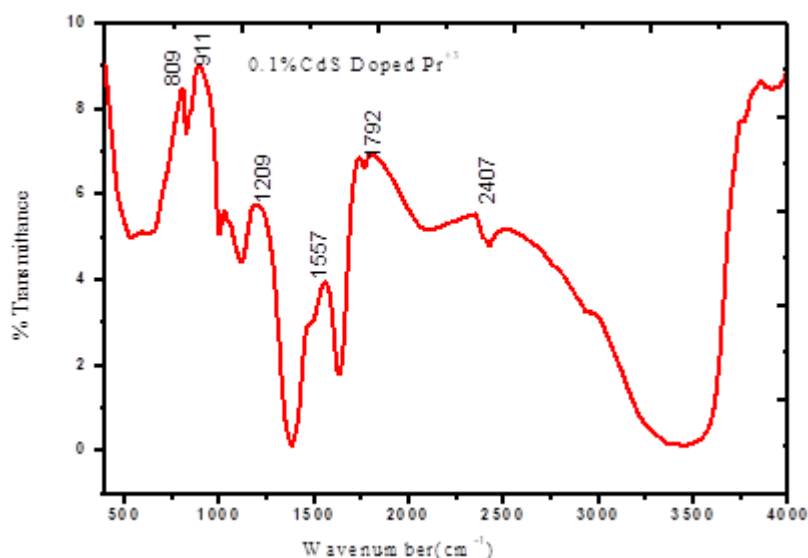
Figure 5: FTIR spectrum of CdS nanomaterial with 0.1mol%Pr^{3+} ion

FTIR spectra is very much useful for structural analysis. The present of hydrogen and Oxygen is the useful characteristic CdS doped Pr^{3+}(0.1mol %) in all infrared group. The absorption peak in the range of 3201-3326 could be attributed to the –OH group of water absorbed by samples. The peak around1622-1644cm^{-1} is assigned to the asymmetric stretching vibration of Cd-S bond from sulfur group. The peak in range 540-612 cm^{-1}are due to Pr^{3+} bond doped CdS nanoparticles.

Conclusions:

The CdS nanoparticles doped with 0.1 mol% of Pr^{3+} ion means a nanomaterial have been prepared by a simple cost effective and eco-friendly precipitation chemical synthesis method. Structural and morphological composition were studied after a successfully synthesis and characterized by using different techniques such XRD TEM, FTIR and EDAX. The XRD study revealed the spherical wurtzite structure without second phase. The TEM images confirmed the spherical morphology of the nano materials.

References:

1. Bokatial, S. R. (2010). Optical properties and up-conversion of Pr^{3+} doped CdS nanoparticles in sol-gel glasses. *Journal of Luminescence, 130*, 1857-1862.

2. Tran, T. Q. H., Hoang, M. H., Do, T. A. T., Le, A. T., Nguyen, T. H., Nguyen, T. D., & Man, M. T. (2021). Nanostructure and photoluminescence dynamics of praseodymium doped hexagonal LaF_2 nanocrystals. *Journal of Luminescence, 237*, 118162.

3. Srivastava, A. M. (2016). Aspects of Pr^{3+} luminescence. *Journal of Luminescence, 169*, 445-449.

4. Goyal, P., Sharma, Y. K., Pal, S., Bind, U. C., Huang, S. C., & Chung, S. L. (2018). Radiative properties of Er^{3+} doped borosilicate glasses for fiber optics application. *Materials Today: Proceedings, 5*, 344-350.

5. Sharma, Y. K., Goyal, P., Pal, S., & Bind, U. C. (2016). Laser action in praseodymium doped borosilicate glasses in the visible region. *Journal Name, 3*, 1031-1035.

6. Pal, S. (2016). *Synthesis and characterization of nanomaterial with rare earth ions* (Doctoral dissertation, Kumaun University, Nainital, India).

7. Bykkam, S., Ahmadipour, M., Narisngam, S., Kalagadda, V. R., & Chakrachidurala, S. (2015). Extensive studies on X-ray diffraction of green synthesized silver nanoparticles. *Advances in Nanoparticles, 4*, 110.

8. Bykkam, S., Ahmadipour, M., Narisngam, S., Kalagadda, V. R., & Chakrachidurala, S. (2015). Extensive studies on X-ray diffraction of green synthesized silver nanoparticles. *Advances in Nanoparticles, 4*, 110.

9. Wu, J., Liu, Q., Gao, P., & Zhu, Z. (2011). Influence of praseodymium and nitrogen co-doping on the photocatalytic activity of TiO_2. *Materials Research Bulletin, 46*, 1176-1183.

10. Nath, D., Singh, F., & Das, R. (2020). X-ray diffraction analysis by Williamson-Hall, Halder-Wagner and size-strain plot methods of CdSe nanoparticles—a comparative study. *Materials Chemistry and Physics, 239*, 122021.

11. Sarkar, S., & Das, R. (2018). Determination of structural elements of synthesized silver nano-hexagon from X-ray diffraction analysis. *Indian Journal of Pure and Applied Physics, 56*, 765-772.

12. De, M., & Sen Gupta, S. P. (1984). Lattice imperfection studies in polycrystalline materials by X-ray diffraction line profile analysis. *Pramana, 23*, 721-744.

THERMAL ANALYSIS AND SIMULATION OF FRICTION WELDING FOR METALLIC POLYMER COMPOSITES

Senkathir S*, S. Muralidharan and A. C Arunraj

Department of Mechanical Engineering, College of Engineering and Technology,

SRM Institute of Science and Technology, SRM Nagar,

Kattankulathur - 603 203, Chengalpattu District, Tamil Nadu

*Corresponding author E-mail: senkaths@srmist.edu.in

Abstract:

Poly-Ether-Ether-Ketone (PEEK) is a versatile polymer with strong mechanical properties, making it ideal for aerospace, electronics, and medical implant applications. PEEK-Al, composites enhance these properties, making them suitable for aerospace, electronics, and medical implant applications. Rotational Friction Welding is a superior joining solution that ensures high strength and joint quality while minimizing energy consumption and the need for additional materials. This research aims to develop a rotational friction welding simulation model for PEEK-Al using standard welding parameters for thermal analysis. The results will help identify optimal welding parameters and conditions for various composite materials. The research establishes the foundation for simulation and thermal analysis of the Rotational Friction Welding process for selected PEEK-metal composites.

Keywords: Friction Welding Process; FWP; PEEK; PEEK-Al.

Introduction:

Poly-Ether-Ether-Ketone (PEEK) is a highly versatile polymer material that combines various properties such as high mechanical resistance, wear resistance, chemical resistance, light weight and good electrical insulation. Due to its low melting point PEEK or PEEK composites cannot be joined efficiently through many processes without having large amounts of material usage (eg: fasteners). The Rotational Friction Welding process is used in this case as it provides a strong joint between PEEK parts without requiring high energy use or fasteners, and friction welding process results in stronger joint strength compared to other weld processes. The friction welding process also eliminates the need for filler materials unlike traditional welding methods. Other benefits of rotational friction welding include localized heat affected zone, ie the heat generation is limited to the weld area and does not spread to other areas of the parts. Thus, it is highly suitable for joining of polymer or metallic polymer composite materials Composite materials such as PEEK-Aluminium, PEEK-Copper, PEEK-Titanium enhance specific properties

of PEEK such as mechanical strength, chemical resistance, thermal resistance, electrical conductivity, etc. which make them highly suitable for more specific applications where a large degree of optimization is required in material properties. Simulation of friction welding allows for a cost-effective method of analysing the welding process and outcome for the required material. Use of advanced Finite Element Analysis methods can help provide a highly accurate simulation which can be comparable to experimental results. Employing a variable speed rotational friction welding procedure rather than a constant speed process results in a higher level of efficiency when connecting PEEK material [1] While the RFW process was shown to have a lower peak temperature in comparison to other joining processes, the study underlines the association between peak temperature and the quality of the weld produced by the material.[2] how weld quality and other metrics are affected by friction time. And it gives you a way to figure out the best friction time by taking important aspects into account.[3] Fusion bonding techniques enable superior quality in the joining of thermoplastic materials. Minimize surface preparation and remove stress from mechanical fastening. Fusion bonding proves effective for joining dissimilar materials.[4] Abaqus software, in conjunction with FORTRAN and Python, is utilized to execute a sophisticated friction welding simulation employing Inconel 718 material. The results of thermal analysis and microstructure analysis are presented accordingly.[5] Modifying the rotational speeds in rotary friction welding of PEEK rods significantly improves bending strength by up to 140% and decreases cycle time by 6%. Peak temperatures reaching 377°C, exceeding PEEK's melting point, greatly enhance weld quality. The utilization of a CNC lathe in conjunction with measurement tools demonstrates that variable speeds improve weld properties in comparison to fixed speeds.

The forecasts regarding peak temperatures in rotary friction welding, as analyzed through COMSOL software, indicate an average error of 15°C. Increasing rotational speed enhances mechanical properties, including bending strength and impact energy. Determining the optimal friction time is crucial for producing high-quality welds and facilitating efficient solder joint formation. Numerical simulations explore heat transfer and the heat affected zone to refine welding conditions, with experimental validation confirming the accuracy of these simulations and the proposed parameters. Fusion bonding techniques, such as ultrasonic and induction welding, efficiently unite thermoplastic composites by reducing the need for surface preparation and allowing for the integration of dissimilar materials, even when their properties vary. There is a significant lack of thorough investigations into the friction welding of metallic polymer composites, particularly those incorporating varying PEEK content alongside Al,The current literature does not provide thorough insights into heat generation during the friction welding

process of these specific composite materials. This investigation explores the friction welding of PEEK-metal composites with different PEEK content, focusing on thermal analysis and heat generation to improve weldability. The aim is to create a simulation for friction welding involving PEEK -Aluminium, Copper, and Titanium metallic polymer composites, with varying PEEK content, using Abaqus software. The aim is to explore heat generation and perform a thermal analysis within the framework of friction welding simulation. The aim is to determine the optimal boundary conditions and parameters that will produce the highest weld quality and energy efficiency for the chosen materials.

Experimental Setup and Methodology:

1. Methodology

Figure.1 outlines the steps involved in simulating friction welding. It begins with designing a 3D model of cylinders using CAD software. The model is then transferred to Abaqus CAE software, where material properties are defined. After that, essential parameters and boundary conditions for friction welding are established, followed by running the simulation. Lastly, the generated results are examined to assess heat production, and necessary adjustments are made to enhance weld quality and energy efficiency.
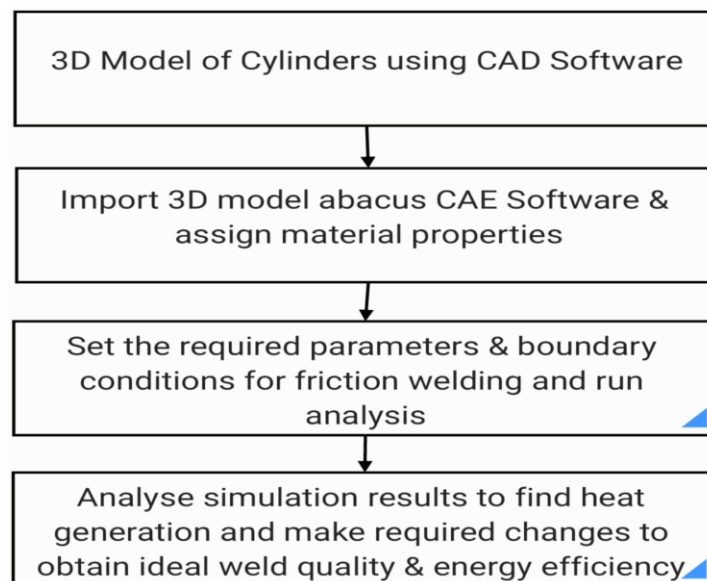
Figure 1: Methodology used for the Composite analysis

2. Material Properties

The simulation is carried out for composites made of PEEK-Aluminium, PEEK-Copper, and PEEK-Titanium. A total of four different material combinations are utilized for each composite, with the percentage of metal ranging from ten to twenty to thirty to forty percent for all composite materials. The Rule-of-Mixture approach is utilized in order to compute the material properties that can seen in Table 1. This method makes use of the volume % distribution

of the materials in order to make predictions regarding the material properties of composites by utilizing the property values of the individual materials that are present in the composite.

Table 1: PEEK-Aluminium Material Properties

PEEK %	Al %	Density (g/mm³) (xE-03)	Young's Modulus (N/mm²)	Poisson's Ratio	Thermal Conductivity (W/m degC) (xE-03)	Thermal Co-eff Expansion (/degC) (xE-05)	Specific Heat Capacity (J/g degC)
90	10	1.44	10130	0.375	3.6	4.46	1.35
80	20	1.58	16560	0.37	3.201	4.22	1.3
70	30	1.72	22990	0.365	2.801	3.98	1.25
60	40	1.86	29420	0.36	2.402	3.74	1.2

3. Experimental Setup

3.1 Dimensions and Parameters

The simulation model uses two cylinders of the following dimensions are in Table 2 and the friction welding parameters used are as in Table 3:

Table 2: PEEK-Aluminium Model dimension

Cylinder 1 (Load Cylinder)	Value
Diameter	25mm
Length	150mm
Cylinder 2 (Load Cylinder)	
Diameter	25mm
Length	250mm

Table 3: Welding Parameters

Parameter	Value
Spindle Speed	800 rpm
Soft Load	400 N
Soft Load Time	6 sec
Friction Load	450 N
Friction Load Time	30 sec
Forge Load	100 N
Forge Load Time	8 sec
Cooling Time	7 sec

3.2 Defining Model and Properties
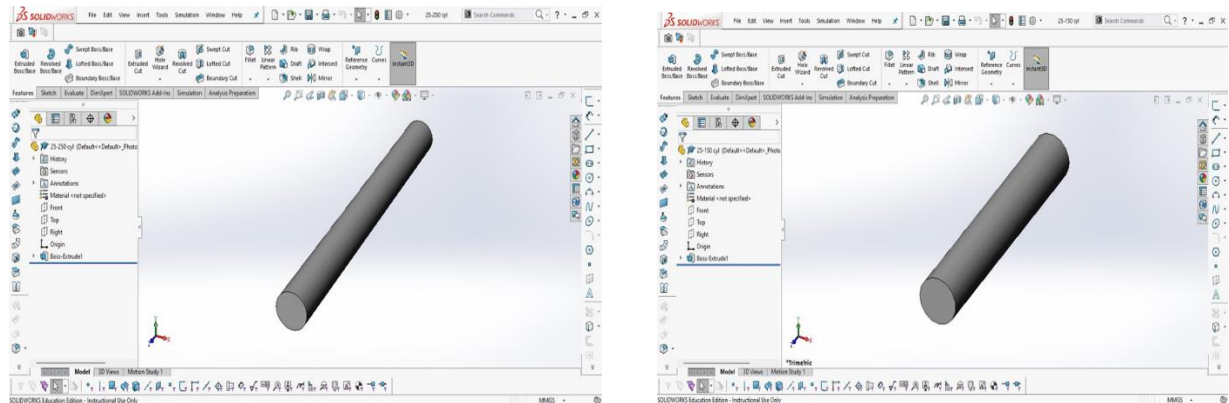
Figure 2: CAD Model 1 and 2

SolidWorks 2017 CAD software is used to create the model of cylinders as shown in figure.2. The CAD model is imported into Abaqus CAE software and Material Property is defined as follows: Material property of PEEK-Al composites is young modules, passion ratio and specific heat   calculated by rule of mixture The defined properties are assigned using a Section module which assigns the material properties to the selected geometry. The two cylinders are aligned using assembly module, which is depicted in figure.3
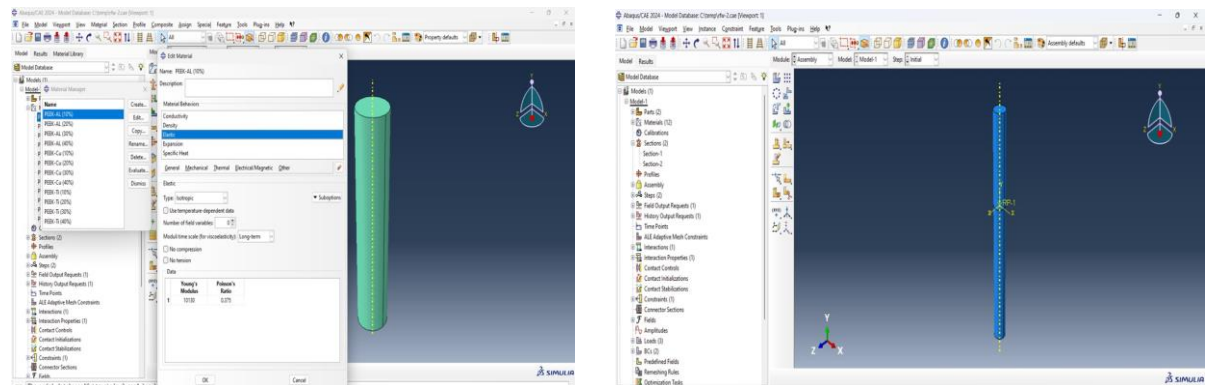
Figure 3: Material Property input and assembling

3.3 Boundary Conditions

In addition to the increments that are set for each step, the time length of each step is defined by utilizing the step module. It is the surface-to-surface type interaction that is selected, which results in the interaction type being generated between the contact surfaces. For the purpose of defining friction and other attributes between the contact surfaces, the interaction property is utilized instead. Using load management, the active load on each step is assigned to individual steps. The mesh is defined in the following manner for both cylinders (defining the mesh specifically for each cylinder provides for more mesh accuracy than meshing the assembly combined). The pixel size is 0.25, and the mesh parameters are a tetrahedron configuration. The type of element is chosen so that the analysis may carry out calculations for the combined

temperature and displacement of the elements that are provided which are shown in figure.4
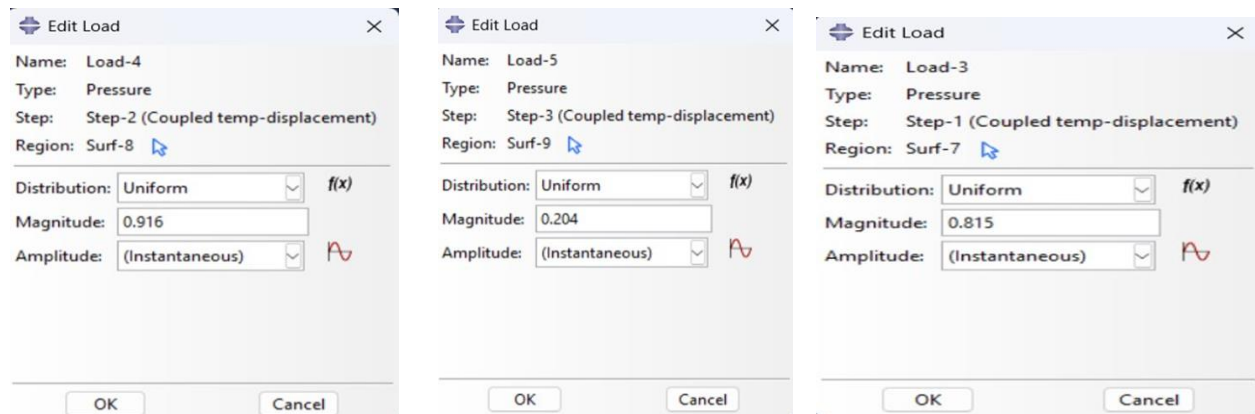
Figure 4: The active load on each step is assigned using load manager

Results and Discussion:

The following simulation results were found for PEEK-Al composite in show in Figure 5. The graph shows us the working temperature during friction welding process is same for all the composites (Figure.6). The Abaqus CAE software was utilized in order to carry out the simulation of Rotational Friction Welding for PEEK-Aluminium composites with metal compositions of 10%, 20%, 30%, and 40%. The Rule-of-Mixture equations were utilized in order to ascertain the parameters of the composite material. Throughout the entirety of the welding process, including the Soft Load, Friction Load, Forge Load, and Initial Cooling stages, the nodal temperatures were continually monitored and recorded. The results that were obtained can be employed to ascertain the amount of heat that is generated during the welding process or any single phase for the particular model, material, and welding parameters that have been specifically selected.
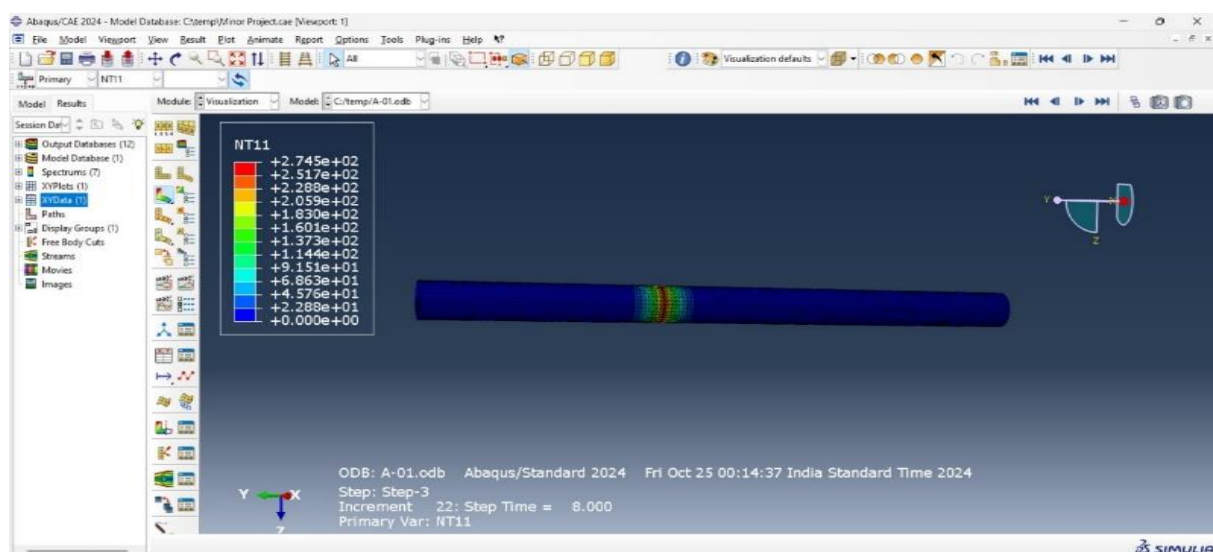
Figure 5: simulation of composite

During the welding process, the nodal temperature values can be used to identify

additional thermal properties by employing appropriate FEA equations. These equations can determine the optimal weld parameters for the material in question, which in turn can improve the efficiency of the process and result in stronger joints and welds of superior quality. PEEK-Al is exploited in a significant manner in the field of aviation applications. Temperature is measured for all four compositions of composites in different welding span
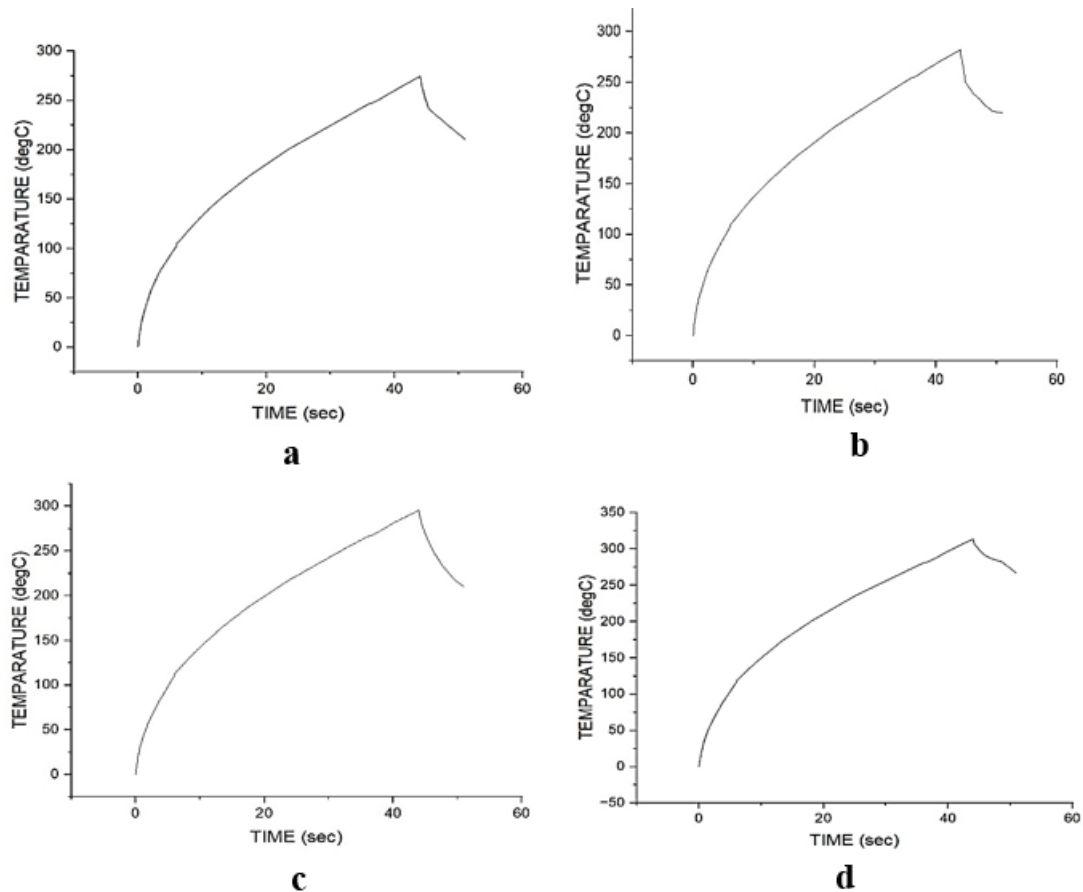
Figure 6: (a) 40% PEEK-Al Graph   (b) 40% PEEK-Al Graph

(c) 40% PEEK-Al Graph   (d) 40% PEEK-Al Graph

Conclusion:

The following conclusion were obtained from this study.

- Utilizes a FEA technique for optimizing the welding process of polymer materials.
- Current model uses basic parameters and boundary conditions. Future work could include increasing mesh density and adjusting mesh type and configuration. More over current boundary conditions could be improved for better accurate simulation results.
- Advanced Finite Element Analysis techniques could be used to refine the model and programming languages like Python and FORTRAN could be used to compare simulation models with experimental outcomes.

References:

1. Kuo, C.-C., Liang, H.-X., Huang, S.-H., & Tseng, S.-F. (2023). Rotary friction welding of polyetheretherketone biopolymer rods using variable rotational speed. *Polymers, 20*(15), 4077.

2. Kuo, C.-C., Gurumurthy, N., Chen, H.-W., & Huang, S.-H. (2023). Experimentation and numerical modeling of peak temperature in the weld joint during rotary friction welding of dissimilar plastic rods. *Polymers, 9*(15), 2124.

3. Abdi, S., Chikh, S., & Djamel, M. (2017). Thermal analysis during a rotational friction welding. *Applied Thermal Engineering, 110*, 1543-1553.

4. Ageorges, D. C., Ye, L., & Hou, M. (2001). Advances in fusion bonding techniques for joining thermoplastic matrix composites: A review. *Composites Part A: Applied Science and Manufacturing, 32*(6), 839-857.

5. Mani, H., Taherizadeh, A., Sadeghian, B., & Cavalier, P. (2024). Thermal-mechanical and microstructural simulation of rotary friction welding processes by using finite element method. *Materials, 17*(4), 815.

EXPLORING THE BIOLOGICAL POTENTIAL OF 1,3,4-THIADIAZOLE DERIVATIVES: MECHANISMS, ACTIVITIES, AND THERAPEUTIC APPLICATIONS

Bharti Bansal and Monika Gupta*

Amar Shaheed Baba Ajit Singh Jhujhar Singh Memorial College of Pharmacy,

Bela, Ropar, India

*Corresponding author E-mail: monikaguptaa@gmail.com

Abstract:

Thiadiazole is a heterocyclic compound which contains carbon, nitrogen and sulfur atoms in its five-membered ring. The thiadiazoles have various isomers such as 1,2,4-thidiazole, 1,2,5-thiadiazole, 1,2,3-thiadiazole and 1,3,4-thiadiazole, these isomers are widely recognized for their diverse biological activities. In these days, 1,3,4-thiadiazole is widely used in medicinal chemistry, as this scaffold exhibits remarkable physicochemical properties such as solubility, stability, and electronic characteristics, to make this scaffold more valuable in medical sciences.1,3,4-thiadiazole derivatives exhibits a wide range of biological activities such as anti-cancer, anti-proliferative, anti-convulsant, anti-hypertensive, anti-diabetic or anti-inflammatory and anti-alzheimer activity. As this scaffold used in medicinal as well as pharmaceutical sciences they are also used in agrochemical, corrosion inhibitors and dyes. This chapter highlights the importance of 1,3,4-thiadiazole derivatives in modern science and technology by studying their biological activities and structural characteristics, functionalization, and wide range of applications.
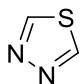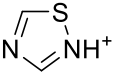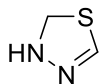
Keywords: 1,3,4-thiadiazole, Anti Diabetics, Anti Convulsant, Anticancer, Anti-Alzhiemer's and Anti Tubercular Thidaizole Derivatives

Introduction:

Ring-shaped compounds made up of carbon, nitrogen, sulfur, and oxygen are known as heterocyclic compounds. Pyrrole, furan, and thiophene are examples of heterocyclic compounds with a single non-carbon atom; triazene, azole, thiazole, thiadiazole, oxadiazole, and other heterocyclic molecules have multiple non-carbon atoms(Wassel *et al.*, 2021) . 1,3,4-thiadiazole has become a crucial research topic because of its intriguing pharmacological and biological characteristics. The various substituted derivatives, or variations, of the 1,3,4-thiadiazole molecule are of special interest to researchers (Serban *et al.*, 2018).
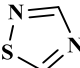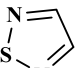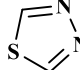
A class of five-membered heterocyclic compounds known as 1,3,4-thiadiazole is important in medicinal chemistry due to its wide range of biological activities. Among the many biological activities that can be developed using the 1,3,4-thiadiazole scaffold are antimicrobial, anticonvulsant, anti-cancer, antibacterial, anti-oxidant, anti-hypertensive, anti-diabetic, anti-leishmanial, anti-histamine, anti-depressive, anti-tubercular, anti-tumor, anti-proliferative, and anti-inflammatory compounds.(Mohamed *et al.*, 2022).

Table 1: 1,3,4-Thiadiazoles are classified into three main subclasses based on their electronic structure and aromaticity (Sharma *et al.*, 2013)

Sr. No.	Subclasses	Key Aspects	Examples
1.	Aromatic Thiadiazoles	The most common type. Stable and aromatic structures. E.g.:1,3,4-Thiadiazole.	1,3,4 thiadiazole
2.	Mesomeric Thiadiazoles	A system of delocalized electrons. Unique reactivity. E.g.: 1,2,4-Thiadiazolium salts	1,2,4-thiadiazolium
3.	Non-Aromatic Thiadiazoles	Forms with partial reductions. Conjugation variations. E.g.: 1,3,4-Thiadiazoline	1,3,4-thiadiazoline

In 1,3,4-thiadiazole derivatives the presence of N-C-S moietymustcontributein various biological properties.There are other different four isomeric forms thiadiazoles such as 1,2,5-thiadiazole, 1,2,4-thiadiazole, 1,2,3-thiadiazole and 1,3,4-thiadiazole. Because of its wide range of pharmacological activities, 1,3,4-thiadiazole is the most well-known and studied heterocyclic nucleus among them. Thiadiazoles have also been used in a variety of industries, such as plastic, dye, and polymer manufacturing, as well as agriculture (Kumar *et al.*, 2020).

Table 2: Different forms of thiadiazole along with their uses and annotations (Tokareva *et al.*, 2024)

Sr. No.	Thiadiazole	Annotations	Applications
1.	1,2,4-thiadiazole	A five-membered heterocyclic ring consists carbon, nitrogen and sulfur atoms. Having stable e⁻ arrangement&are aromatic in nature. Commonly found in a variety of bioactive substances.	Used in pharma-ceutical industries for creating anti-viral, anti-tubercular &anti-cancer drugs. Utilized in agro-chemicals as fungi-cides &herbicides.
2.	1,2,5- thiadiazole	A five-membered ring with nitrogen atom opposite to the sulfur atoms at positions 1 & 2. Compared to other isomers, they are less common.	Useful in electro and photochemical applications. Useful in electronic and optical materials.
3.	1,2,3-thiadiazole	A five-membered ring with two adjacent nitrogen atoms and one sulfur atom. Exhibits aromaticity because of delocalizedπ-electrons,less stable.	Intermediatesin organic synthesis. Useful as a potential for anti-microbial & anti-inflammatory properties.
4.	1,3,4- thiadiazole	A highly stable five-membered heterocyclic ring with a sulfur atom consisting of two nitrogen atoms. Chosen due to its higher aromaticity, stability& adaptability	Used to create anti-bacterial, anti-cancer&anti-diabetic drugs. Used in polymer and material's chemistry due to their e⁻donating properties.

Properties Of 1,3,4-Thiadiazole

Table 3: Chemical and physical characteristics of 1,3,4-thiadiazole

Properties	1,3,4-Thiadiazole
Chemical formula	5-membered heterocyclic ring that contains carbon sulfur and nitrogen
Molecular formula	$C_2H_2N_2S$
Functional group	Possibly substitution at C-5 and C-2 in thiadiazole ring
Pharmacokinetics	Moderate solubility, metabolized in the liver, excreted renally
Biological activities	Antimicrobial, anti-inflammatory, anti-convulsant, anti-cancer, anti-hypertensive
Physicochemical properties	Polar, Aromatic and e⁻-rich
Toxicity	Low to moderate, can cause hepatotoxicity in some cases
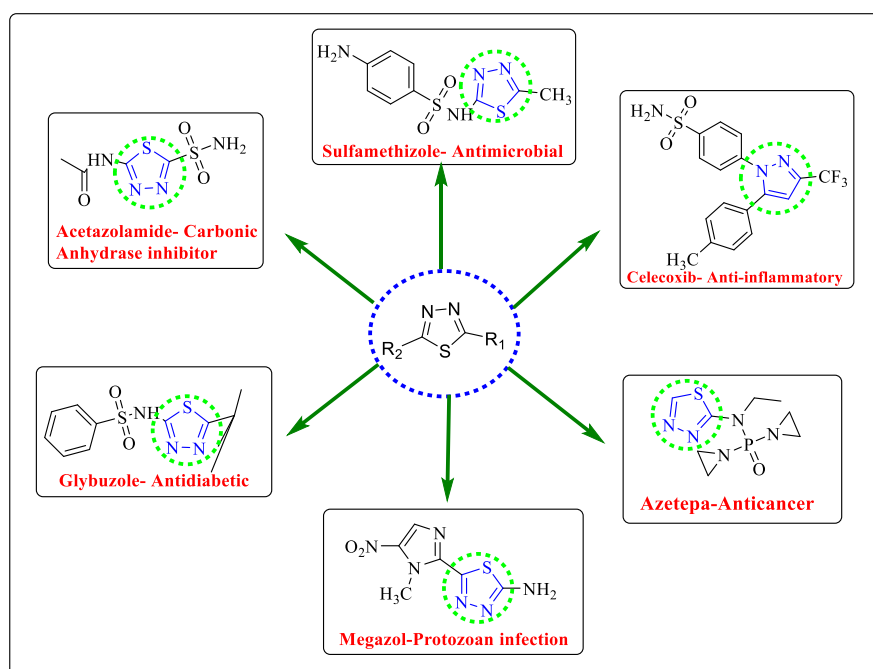
Figure 1: Various marketed drugs containing 1,3,4-thiadiazole

Biological Activities

Anti-Diabetic Activity

The most common and chronic metabolic disease, Diabetes Mellitus (DM) which is basically identifies by higher blood glucose level in the body. The insufficient level of blood glucose levels in the body is the major sign of diabetes mellitus, a condition which is caused by an excessive intake of carbohydrates which also affects the insulin secretion(Hasan *et al.*, 2023) . According to recent studies, diabetes mellitus, an increasingly common condition, affects 20% of

people worldwide. Patients with type-2 diabetes are initially treated and managed primarily with dietary and lifestyle modifications, whereas those with type-1 diabetes are primarily treated with insulin. In type-2 diabetes mellitus, insulin is essential when blood sugar levels cannot be controlled by diet, exercise, weight loss, or oral medications. People with diabetes are most likely to have type-2 diabetes. Simple lifestyle modifications can help prevent type-2 diabetes and its complications. Inhibiting the enzymes α-amylase and α-glucosidase (starch hydrolases) is one way to manage diabetes mellitus by controlling the digestion of starchy foods(zahid ali, wajid rehman, 2024).

Mechanism of Action
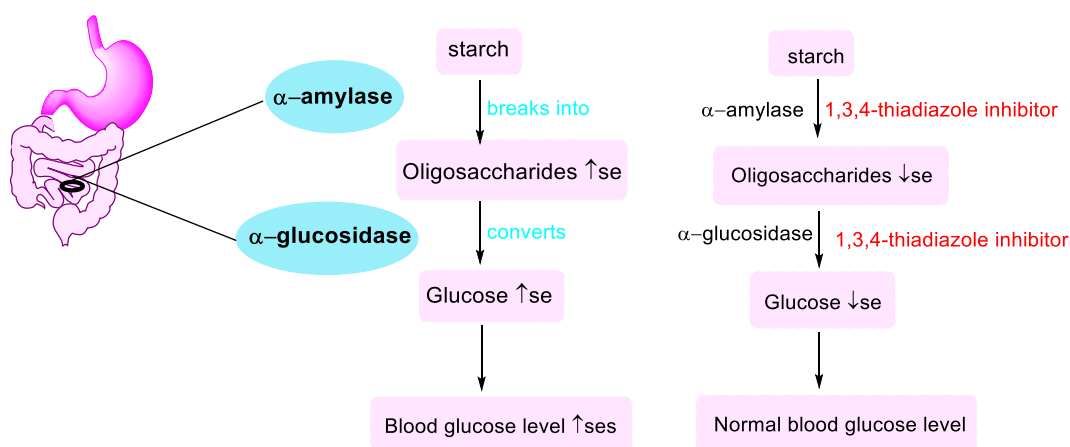
Figure 2: Inhibition of α-amylase and α-glucosidase enzymes by 1,3,4-thiadiazole

Ali, Z., Rehma, *et al.* (2024) they have worked out for the synthesis of 2-hydrazinyl-5-(4-nitrophenyl)-1,3,4-thiadiazole-bearing Schiff base derivatives investigating against their inhibition of α-glucosidase enzyme. All over, a novel series of (1-12) derivatives are synthesized and among of them, compound **3**demonstrated excellent inhibition against α-glucosidase enzymes with an IC_{50} value between 18.10 ± 0.20 and 1.10 ± 0.10 μM(Zahoor *et al.*, 2024).
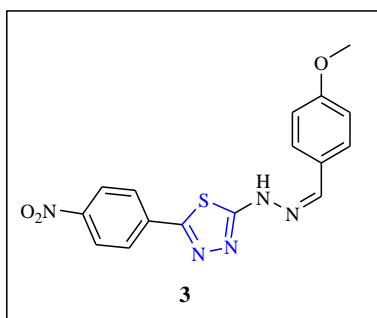

Abbasi, S. A. *et al.* (2024) have prepared thiadiazole-bearing thiosemicarbazide (**1 - 20),**and studied the anti-diabetic activity by inhibiting the α-amylase and α-glucosidase enzymes. Out of all the produced analogues, the analogue**19** showed the greatest potency(Abbasi *et al.*, 2024)**.**
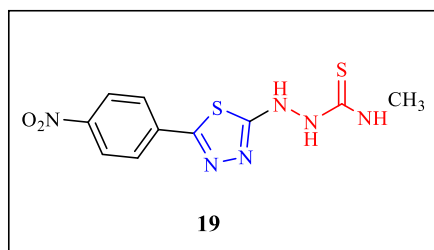
Anti-Cancer Activity

A serious and complicated human disease, Cancer i.e. characterized by uncontrolled cell proliferation which may also having the ability to spread other areas of the body. According to the recent studies, it is acknowledged as the World's second most common cause of death.one out of every six fatalities is due to Cancer. In worldwide, about 18.1 million people received a cancer diagnosis in 2018, and by 2040, the figure is predicted to rise to 29.4 million. There are also various treatments methods, access to therapy, treatment sustainability, and also lifestyle plays the significant role in this distribution, which is why this number varies throughout nations(Serag *et al.*, 2025).

Mechanism of Action
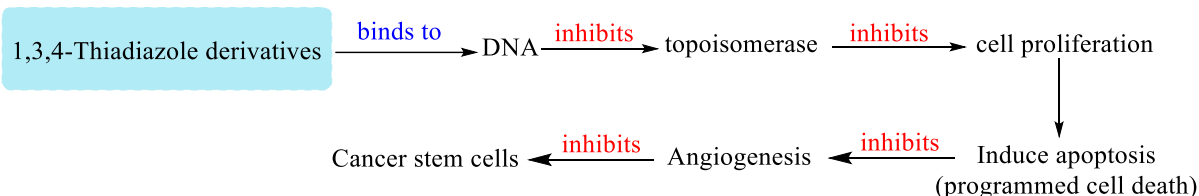
Figure 3: Anticancer Activity Mechanism of Thiadiazoles.

Kalagara, S. *et al.* 2025 synthesized a novel series of aryl substituted indole-1,3,4-thiadiazole derivatives **(10a–j).** These compounds were synthesized for investigating their anti-cancer properties against four human cancer cell lines like MCF-7 (breast cancer), A549 (lung cancer). Among the synthesized compounds, three compounds **10a**, **10b** and **10c** displayed more cytotoxic activity than positive control.(Kalagara *et al.*, 2025)
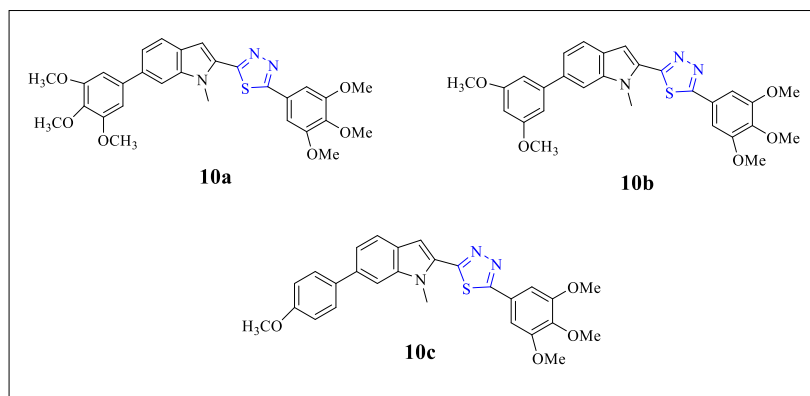
Kamel, M. G. *et al.* 2024 synthesized fifteen new pyrazole compounds bearing chalcone (4–10), thiazole (16–19) and thiadiazole (23–26) moieties. Three pyrazolyl-chalcone derivatives (4, 5, and 7) and a pyrazolyl-thiadiazole derivative **(25)** showed potent anti-cancer activity against the PaCa-2 cell line. Compound 25 showed potent anti-cancer activity against the PC3 cell line with an IC_{50} value of 11.8 mg mL^{-1}. Compound **25** exhibited the strongest anti-cancer effect among them against the PC¬3 cell line, with an IC_{50} value of 11.8 μg mL^{-1}.(Kamel *et al.*, 2024)

25
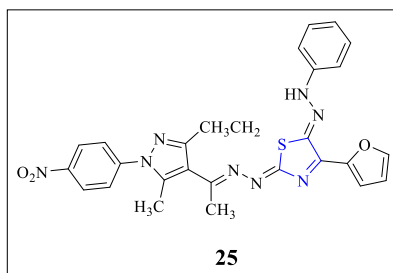
Anti-Alzheimer's Activity

The primary cause of dementia and one of the most prevalent neurodegenerative diseases is Alzheimer's disease (AD). The patient first experiences mild cognitive impairment before all aspects of their life functions is gradually affected.The primary cause of dementia and one of the most prevalent neurodegenerative diseases is Alzheimer's disease (AD). The patient first experiences mild cognitive impairment before all aspects of their life functions is gradually affected. The one degenerative disease which is more common in older adults is Alzheimer's. The WHO estimates that 82 million populations will suffer from dementia in 2030 or in 2050 there will be152 million, with AD accounting for 60-70% by these cases. By 2050, there will people be 106.2 million cases globally with 1 in 85 people having AD. Acetylcholine is actually a neurotransmitter i.e. linked to Alzheimer's disease (AD) and is necessary for cognitive function. Acetylcholine has an effect on several brain functions, including focus, memory and learning. In Alzheimer's disease, certain areas of the brain, particularly these involved in memory and cognition, gradually lose their acetylcholine- producing neurons.(Cebeci *et al.*, 2024)

Mechanism of Action
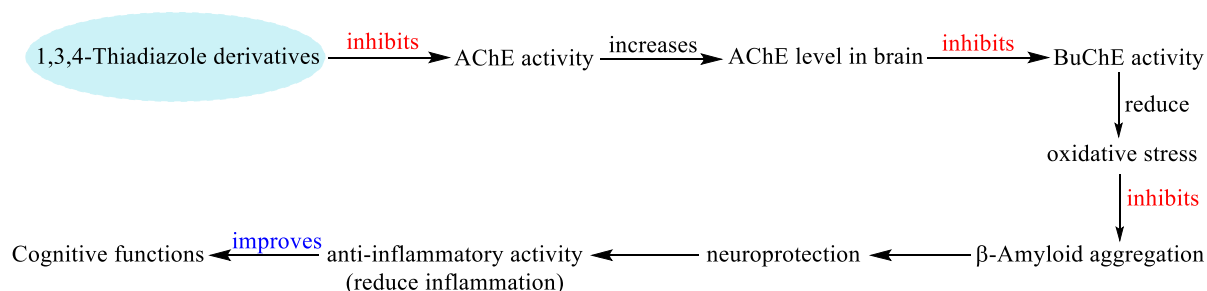
Figure 4: 1,3,4-Thiadiazole derivatives inhibiting enzymes for treating Alzheimer's Activity

Kaya, B. *et al.* 2024 were produced five new thiadiazole analogs and their anti-cholinesterase activity assessed for finding anti-alzheimer medicines. Out of all the synthesized analogues the compound **6e** has the greatest inhibition against both examined enzymes when compared to the standard medicines.(Kaya *et al.*, 2024)


6e
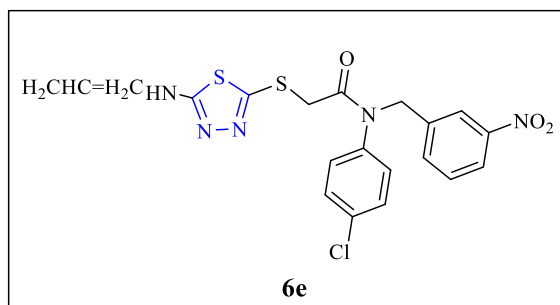
Mohammadi-Farani *et al.* 2024 produced several novel compounds with the 1,3,4-thiadaizole nucleus in order to evaluate their potential anti-Alzheimer's effects. With a fluorine atom in the meta position of the phenyl ring (IC$_{50}$ = 1.82 ± 0.6 µM), derivative **7e** was the most potent chemical compound in this series.(Mohammadi-Farani *et al.*, 2024)

7e
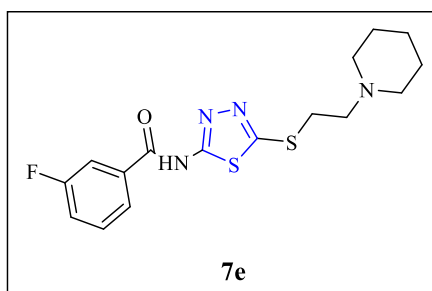
Anti-Bacterial Activity

Infectious diseases caused by bacteria have rapidly increased in recent years. Despite many significant developments in anti-bacterial therapy, the widespread use and abuse of antibiotic has led to the emergence of antibiotic resistance, a serious public health concern(Ulusoy Güzeldemirci *et al.*, 2017).

Mechanism of Action
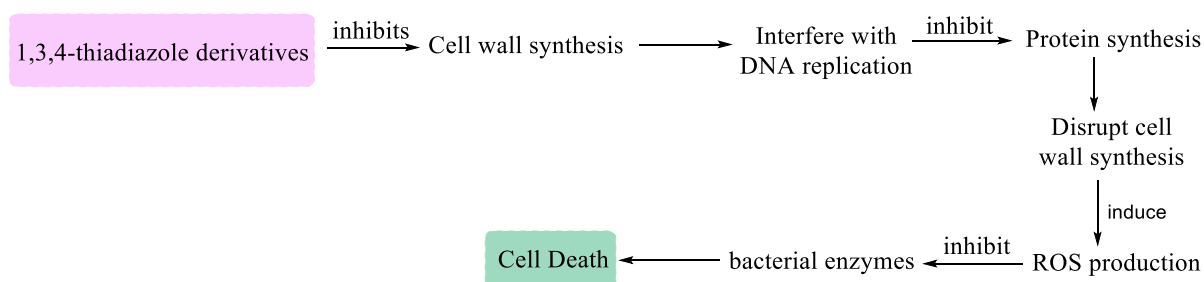
Figure 5: Bacterial activity inhibitiory mechanism of 1,3,4-thiadiazole derivatives

Kalyani, M. *et al.* 2024 Trimethylsilyl isothiocynates were used to create a range of pyrimidinyl oxa/thia/thiazole. Each of the 15 compounds they created to test for antibacterial properties outperformed the reference drug by a remarkable margin. Among compounds 3e, 5e, and 7a, more antibacterial activity was shown; compound 5, which contains 1,3,4-thiadiazole, exhibited the strongest antibacterial activity.(Kalyani *et al.*, 2024)


5
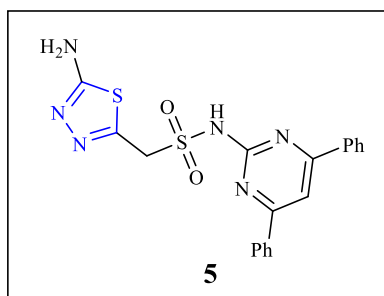
Yang, M. *et al.* 2025synthesized a series of derivatives of various compounds containing thiadiazole, morpholine, and urea as the pharmacophore by combining active substructure fragments, against the anti-bacterial activity which were evaluated. The results showed that the derivative **1** inhibited *Pseudomonas syringae* pv. *Actinidiae* by 35.06 %.(Yang *et al.*, 2025)

1
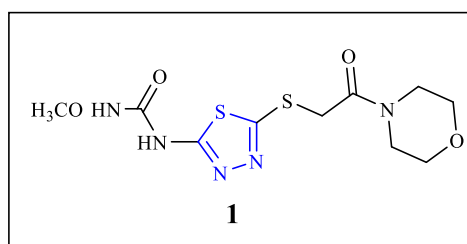
Anti-Convulsant Activity

Seizures, another name for convulsions, are sudden, uncontrollable electrical disruptions of the brain. Rapid, uncontrollable muscle contractions that results in uncontrollable movement and shaking are the hallmark of convulsions. It causes profound changes in consciousness, emotions, movements, and behavior. Any age can experience convulsions which can either be a one-time occurrence or a chronic condition requiring ongoing medical attention.Several modifications to the 1,3,4-thiadiazole moiety have shown good potency as less toxic and highly effective anti-convulsant medications.(V *et al.*, 2024)

Mechanism of Action
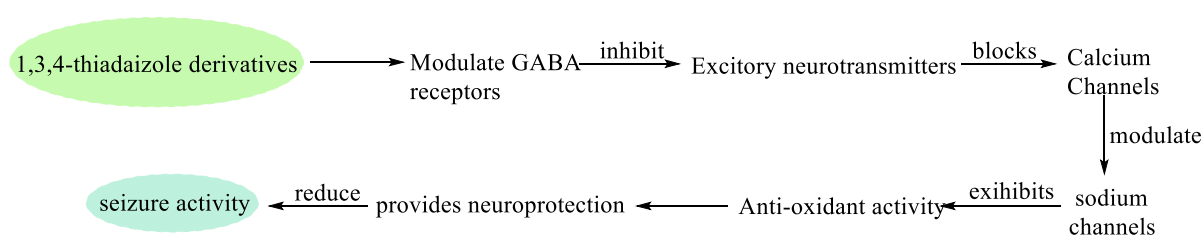
Figure 6: Mechanism of 1,3,4-thiadaizole derivatives as anti-convulsants

Karaküçük-İyidoğan *et al.* 2024 studied the design, synthesis, anti-convulsant evaluation of 1,3,4-thiadiazole derivatives, they had prepared five derivatives of 1,3,4-Thiadiazole analog; among of them **5b** and **5c** displayed significant anticonvulsant activity with ED_{50} values of 170.66 and 107.79 mg/kg, respectively.(Karaküçük-İyidoğan *et al.*, 2024)
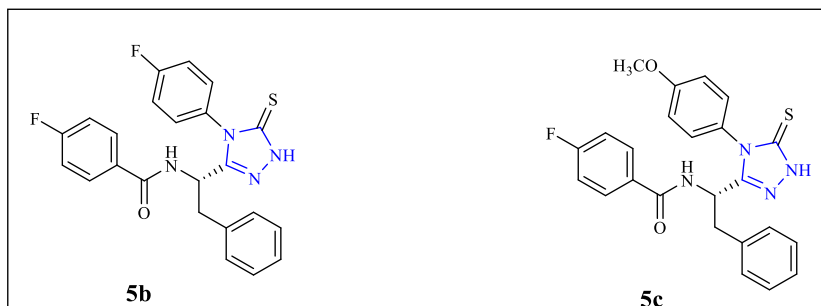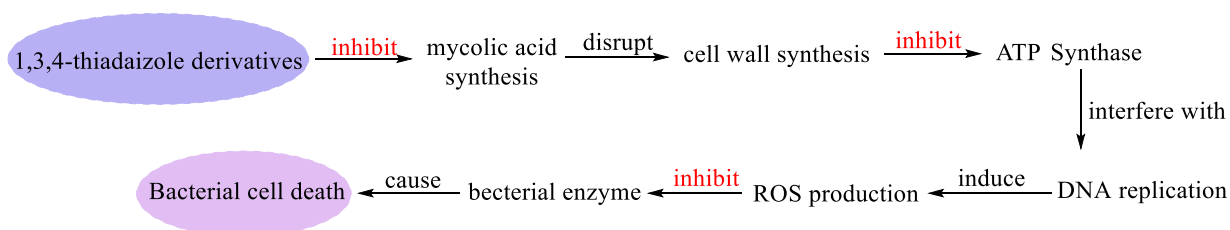

Anti-Tuberculosis Activity

Millions of people worldwide suffer from tuberculosis, a deadly bacterial disease. Whether there are treatments for it, the bacterium's nature makes it difficult to create new ones. Because drug resistant TB is becoming more common, treating it is becoming more difficult. Therefore, we need to develop new TB medications that are more effective, safer and capable of combating these resistant strains. Heterocyclic are compounds that have historically been used by researchers to create new medications. Heterocyclic substances like 1,3,4-thiadiazole have shown a great deal of promise in the development of novel medications. Additionally, thiadiazole have demonstrated promise in the treatment of cancer, infections and other issues.(THOMAS *et al.*, 2023)

Mechanism of Action

Figure 6: Anti-Tubercular activity of 1,3,4-thiadaizole derivatives

Patel, V. M. *et al.* 2025 synthesized N-Mannich bases (2a-j) of 2-(pyridine-4-yl)-1H-benzo[d]imidazole by combining 1,3,5-thiadiazole (2f-j) with benzothiazole (2a-e) under microwave irradiation. Rifampicin and the penta-fluoro substituted 1,3,5-thiadiazole molecule (2h) were similar in their ability to inhibit M. tuberculosis in primary screening (MIC = 6.25 µg/mL). Compound **2h**demonstrated good binding energy in the receptor's active pocket (PDB ID: 4cod).(Patel *et al.*, 2025)

Kendre, B. V. *et al.* 2025 synthesized and designed a new series of 12 chromone fused 1,3,4-thiadiazoles using a quick and easy synthesis method that begins with a 3-formyl chromone. Additionally, the experimental results showed that compounds **5d** and **5f** had excellent anti-tubercular capability against Mtb, with MICs of 3.0 and 4.0µg ml^{-1}.(Kendre *et al.*, 2025)

Shaikh, S. A. *et al.* 2024 synthesized a novel series of thiadiazole-thiazole-acetamide derivatives (4a-4k) by using TBAB as catalyst and butylating agent. The structures of the newly synthesized compounds are well confirmed by different spectroscopic techniques such as FT-IR, ^{1}H-NMR, ^{13}C-NMR and MS. DEPT and 2-D techniques as COSY, HETCOR and HMBC confirmed compound **4e.** The synthesized compounds exhibit moderate to high radical scavenging activities.(Shaikh *et al.*, 2024)

4e
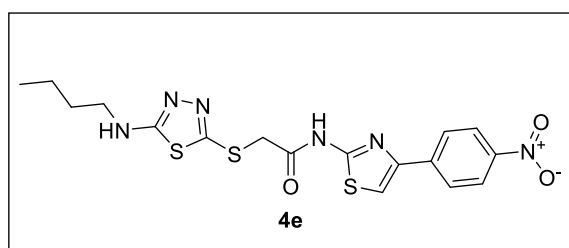
Conclusion:

In conclusion, the derivatives of 1,3,4-thiadiazole were identified as an important class of heterocyclic compounds with a wide range of therapeutic applications. Their unique structural and electronic characteristics allows them to show a wide range of pharmacological uses. This chapter, highlights the ability of 1,3,4-thiadiazole derivatives to treat various diseases by studying their structural variations and medical applications. The review of their medicinal uses shows, they can effectively treat diabetes, cancer, alzheimer, inflammation, neurological disorders, and infectious diseases. Although, their ability for treatment is motivating, the future research is required to optimize their therapeutic properties, enhance target selectivity and minimize toxicity. Future study will be enhanced by focusing on structure activity relationship, clinical evaluation and molecular docking.

References:

1. Abbasi, S. A., Rahim, F., Hussain, R., Khan, S., Ullah, H., Iqbal, T., Iqbal, N., Khan, H. U., Khan, S., Iqbal, R., Shah, S. A. A., Al Obaid, S., & Ansari, M. J. (2024). Synthesis of modified 1,3,4-thiadiazole incorporating substituted thiosemicarbazide derivatives: Elucidating the in vitro and in silico studies to develop promising anti-diabetic agent. *Results in Chemistry*, *8*, 101556. https://doi.org/10.1016/j.rechem.2024.101556

2. Kumar, A. , Kumar G., (2020). Synthesis, Characterization and Antibacterial activity of

halogen dcerivatives1, 3, 4- thiadiazole. *International Journal of Pharmacy and Life Sciences*, *11*(1).

3. Cebeci, A. N., Osmaniye, D., Sağlık Özkan, B. N., & Kaplancıklı, Z. A. (2024). Synthesis of new 1,3,4-thiadiazole derivatives, investigation of their AChE effects. *European Journal of Life Sciences*, *3*(2), 66–71. https://doi.org/10.55971/EJLS.1497661

4. Georgeta Serban1,*Oana Stanasel2, *eugenia Serban3Sanda Bota. (2018). 2-Amino-1,3,4-thiadiazole as a potential scaffoldfor promising antimicrobial agents. *Drug Design, Development and Therapy*, *12*, 1545–1566.

5. Hasan, T., Islam, A., Riva, R. ara khanom, Rahman, M. N., Ahmed, S., Islam, M. A., & Daula, A. F. M. S. U. (2023). Phytochemicals from Zingiber capitatum rhizome as potential α-glucosidase, α-amylase, and glycogen phosphorylase inhibitors for the management of Type-II diabetes mellitus: Inferences from in vitro, in vivo and in-silico investigations. *Arabian Journal of Chemistry*, *16*(10), 105128. https://doi.org/10.1016/j.arabjc.2023.105128

6. Kalagara, S., Baddam, S. R., Ganta, S., Vudari, B., Enaganti, S., Damarancha, A., & Eppakayala, L. (2025). Synthesis and biological evaluation of aryl derivatives of indole-1,3,4-thiadiazole as anticancer agents. *Synthetic Communications*, *55*(2), 138–145. https://doi.org/10.1080/00397911.2024.2431034

7. Kalyani, M., Sireesha, S. M., Reddy, G. D., & Padmavathi, V. (2024). Facile synthesis of pyrimidine substituted-1,3,4-oxadiazole, 1,3,4-thiadiazole and 1,2,4-triazole derivatives and their antimicrobial activity correlated with molecular docking studies. *Journal of Molecular Structure*, *1312*, 138563. https://doi.org/10.1016/j.molstruc.2024.138563

8. Kamel, M. G., Sroor, F. M., Hanafy, M. K., Mahrous, K. F., & Hassaneen, H. M. (2024). Design, synthesis and potent anti-pancreatic cancer activity of new pyrazole derivatives bearing chalcone, thiazole and thiadiazole moieties: gene expression, DNA fragmentation, cell cycle arrest and SAR. *RSC Advances*, *14*(37), 26954–26970. https://doi.org/10.1039/D4RA03005B

9. Karaküçük-İyidoğan, A., Başaran, E., Tatar-Yılmaz, G., & Oruç-Emre, E. E. (2024). Development of new chiral 1,2,4-triazole-3-thiones and 1,3,4-thiadiazoles with promising in vivo anticonvulsant activity targeting GABAergic system and voltage-gated sodium channels (VGSCs). *Bioorganic Chemistry*, *151*, 107662. https://doi.org/10.1016/j.bioorg.2024.107662

10. Kaya, B., Acar Çevik, U., Çiftci, B., Isık, M., Kaplancıklı, Z. A., & Beydemir, Ş. (2024). Design, Synthesis and Cholinesterase Inhibitory Activity of Novel 1,3,4-Thiadiazole

Derivatives. *Cumhuriyet Science Journal*, *45*(3), 503–509. https://doi.org/10.17776/csj.1449622

11. Kemskyi, S., Grozav, A., Chornous, V., Yakovychuk, N., Fedoriv, M., Melnyk, D., Melnyk, O., & Vovk, M. (2024). Synthesis, antimicrobial activity, DFT-calculation, and docking of 4-(1,3,4-thiadiazol-2-yl)-containing polysubstituted pyrroles. *Current Chemistry Letters*, *13*(4), 761–776. https://doi.org/10.5267/j.ccl.2024.3.005

12. Kendre, B. V, Hardas, P. S., Pat, R. C., Kendre, R. B., Landge, M. G., & Bhusare, S. R. (2025). Design, Synthesis and Biological Evaluation of Chromone Fused 1, 3, 4-Thiadiazoles as Highly Potent Nontoxic Inhibitors of Enoyl-Acyl Carrier Proteins in M. tuberculosis. *International Journal of New Chemistry*, *12*(4), 581–606.

13. Mohamed, A. E., Elgammal, W. E., Dawaba, A. M., Ibrahim, A. G., Fouda, A., & Hassan, S. M. (2022). A novel 1,3,4-thiadiazole modified chitosan: synthesis, characterization, antimicrobial activity, and release study from film dressings. *Applied Biological Chemistry*, *65*(1), 54. https://doi.org/10.1186/s13765-022-00725-7

14. Mohammadi-Farani, A., Takesh, M., Mohammadi, M., Hosseini, A., Aliabadi, A., & Aliabadi, A. (2024). Synthesis, Docking and Acetylcholinesterase Inhibitory Evaluation of 1,3,4-Thiadiazole Derivatives as Potential Anti-Alzheimer Agents. *Pharmaceutical Sciences*. https://doi.org/10.34172/PS.2024.7

15. Patel, V. M., Patel, N. B., Chan-Bacab, M. J., Rivera, G., Humal, T. R., & Gamit, A. S. (2025). Synthesis and computational studies of 1,3,4-thiadiazole and benzothiazole clubbed benzimidazole analogous as anti-tubercular and anti-protozoal agent. *Journal of Molecular Structure*, *1319*, 139326. https://doi.org/10.1016/j.molstruc.2024.139326

16. Serag, M. I., Tawfik, S. S., Eisa, H. M., & Badr, S. M. I. (2025). Design, Synthesis, Biological Evaluation and Molecular Docking Study of New 1,3,4-Thiadiazole-Based Compounds as EGFR Inhibitors. *Drug Development Research*, *86*(1). https://doi.org/10.1002/ddr.70035

17. Shaikh, S. A., Labhade, S. R., Kale, R. R., Pachorkar, P. Y., Meshram, R. J., Jain, K. S., Labhade, H. S., Bhanushali, D. D., More, R. A., Nerkar, C. K., Chobe, S. S., Marathe, A. N., Wakchaure, S. N., & Boraste, D. R. (2024). Thiadiazole-thiazole derivatives as potent anti-tubercular agents: Synthesis, biological evaluation, and In silico docking studies. *European Journal of Medicinal Chemistry Reports*, *12*, 100183. https://doi.org/10.1016/j.ejmcr.2024.100183

18. Sharma, B., Verma, A., Prajapati, S., & Sharma, U. K. (2013). Synthetic Methods, Chemistry, and the Anticonvulsant Activity of Thiadiazoles. *International Journal of*

Medicinal Chemistry, *2013*, 1–16. https://doi.org/10.1155/2013/348948

19. Thomas, A., B., V., K. U., S. S., & M. V., V. (2023). Development of Novel 1, 3, 4-Thiadiazoles As Antitubercular Agents-Synthesis And In Vitro Screening. *International Journal of Current Pharmaceutical Research*, 37–41. https://doi.org/10.22159/ijcpr.2023v15i3.3009

20. Tokareva, M. A., Glukhareva, T. V., & Keaveney, S. T. (2024). Recent Advances in the Denitrogenative Annulation Reactions of 1,2,3-Thiadiazoles. *ChemCatChem*, *16*(14). https://doi.org/10.1002/cctc.202301488

21. Ulusoy Güzeldemirci, N., Karaman, B., & Küçükbasmaci, Ö. (2017). Antibacterial, Antitubercular and Antiviral Activity Evaluations of Some Arylidenehydrazide Derivatives Bearing Imidazo[2,1-b]thiazole Moiety. *Turkish Journal of Pharmaceutical Sciences*, *14*(2), 157–163. https://doi.org/10.4274/tjps.25743

22. V, V., Nafiya, F., A, H., M M, M. K., N, N., & Saji, S. (2024). In-Silico Design of Thiadiazole Derivatives as Anticonvulsant Agents. *Asian Journal of Pharmaceutical Research and Development*, *12*(4), 85–91. https://doi.org/10.22270/ajprd.v12i4.1445

23. Wassel, M. M. S., Ammar, Y. A., Elhag Ali, G. A. M., Belal, A., Mehany, A. B. M., & Ragab, A. (2021). Development of adamantane scaffold containing 1,3,4-thiadiazole derivatives: Design, synthesis, anti-proliferative activity and molecular docking study targeting EGFR. *Bioorganic Chemistry*, *110*, 104794. https://doi.org/10.1016/j.bioorg.2021.104794

24. Yang, M., Zhou, Z., Liu, D., Wu, Y., He, D., Feng, N., Zhou, Y., Li, C., Liu, B., Chen, D., Sun, Y., & Wang, Z. (2025). Synthesis, crystal structure and biological evaluation of thiadiazole derivatives containing urea moiety as anti-bacterial agents. *Journal of Molecular Structure*, *1326*, 141073. https://doi.org/10.1016/j.molstruc.2024.141073

25. Zahid ali, wajid rehman, liaqat rashid. (2024). New 1,3,4-Thiadiazole Derivatives as α-Glucosidase Inhibitors:Design, Synthesis, DFT, ADME, and In Vitro Enzymatic Studies. *ACS Omega*, *9*, 7480–7490.

26. Zahoor, T., Khan, S., Chinnam, S., Iqbal, T., Hussain, R., Khan, Y., Ullah, H., Daud, S., Rahman, R., Iqbal, R., Aljowaie, R. M., & Aghayeva, S. (2024). A combined in vitro and in silico approach of thiadiazole based Schiff base derivatives as multipotent inhibitor: Synthesis, spectral analysis, antidiabetic and antimicrobial activity. *Results in Chemistry*, *9*, 101671. https://doi.org/10.1016/j.rechem.2024.101671

APPLICATION OF ARTIFICIAL INTELLIGENCE AND MACHINE LEARNING IN OFFSHORE OPERATIONS: A COMPREHENSIVE REVIEW

Gitam Parasar and Prasenjit Talukdar*

Department of Petroleum Engineering,

DUIET, Dibrugarh University, Assam-786004, India

*Corresponding author E-mail: prasenjit_duiet@dibru.ac.in

Abstract:

Artificial Intelligence (AI) and Machine Learning (ML) are transforming offshore industries, making operations safer, more efficient, and smarter. These technologies are playing a crucial role in oil and gas, renewable energy, and maritime navigation by automating complex tasks, improving decision-making, and predicting potential failures before they happen. By analyzing a large amount of real-time data, AI-driven models help in predictive maintenance, risk assessment, and operational optimization. Techniques like artificial neural networks (ANN), long short-term memory (LSTM), and reinforcement learning are being used to enhance efficiency—from optimizing oil extraction to improving offshore wind farm performance. The shift towards AI-powered automation has made offshore work less dependent on manual efforts, reducing risks and operational costs. However, challenges such as computational demands, the need for transparent AI models, and adaptive learning still need to be addressed. As AI and ML continue to evolve, they promise to bring even greater innovation, sustainability, and efficiency to offshore operations.

Keywords: Artificial Intelligence (AI), Machine Learning (ML), Offshore Operations, Neural Networks (ANN), Long Short-Term Memory (LSTM), Reinforcement Learning, Oil and Gas, Renewable Energy

Introduction:

Artificial Intelligence (AI) and Machine Learning (ML) are revolutionizing offshore operations by enhancing safety, efficiency, and decision-making across various industries, including oil and gas, renewable energy, and maritime navigation. These technologies leverage advanced algorithms, deep learning architectures, and data-driven models to optimize complex processes, and improve predictive accuracy.

AI and ML have demonstrated their potential in predictive maintenance, anomaly detection, risk assessment, and operational optimization. By analysing vast amounts of real-time data, these models can forecast equipment failures, enhance energy management, and improve

navigation systems. Techniques such as artificial neural networks (ANN), long short-term memory (LSTM), support vector machines (SVM), and reinforcement learning are being applied to tackle industry-specific challenges, from optimizing oil production rates to improving offshore wind farm efficiency.

The integration of AI-driven automation has led to safer and more cost-effective offshore operations, reducing the reliance on traditional, labour-intensive methods. However, challenges remain, including the need for robust computational resources, explainable AI models, and adaptive learning techniques to further enhance real-world applicability. As AI and ML continue to evolve, they hold the potential to drive innovation, sustainability, and operational excellence in offshore environments.

1.   Significance of Artificial Intelligence

Artificial Intelligence (AI) is transforming offshore operations by improving anomaly detection, predictive maintenance, and decision-making. Advanced deep learning models like Long Short-Term Memory (LSTM) and Gated Recurrent Unit (GRU) help classify production anomalies more efficiently, enhancing both safety and operational performance. Genetic algorithms further refine these models by optimizing their hyperparameters, leading to better accuracy compared to traditional methods. AI-driven solutions not only cut maintenance costs but also improve reliability in offshore environments. However, challenges remain, such as the need for high computational power and the development of explainable AI to improve trust and interpretability. As AI continues to advance, its role in optimizing offshore operations will become even more critical. (Bayazitova *et al.*, 2024)

1.1.   Artificial Intelligence (AI) in Offshore Wind Energy

Artificial intelligence (AI) enhances offshore wind energy operations by enabling automation, real-time decision-making, and intelligent energy management. AI-driven systems process vast amounts of wind turbine data, allowing operators to make timely adjustments that optimize wind farm performance. Additionally, AI identifies key trends and methodologies, supporting innovation and addressing research gaps in offshore wind energy. These advancements contribute to improved operational efficiency, sustainability, and long-term reliability in wind power generation. (Das *et al.*, 2024)

1.2.   Artificial Intelligence (AI) in Offshore Service Management

Artificial Intelligence (AI) is also transforming the landscape of offshore service management, particularly regarding project selection. AI-based decision support tools enable vendors to shortlist projects to consider with more accuracy and efficiency, effectively reducing risk and complexity. It means smarter decisions, better resource allocation, and smoother

operations. The progression of AI will create more operational efficiency and make the management of offshore projects more future-ready. (Ikram *et al.*, 2023)

1.3. Artificial Intelligence (AI) in Wellbore Instability Management

Artificial intelligence (AI) provides a robust solution for addressing wellbore instability in offshore drilling operations. Traditional physics-based models often struggle with accurately determining empirical coefficients, limiting their predictive effectiveness. AI enhances wellbore stability predictions by efficiently analyzing complex nonlinear relationships, improving drilling performance, and enabling real-time data processing. Future developments should focus on integrating hybrid AI-physics models and adaptive learning techniques to further enhance predictive accuracy and operational safety.

1.4. Artificial Intelligence (AI) in Oil Production Rate Estimation

Artificial intelligence (AI) plays a crucial role in optimizing oil production rate estimation for offshore operations, especially in challenging high gas-oil ratio (GOR) and high water cut (WC) conditions. Traditional methods, such as test separators and multiphase flow meters (MPFMs), are costly, complex, and often inaccurate under extreme flow scenarios. AI-based solutions offer a more efficient and reliable alternative by leveraging data-driven approaches to predict oil flow rates accurately. By analysing critical parameters such as choke size, upstream and downstream pressures, GOR, and WC, AI models enhance production forecasting and well performance evaluation(Al Dhaif *et al.*, 2021)

1.5. Artificial Intelligence (AI) in Offshore Resource Exploration

Artificial intelligence (AI) is revolutionizing offshore resource exploration by enabling scalable and automated solutions for detecting and estimating polymetallic nodule abundance on the seafloor. Traditional manual methods for nodule identification and quantification are labour-intensive and prone to inconsistencies. AI-driven deep learning (DL) models offer a more efficient alternative by analysing seafloor images and improving estimation accuracy. By integrating AI with seabed sampling, researchers gain deeper insights into nodule distribution variability, enhancing exploration strategies and optimizing deep-sea mining operations. (Tomczak *et al.*, 2024)

1.6. Artificial Intelligence (AI) in Offshore Pipeline Integrity Management

Artificial intelligence (AI) is transforming offshore pipeline integrity management by integrating advanced modelling techniques to assess structural health and failure risks. By combining AI with finite element analysis (FEA), researchers can predict the remaining useful life (RUL) and probability of failure (POF) of corroded pipelines with greater precision. Traditional failure pressure equations often yield overly conservative estimates, but AI-driven

models improve accuracy, reducing estimation errors and optimizing maintenance strategies. These advancements enable risk-based inspection approaches that enhance pipeline safety and longevity in offshore environments.

1.7.   Artificial Intelligence (AI) in Offshore Oil and Gas Operations

AI is transforming offshore oil and gas operations by enabling data-driven decision-making in exploration, drilling, reservoir management, and production. By processing vast amounts of data, AI enhances resource extraction, automates workflows, and improves operational safety. AI-powered techniques, such as artificial neural networks (ANN) and adaptive learning models (ALM), help optimize complex processes, leading to more efficient and sustainable offshore operations(Sircar *et al.*, 2021)

Machine learning (ML) is playing a crucial role in improving safety, reliability, and efficiency in offshore operations by enabling fault detection, anomaly identification, risk assessment, and system prognosis. The use of supervised, unsupervised, and semi-supervised learning methods allows for predictive maintenance, early failure detection, and optimized decision-making, reducing operational risks in offshore environments. The integration of digitalization and remote sensing technologies has significantly increased data availability, enhancing the accuracy of ML models. However, challenges such as data scarcity, trust in AI-driven decisions, and model interpretability need to be addressed. Strengthening data governance, improving model transparency, and fostering interdisciplinary collaboration will be essential to fully leverage AI and ML for safer and more efficient offshore operations.

1.8.   Artificial Intelligence (AI) in Offshore Oil Production

AI is revolutionizing offshore oil production by enabling more accurate and efficient decision-making processes. By leveraging AI techniques such as Support Vector Machine (SVM) and Random Forest (RF), offshore operations can improve oil flow rate predictions, optimize resource extraction, and enhance production efficiency. AI-driven models analyse key parameters like upstream and downstream pressures, gas-oil ratio (GOR), and choke size to provide superior predictions compared to traditional empirical methods.(Ibrahim *et al.*, 2021)

1.9.   Artificial Intelligence (AI) in Offshore Drilling

AI is transforming offshore drilling by improving decision-making, optimizing operations, and reducing uncertainties. By utilizing an Artificial Neural Network (ANN) model, AI enhances real-time predictions of the Rate of Penetration (ROP), allowing for more efficient and cost-effective drilling processes. AI-driven insights contribute to safer offshore hydrocarbon extraction and streamlined operations. (Almomen *et al.*, 2024)

1.10. Artificial Intelligence (AI) in Autonomous Offshore Operations

AI is revolutionizing offshore operations by enabling autonomous ships to navigate more efficiently and safely. A major application of AI in this field is ship collision avoidance and mission planning, where intelligent systems help vessels minimize risks while optimizing routes. AI-driven navigation enhances decision-making by integrating real-time data, making offshore operations more reliable and effective. (Sarhadi *et al.*, 2022)

1.11. Artificial Intelligence (AI) in Maritime Safety

AI is transforming maritime safety by enabling real-time collision damage prediction and risk assessment. By leveraging deep learning techniques such as Long Short-Term Memory (LSTM) networks and Transformer models, AI-driven systems can analyse vast datasets and predict the extent of ship collision damage with high accuracy. This enhances decision-making and improves navigation in congested offshore environments, making operations safer and more reliable. (Shabani *et al.*, 2025)

1.12. Artificial Intelligence (AI) in Offshore Wind Turbine Fault Detection

AI is revolutionizing fault detection in floating offshore wind turbines (FOWTs) by enabling real-time monitoring and predictive maintenance. Using deep learning techniques, particularly neural networks with 1D convolutional operations, AI-driven systems continuously analyse turbine signals to detect potential faults. This technology enhances traditional inspection methods, which are often challenging in offshore environments, by offering a more efficient and automated approach to identifying malfunctions in key subsystems like pitch control and generators. (Fernandez-Navamuel *et al.*, 2024)

1.13. Artificial Intelligence (AI) in Offshore Multi-Use Platforms (MUPs)

AI is transforming the development of offshore multi-use platforms (MUPs) by analysing extensive research data to identify emerging trends and technological synergies. These platforms integrate energy production, aquaculture, and freshwater generation, offering sustainable solutions for coastal and island communities. AI-driven text analysis has helped map out common technology combinations, such as wind and wave energy, while also revealing gaps in research, particularly in modular and mobile platform designs. (Xylia *et al.*, 2023)

1.14. Artificial Intelligence (AI) in Offshore Renewable Energy

As the demand for cleaner energy grows, AI is playing a pivotal role in optimizing offshore renewable energy sources like wind and wave power. These energy systems face significant challenges, including harsh environmental conditions, high maintenance costs, and unpredictable energy generation. AI-driven models enhance forecasting for wind and wave patterns, ensuring better integration into the energy grid. By analysing vast amounts of real-time

data, AI helps improve energy efficiency and grid stability, making offshore renewables more viable and scalable. (Allal *et al.*, 2024)

1.15. Enhancing Decision-Support Systems (DSS) with AI

The study highlights how AI-powered decision-support systems (DSS) can provide real-time risk warnings to vessel crews, potentially preventing accidents before they occur. However, the current model has limitations, as it relies solely on Norwegian data and lacks crucial variables like weather conditions, vessel position, and traffic density. Future research should integrate additional data sources, such as GPS and AIS history, to refine risk predictions. By continuously advancing AI-driven maritime safety systems, offshore operations can become safer, smarter, and more proactive in preventing accidents.(Munim *et al.*, 2024)

1.16. AI-Driven Monitoring for Offshore Wind Turbines

AI and machine learning are transforming offshore wind farm operations by improving the monitoring and maintenance of floating offshore wind turbines (FOWTs). This study presents a deep learning-based method that detects and classifies faults in key control subsystems, such as pitch sensors, actuators, and generators. By analysing synthetic signals from simulations, the model continuously assesses turbine health, enabling real-time fault detection. This proactive approach enhances maintenance efficiency and minimizes the need for in-person inspections, which are particularly challenging in offshore environments. (Pacis *et al.*, 2023)

2. Significance of Machine Learning

Machine learning (ML) is transforming offshore operations by enabling advanced anomaly detection, predictive maintenance, and operational optimization. Deep learning architectures like long short-term memory (LSTM) and gated recurrent unit (GRU) networks effectively classify anomalies in production data, improving safety and efficiency. Additionally, genetic algorithms for hyperparameter optimization enhance model performance, achieving superior accuracy compared to traditional methods.

These ML-driven advancements reduce maintenance costs, improve decision-making, and enhance operational reliability. However, challenges remain, including the need for robust computational resources and explainable AI to ensure transparency and trust in real-world applications. As ML continues to evolve, it will play an increasingly crucial role in optimizing offshore operations. (Bayazitova *et al.*, 2024)

2.1. Machine Learning (ML) in Offshore Wind Energy

Machine learning (ML) plays a critical role in improving predictive accuracy and forecasting capabilities in offshore wind energy. By integrating ML and deep learning (DL) techniques, researchers can develop more precise models that handle environmental variability

effectively. ML-driven data analysis enhances energy trading strategies, optimizes wind turbine operations, and ensures efficient power generation. As ML continues to advance, it will further contribute to automation, reducing reliance on manual intervention while increasing the overall efficiency of offshore wind farms. (Das *et al.*, 2024)

2.2. Machine Learning (ML) in Offshore Service Management

Machine learning (ML) techniques, particularly the Deep Extreme Learning Machine (DELM)-based model, significantly improve predictive performance in offshore service management. The model utilizes an advanced Extreme Learning Machine (ELM) algorithm with multiple hidden layers, random weights, and biases, enabling high training and testing accuracy. This ML-driven approach enhances project evaluation, allowing vendors to assess multiple variables for better decision-making. The results highlight the effectiveness of ML in refining project selection processes and improving overall offshore operations.(Ikram *et al.*, 2023)

2.3. Machine Learning (ML) in Wellbore Instability Management

Machine learning (ML) techniques play a crucial role in optimizing wellbore stability by leveraging data-driven approaches to improve prediction accuracy. ML models can process vast amounts of drilling data, identifying patterns that traditional methods might overlook. By refining empirical coefficients and optimizing drilling parameters, ML contributes to safer and more efficient offshore drilling operations. Further advancements in real-time data integration and adaptive learning will continue to enhance the reliability and cost-effectiveness of wellbore management. (Tamascelli *et al.*, 2024)

2.4. Machine Learning (ML) in Oil Production Rate Estimation

Machine learning (ML) techniques, including artificial neural networks (ANN), adaptive network-based fuzzy inference systems (ANFIS), and functional networks (FN), significantly improve the accuracy and efficiency of oil production rate estimation. These models utilize vast datasets to identify complex relationships between key parameters, enabling more precise predictions compared to traditional methods. By applying ML algorithms to 550 data points from volatile oil and gas condensate wells in the Middle East, this study highlights the ability of ML to reduce operational costs, optimize decision-making, and enhance overall offshore oil field management(Al Dhaif *et al.*, 2021)

2.5. Machine Learning (ML) and Deep Learning (DL) in Seafloor Analysis

Machine learning (ML), particularly deep learning (DL), plays a crucial role in processing vast amounts of seafloor image data to detect and quantify polymetallic nodules. DL models can identify patterns and anomalies with high precision, reducing the need for extensive human intervention. This study demonstrates the potential of DL-based approaches to improve

estimation accuracy and resource assessment. Future advancements, including self-supervised learning and real-time data analysis using autonomous underwater vehicles, could further refine these techniques, making offshore resource exploration more efficient, sustainable, and data-driven. (Tomczak *et al.*, 2024)

2.6. Machine Learning (ML) and Probabilistic Failure Prediction

Machine learning (ML) models, particularly neural networks, outperform conventional methods in predicting pipeline failure by analysing vast datasets generated through FEA simulations. By processing over 266,000 stress condition models, ML algorithms refine risk assessment, demonstrating a 15% reduction in conservative failure pressure estimates. The study also applies probabilistic modelling using the Waybill distribution, revealing that failure pressure declines by 65–76% over a 30-year period. Additionally, findings indicate that pipeline age, internal pressure, and defect spacing significantly impact failure risk. These insights support more accurate predictive maintenance strategies, improving operational efficiency and reliability in offshore pipeline management. (Hosseinzadeh *et al.*, 2025)

2.7. Machine Learning (ML) for Predictive Maintenance and Production Optimization

Machine learning (ML) plays a crucial role in predictive maintenance, reducing downtime and operational risks by forecasting equipment failures and optimizing drilling parameters. Supervised learning and fuzzy logic models enhance reservoir analysis, ensuring better production efficiency. By leveraging ML-driven data analytics, offshore operations can become more automated, cost-effective, and sustainable, driving significant advancements in the oil and gas industry. (Sircar *et al.*, 2021)

Machine learning (ML) enhances the efficiency and adaptability of MUPs by systematically organizing research and optimizing platform configurations. Despite their potential, economic assessments and real-world feasibility studies, especially outside Europe, remain limited. AI and ML can bridge these gaps by improving design strategies, evaluating cost-effectiveness, and facilitating global knowledge sharing. As these technologies advance, they will play a crucial role in making MUPs more viable, resilient, and scalable for sustainable offshore development. (Xylia *et al.*, 2023)

Machine learning (ML) plays a vital role in advancing predictive maintenance for offshore wind farms. By training AI models to recognize patterns in turbine data, ML improves fault diagnosis and reduces downtime by enabling faster responses to equipment failures. However, current models face challenges in distinguishing between similar faults and detecting multiple issues simultaneously. Future advancements in AI and ML will focus on enhancing fault

differentiation and multi-fault detection, further improving the reliability and efficiency of offshore wind energy operations(Fernandez-Navamuel *et al.*, 2024)

Machine learning (ML) revolutionizes offshore operations by predicting equipment failures, optimizing energy production, and reducing maintenance costs. ML algorithms process sensor data from offshore platforms to detect anomalies and preemptively address potential issues, minimizing downtime. Autonomous AI-driven maintenance systems further enhance operational safety by reducing the need for risky human inspections in remote offshore environments. By leveraging AI and ML, offshore renewable energy operations become more reliable, cost-effective, and sustainable, accelerating the transition to a cleaner energy future.(Allal *et al.*, 2024)

2.8. Machine Learning (ML) for Flow Rate Prediction and Operational Optimization

Machine learning (ML) models, particularly RF and SVM, significantly enhance flow rate estimations in offshore oil production. RF models, with an absolute average percentage error (AAPE) below 1%, outperform traditional correlations, improving predictive accuracy under various flow conditions. By reducing uncertainties in high-GOR and high-water-cut reservoirs, ML contributes to more efficient and sustainable offshore operations, minimizing risks and optimizing production processes(Ibrahim *et al.*, 2021)

2.9. Machine Learning (ML) for Drilling Performance Optimization

Machine learning (ML), particularly ANN models, plays a crucial role in optimizing offshore drilling performance. Trained on extensive well data, ANN models achieve high predictive accuracy in forecasting ROP, outperforming traditional methods. The integration of empirical equations further validates these predictions, ensuring robust and reliable drilling optimization. Future advancements will focus on expanding validation across different reservoirs and developing predictive models for pre-emptive drilling adjustments, enhancing offshore operational efficiency. (Almomen *et al.*, 2024)

2.10. Machine Learning (ML) for Collision Risk Prediction

Machine learning (ML) plays a critical role in advancing collision damage prediction in offshore operations. Researchers have trained ML models on over 5,500 collision scenarios to improve risk assessments and proactive decision-making. These models significantly outperform traditional methods, offering real-time insights that help ships avoid potential hazards. Validated through real-world applications in the Gulf of Finland, this AI-powered approach enhances maritime safety, reduces risks, and improves the overall efficiency of offshore operations. (Shabani *et al.*, 2025)

AutoML is proving to be a game-changer in maritime safety by enhancing accident prediction and risk management at sea. By analyzing accident data in Norwegian waters, this study identified key influencing factors, such as navigation area and operational phase—an insight not previously emphasized in maritime safety research. The findings suggest that tree-based models, particularly LightGBM, offer the highest accuracy in predicting accidents, making them valuable for improving maritime risk assessments. (Munim *et al.*, 2024)

AutoML is proving to be a powerful tool in maritime safety, helping predict accidents and improve risk management at sea. This study applied AutoML to analyze accident data in Norwegian waters, identifying key factors such as navigation area and operational phase that influence maritime incidents. Interestingly, the operational phase had not been highlighted in previous research, making it a valuable new insight for decision-making. The study found that tree-based models, particularly LightGBM, performed best in predicting accidents. These insights could support the development of decision-support systems (DSS) that provide real-time risk warnings to vessel crews, potentially preventing accidents before they happen. However, the study had some limitations—it relied solely on Norwegian data and lacked variables like weather conditions, vessel position, and traffic density, which could enhance model accuracy. Future research could expand these models to other regions and integrate additional data sources, such as GPS and AIS history, to refine risk predictions. By continuously improving these AI-driven systems, maritime operations can become safer, smarter, and more proactive in preventing accidents.(Munim *et al.*, 2024)

Challenges of AI and ML in Offshore Operations

The adoption of artificial intelligence (AI) and machine learning (ML) in offshore operations faces several significant challenges. One of the primary obstacles is the requirement for vast computational resources, as AI-driven models demand substantial processing power and storage capacity to function effectively. Additionally, the availability of high-quality, labelled datasets for offshore environments remains limited, making it difficult to train and validate AI models with high accuracy. Another major challenge is the interpretability of AI models—many operate as "black boxes," meaning their decision-making processes are not easily understood by engineers and operators. This lack of transparency raises concerns about trust, regulatory compliance, and accountability in high-risk offshore operations. Furthermore, cybersecurity risks pose a growing challenge, as AI-driven offshore systems rely on interconnected digital infrastructure that could be vulnerable to cyber threats, hacking, and data breaches. Without robust security frameworks, sensitive operational data could be compromised, leading to significant financial and safety risks.

Future of AI and ML in Offshore Operations

Despite these challenges, the future of AI and ML in offshore operations is highly promising, with advancements that could drive greater efficiency, safety, and sustainability. One key area of progress is the integration of hybrid AI-physics models, which combine data-driven insights with established engineering principles to improve predictive accuracy. The adoption of reinforcement learning and self-supervised learning will allow AI systems to refine their performance over time with minimal human intervention, enabling more autonomous offshore operations. Additionally, digital twin technology—AI-powered virtual replicas of offshore assets—will revolutionize predictive maintenance by enabling real-time monitoring and proactive issue detection. Edge computing is another area of growth, allowing AI models to process data in real-time at offshore sites without relying solely on cloud-based infrastructure. As these technologies continue to evolve, interdisciplinary collaboration among AI researchers, offshore engineers, and policymakers will be essential to overcoming current limitations and unlocking the full potential of AI-driven offshore operations.

Conclusion:

AI and ML are making offshore industries smarter, safer, and more efficient. From predicting equipment failures to optimizing energy use, these technologies are helping companies in oil and gas, renewable energy, and maritime navigation make better decisions and reduce risks. AI is streamlining manual work processes and enhancing efficiency by automating intricate tasks and analysing data in real time. For greater real-world applicability, however, much remains to be solved such as computational demands, explainable AI and adaptive learning. These challenges notwithstanding, the ever-advancing landscape of AI and ML is likely to facilitate innovation, sustainability, and operational excellence in offshore sectors of the economy.

References:

1.   Al Dhaif, R., Ibrahim, A. F., Elkatatny, S., & Al Shehri, D. (2021). Prediction of oil rates using Machine Learning for high gas oil ratio and water cut reservoirs. *Flow Measurement and Instrumentation*, *82*, 102065. https://doi.org/10.1016/J.FLOWMEASINST.2021.102065

2.   Allal, Z., Noura, H. N., Salman, O., & Chahine, K. (2024). Machine learning solutions for renewable energy systems: Applications, challenges, limitations, and future directions. *Journal of Environmental Management*, *354*, 120392. https://doi.org/10.1016/J.JENVMAN.2024.120392

3.   Almomen, H., Mahmoud, A. A., Elkatatny, S., & Abdulraheem, A. (2024). Predicting the

Rate of Penetration while Horizontal Drilling through Unconventional Reservoirs Using Artificial Intelligence. *ACS Omega*. https://doi.org/10.1021/acsomega.4c08006

4. Bayazitova, G., Anastasiadou, M., & dos Santos, V. D. (2024). Oil and gas flow anomaly detection on offshore naturally flowing wells using deep neural networks. *Geoenergy Science and Engineering*, *242*(August), 213240. https://doi.org/10.1016/j.geoen.2024.213240

5. Das, P., Mashiata, M., & Iglesias, G. (2024). Big data meets big wind: A scientometric review of machine learning approaches in offshore wind energy. *Energy and AI*, *18*(August), 100418. https://doi.org/10.1016/j.egyai.2024.100418

6. Fernandez-Navamuel, A., Peña-Sanchez, Y., & Nava, V. (2024). Fault detection and identification for control systems in floating offshore wind farms: A supervised Deep Learning methodology. *Ocean Engineering*, *310*(P1), 118678. https://doi.org/10.1016/j.oceaneng.2024.118678

7. Hosseinzadeh, S., Bahaari, M., Abyani, M., & Taheri, M. (2025). Data-driven remaining useful life estimation of subsea pipelines under effect of interacting corrosion defects. *Applied Ocean Research*, *155*, 104438. https://doi.org/10.1016/J.APOR.2025.104438

8. Ibrahim, A. F., Al-Dhaif, R., Elkatatny, S., & Shehri, D. Al. (2021). Applications of Artificial Intelligence to Predict Oil Rate for High Gas-Oil Ratio and Water-Cut Wells. *ACS Omega*, *6*(30), 19484–19493. https://doi.org/10.1021/acsomega.1c01676

9. Ikram, A., Jalil, M. A., Ngah, A. Bin, Raza, S., Khan, A. S., Mahmood, Y., Kama, N., Azmi, A., & Alzayed, A. (2023). Project Assessment in Offshore Software Maintenance Outsourcing Using Deep Extreme Learning Machines. *Computers, Materials and Continua*, *74*(1), 1871–1886. https://doi.org/10.32604/cmc.2023.030818

10. Munim, Z. H., Sørli, M. A., Kim, H., & Alon, I. (2024). Predicting maritime accident risk using Automated Machine Learning. *Reliability Engineering and System Safety*, *248*(August 2023). https://doi.org/10.1016/j.ress.2024.110148

11. Pacis, F. J., Ambrus, A., Alyaev, S., Khosravanian, R., Kristiansen, T. G., & Wiktorski, T. (2023). Improving predictive models for rate of penetration in real drilling operations through transfer learning. *Journal of Computational Science*, *72*(June), 102100. https://doi.org/10.1016/j.jocs.2023.102100

12. Sarhadi, P., Naeem, W., & Athanasopoulos, N. (2022). A Survey of Recent Machine Learning Solutions for Ship Collision Avoidance and Mission Planning. *IFAC-PapersOnLine*, *55*(31), 257–268. https://doi.org/10.1016/j.ifacol.2022.10.440

13. Shabani, M., Kadoch, M., & Mirjalili, S. (2025). A novel metaheuristic-based approach for

prediction of corrosion characteristics in offshore pipelines. *Engineering Failure Analysis*, *170*, 109231. https://doi.org/10.1016/J.ENGFAILANAL.2024.109231

14. Sircar, A., Yadav, K., Rayavarapu, K., Bist, N., & Oza, H. (2021). Application of machine learning and artificial intelligence in oil and gas industry. *Petroleum Research*, *6*(4), 379–391. https://doi.org/10.1016/j.ptlrs.2021.05.009

15. Tamascelli, N., Campari, A., Parhizkar, T., & Paltrinieri, N. (2024). Artificial Intelligence for safety and reliability: A descriptive, bibliometric and interpretative review on machine learning. *Journal of Loss Prevention in the Process Industries*, *90*(July 2023), 105343. https://doi.org/10.1016/j.jlp.2024.105343

16. Tomczak, A., Kogut, T., Kabała, K., Abramowski, T., Ciążela, J., & Giza, A. (2024). Automated estimation of offshore polymetallic nodule abundance based on seafloor imagery using deep learning. *Science of The Total Environment*, *956*, 177225. https://doi.org/10.1016/J.SCITOTENV.2024.177225

17. Xylia, M., Passos, M. V., Piseddu, T., & Barquet, K. (2023). Exploring multi-use platforms: A literature review of marine, multifunctional, modular, and mobile applications (M4s). *Heliyon*, *9*(6), e16372. https://doi.org/10.1016/j.heliyon.2023.e16372

PALLADIUM CATALYZED DECARBOXYLATIVE ALLYLATION REACTIONS: A BRIEF OVERVIEW

Asik Hossian

Department of Chemistry,

Balurghat College, Balurghat, PIN - 733101, Dakshin Dinajpur, West Bengal, India

Corresponding author E-mail: asik.iitg@gmail.com

Abstract:

Palladium-catalyzed decarboxylative allylation reactions have emerged as an extremely efficient method for the construction of carbon-carbon bonds and the ensuing alkenes represent as versatile building blocks in synthetic chemistry. In the decarboxylative allylation reactions, allyl electrophiles coupled with nucleophiles formed via decarboxylation of carboxylic acid derivatives in a chemo-, regio-, and stereo-selective manner. In the reaction palladium serves as the key catalyst to facilitate the formation of coupling products from the carboxylate and the allyl moiety. The coupling partner carboxylic acids are commercially available in large structural varieties at low cost and these compounds are generally stable to air and moisture, easy to store, and simple to handle. Therefore, the decarboxylative allylation reaction has offered a convenient and versatile application in the synthesis of complex molecular frameworks, including natural products and pharmaceuticals. This review summarizes key developments in palladium-catalyzed decarboxylative allylation reactions, providing insights into the reaction mechanisms, synthetic applications, and future directions for improving its efficacy in chemical synthesis.

Keywords: Decarboxylation, Cross-Coupling Reactions, Allylation, Palladium, C-C Bond Formation.

1. Introduction:

Allylic aromatic compounds are ubiquitous structural motifs found in various natural products (**Figure 1**).[1] In addition, these compounds represent important organic intermediates for the synthesis of complex molecular frameworks due to the versatility of olefin functionalizations.[2] Over the past decades, several methods have been used to construct the allylic arenes (**Scheme 1**). In this vein, the transition metal catalyzed allylation of aryl metal species with allylic electrophiles providing the allylated arenes have been reported.[3] Although this protocol is valuable but suffers from the preactivation of arenes which needs stoichiometric amounts of metal that is not environmentally benign. Alternatively, the Lewis acid-catalyzed Friedel-Crafts aromatic allylation reactions are used because it avoids the prior preparation of the

aryl metal species from the arenes.[4] But, these protocols are limited to substrate scopes and harsh reaction conditions which restrict its application. The Tsuji-Trost allylation reaction has also paying attention towards the synthesis of allylated arenes.[5]
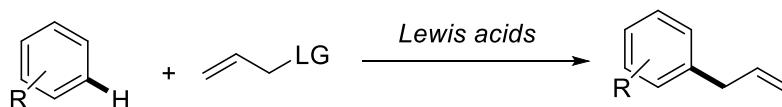

Cathafuran B   Annonidine A   Heptazoline   Mahanimbilol
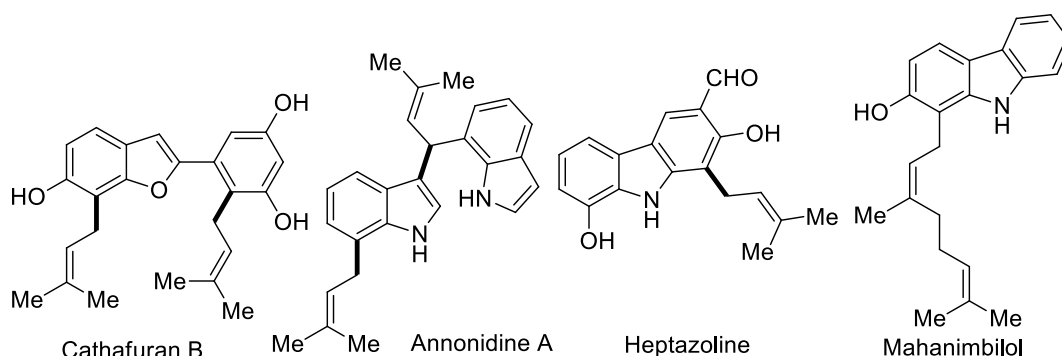
Figure 1: Few selected examples of naturally occurring allylated products

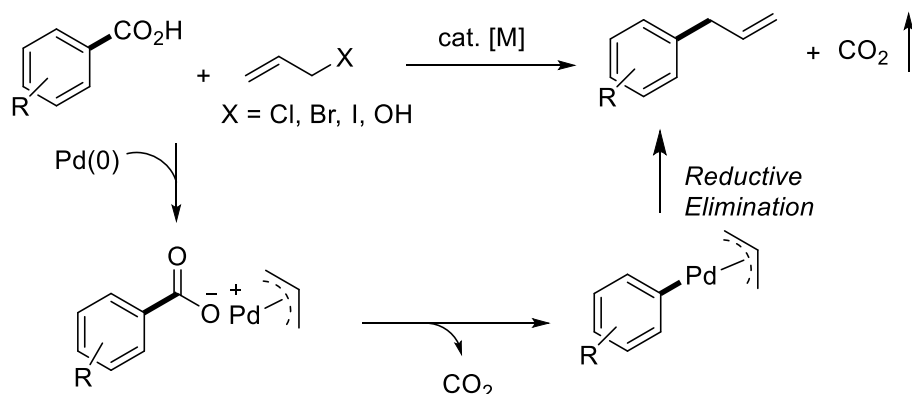a) Conventional allylations with aryl metals
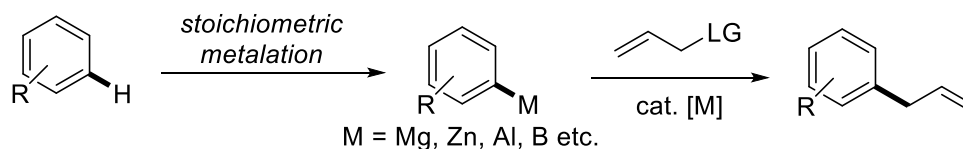
b) Friedel-Crafts allylations

c) Directing group assisted C-H allylations
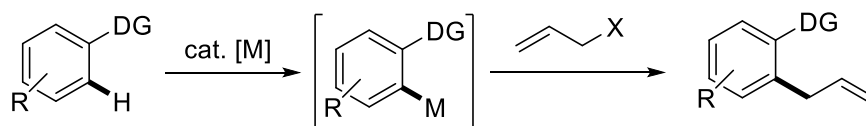
d) Decarboxylative allylations

Scheme 1: Synthesis of aromatic allylic compounds via different methods

Recently, taking the advantages of C-H activation methods, the transition metal catalyzed allylation reactions via C-H activation have been developed using various allylic substitutes.[6] However, the C-H bond activation methods require installation of directing groups in the

substrates to control regioselectivity and subsequent removal of the directing group excludes the synthetic fidelity. To overcome this problem, a regioselective, palladium-catalyzed decarboxylative allylation reaction using inexpensive, commercially available, air and moisture stable aromatic carboxylic acids has been developed (**Scheme 1**). As compared to traditional cross-coupling methods, the decarboxylative cross-couplings has several potential advantages; (i) carboxylic acids are ubiquitous and inexpensive reactants; (ii) decarboxylation can provides the reactive intermediates under neutral conditions; and (iii) the only stoichiometric amount of byproduct is CO_2, which is nontoxic, nonflammable, and easily removed from the reaction medium. Due to remarkable potential of the reaction, decarboxylative allylation reaction has been revealed powerful synthetic method in organic synthesis.[7] In the decarboxylative allylation reactions, a mechanistically distinct decarboxylative metalation occurs to form an organometallic species which have been used as an alternative to aryl halides or organometallic reagents and subsequently coupled with allyl electrophiles affording the coupled allyl products via reductive elimination in a chemo-, regio-, and stereo-selective manner.

2. Decarboxylative allylation reactions

2.1. Palladium catalyzed decarboxylative allylation of allyl esters of acetoacetic acid

In 1980, the Saegusa[8] and Tsuji[9] group first independently showed the palladium catalyzed decarboxylative allylation reactions under very mild conditions. In Tsuji's method, they have used allyl esters of acetoacetic acid in the presence of catalytic amount of $Pd(OAc)_2$ and PPh_3 provided γ,δ-unsaturated methyl ketones in high yield (**Scheme 2, Method A**). In Saegusa's method, they used a variety of acyclic and cyclic keto-esters in the presence of 5.0 mol % of $Pd(PPh_3)_4$ as the catalyst which undergo decarboxylative coupling afforded the desired allylated product with excellent yields (**Scheme 2, Method B**).

Mechanistically, first palladium(0) undergoes an oxidative addition to the allyl ester (**1**) to form a π-allyl-Pd complex and corresponding carboxylate. Then subsequent decarboxylation occurs from the carboxylate, generating the incipient carbanion which is resonance stabilized by the adjacent electron withdrawing keto group. Finally, incipient anion acts as a nucleophile coupled with the electrophile, π-allyl-Pd complex to yield the desired allylated product (**2**) via reductive elimination and regenerating Pd(0) catalyst for next catalytic sequences (**Scheme 2**).
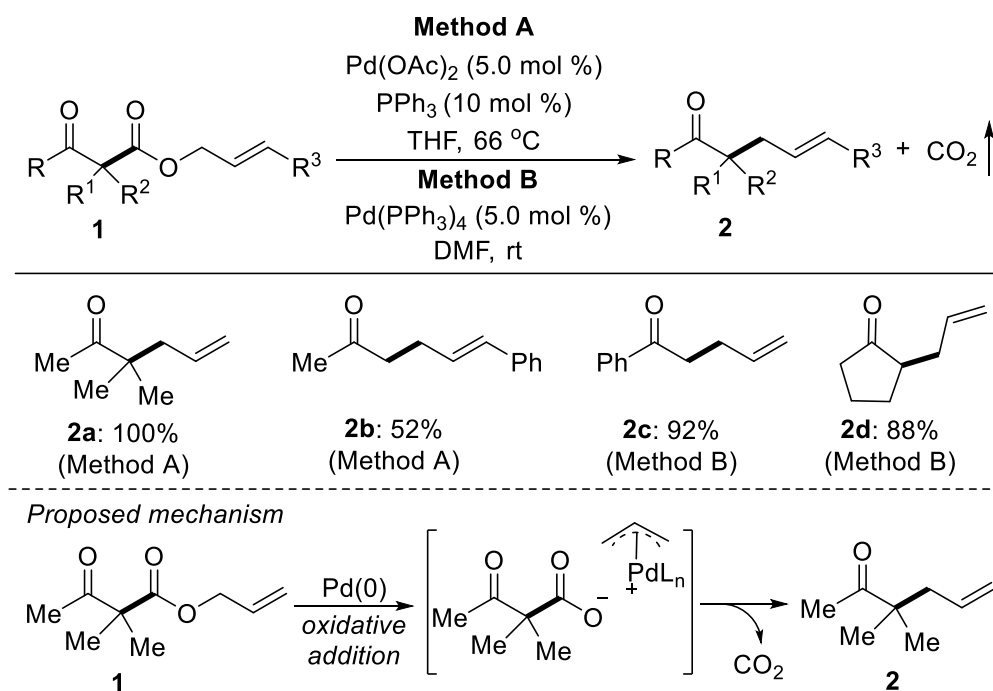
Scheme 2: Palladium catalyzed decarboxylative allylation of allyl esters of acetoacetic acid

2.2. Palladium catalyzed decarboxylative allylation allyl nitroacetic esters

The palladium-catalyzed decarboxylative sp^3-sp^3 allylic alkylation has been widely explored.[10] In sp^3-sp^3 allylation reaction, the incipient anion generates after decarboxylation, which is stabilized by the proximal electron withdrawing groups. In this vein the Tunge group have showed that the allyl nitroacetic esters in the presence of 5.0 mol % $Pd(PPh_3)_4$ undergoes decarboxylative allylation to provide the desired allylation products with excellent yield (**Scheme 3**).[11] A wide range of *α,α*-dialkyl substrates as well as an *α*-phenyl *α*-fluoro ester take part in the reaction efficiently. Here the incipient anion after decarboxylation is stabilized by the proximal nitro group in the reaction. However, the other functional groups such as keto,[12] ester,[13] cyano,[14] sulfone,[15] etc. have also been utilized for this type of stabilization in sp^3-sp^3 decarboxylative allylation reactions.
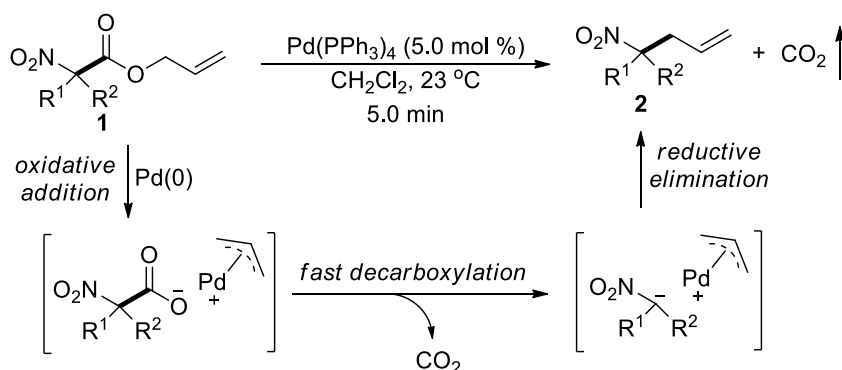
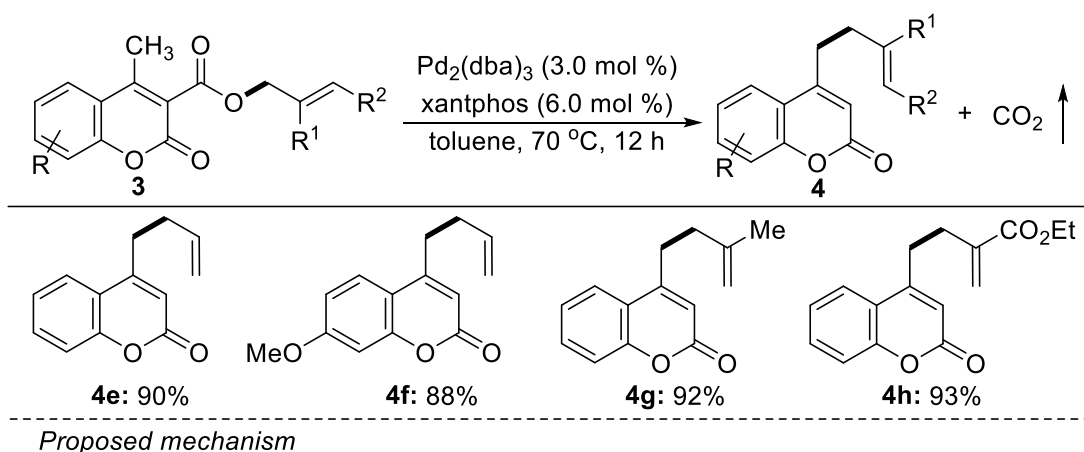**Scheme 3: Palladium catalyzed decarboxylative allylation of allyl nitroacetic esters**

2.3. Palladium catalyzed decarboxylative allylation of allyl esters of 3-carboxylcoumarin derivatives

The decarboxylative sp^2-sp^3 allylation using arene carboxylic acids is not reported earlier due to the instability and rapid protonation of the anion on the sp^2-carbon which is generated after decarboxylation. Therefore, selective sp^2-sp^3 decarboxylative allylation is an extremely challenging target to accomplish. In this vein, Jana *et al.* reported a palladium catalyzed decarboxylative allylation of allyl esters of 3-carboxylcoumarins moiety to furnish allylation product under very mild reaction condition (**Scheme 4**).[16] The reaction is very fascinating due to the formation of functionalized coumarins which are privileged structures in biomedical sciences.[17] Here the anion on sp^2-carbon which is formed after decarboxylation is stabilized by the proximal keto ester group present in the coumarin moiety and regioselective allylation occurred selectively at the C3-carbon of coumarins.
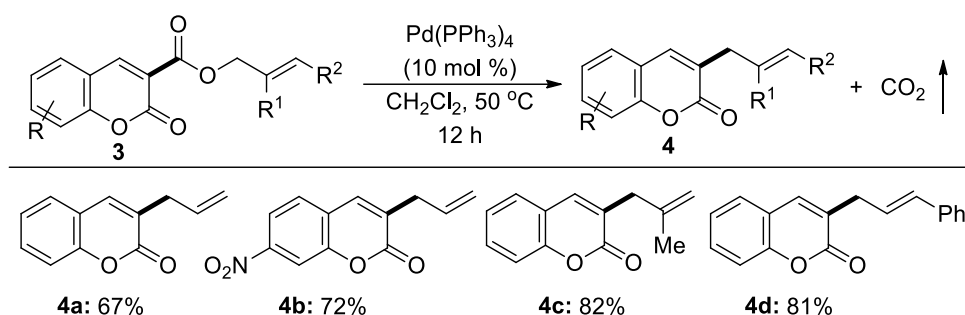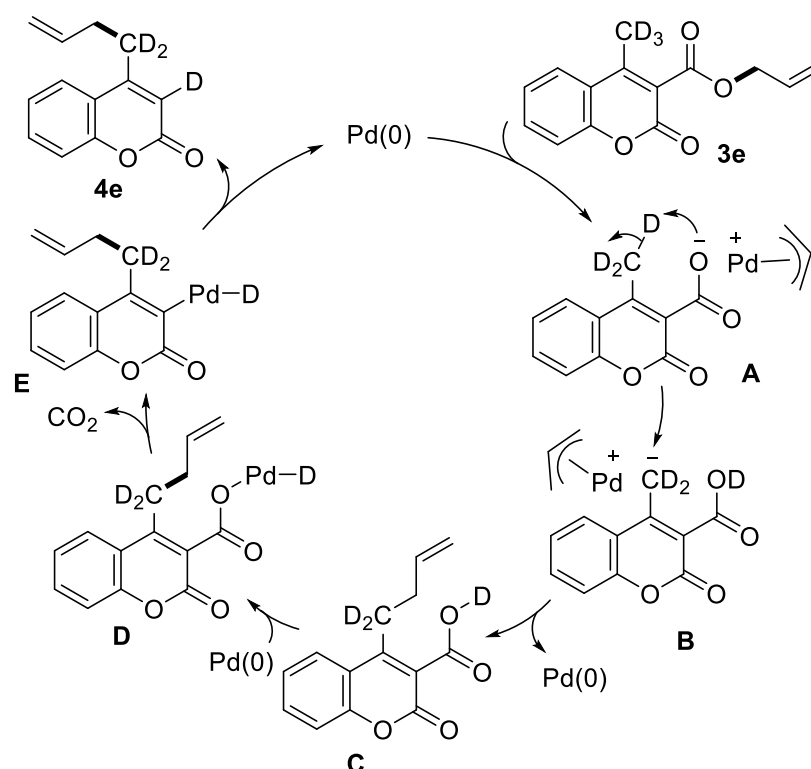

Scheme 4: Decarboxylative allylation of allylic ester of coumarins

Interestingly, when 4-methyl-3-allylcoumarate was used, the reaction did not furnish any desired C3-allylation product, instead a migratory sp^3-sp^3 cross-coupling product was formed. Presumably, this is due to the destabilization of the Csp^2 anion which prefers to migrate at the sp^3-carbon through proton exchange. After rigorous screening, they optimized reaction conditions for this remote decarboxylative γ-allylation of the coumarins moiety in good to excellent yields of allylation product with excellent selectivity at sp^3 center (Scheme 5).[18] To understand the mechanism for this unusual decarboxylative γ-allylation they performed several control experiments and predicted the mechanism of the reaction. Mechanistically, first palladium undergoes oxidative addition with substrates to form a π-allyl palladium complex and the coumarin carboxylate **A**. Then intramolecular 1,5-proton transfer occurs to generate resonance stabilized carbanion at the C4-carbon **B**. Subsequent, reductive elimination of the π-allyl palladium complex forms the C-C bond at C4 position. Finally, palladium catalyzed decarboxylative protonation occurs at C3 position (Scheme 5).

**Scheme 5: Migratory decarboxylative γ-allylation of coumarins**

2.4. Palladium catalyzed intermolecular sp^2-sp^3 decarboxylative allylation using arene carboxylic acids and allyl halides

In 2011, the liu group also reported a palladium catalyzed intermolecular sp^2-sp^3 decarboxylative allylation using arene carboxylic acids and allyl halides (**Scheme 6**).[19] However, the methodology was limited to electron-rich substrates mainly and moderate to low yield of the desired product was obtained. Mechanistically, aryl-palladium species is generated through palladium mediated decarboxylation and subsequently nucleophile attacks to an allyl halide to give the desired aromatic allylic coupling product.

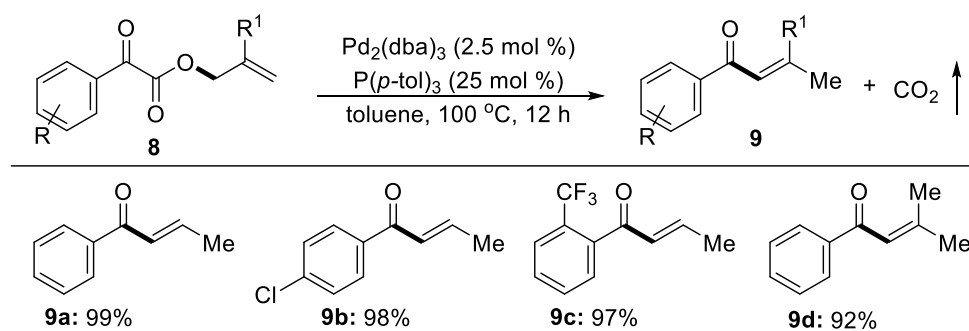## 2.5. Palladium-catalyzed decarboxylative allylation of α-oxocarboxylates

In 2011, Goossen and coworkers have been developed a palladium catalyzed decarboxylative sp^2-sp^3 allylation of non-activated α-oxocarboxylates resulted in α,β-unsaturated

ketones through alkene isomerization (**Scheme 7**).[20] Interestingly, here α-oxocarboxylic acid work as an equivalent of acyl anion donor for this transformation. Mechanistically, first oxidative addition of the carboxylates substrate to Pd(0) lead to the formation of π-allyl-Pd-carboxylate complexes **F**. From the complex **F**, an extrusion of CO_2 leads to the formation of the acyl π-allyl-Pd complex **G**. Finally, reductive elimination of the acyl π-allyl-Pd complex affords the allyl ketone **H**, which is then isomerize to the corresponding stable conjugated vinyl ketone **9** with the help of palladium (**Scheme 7**).
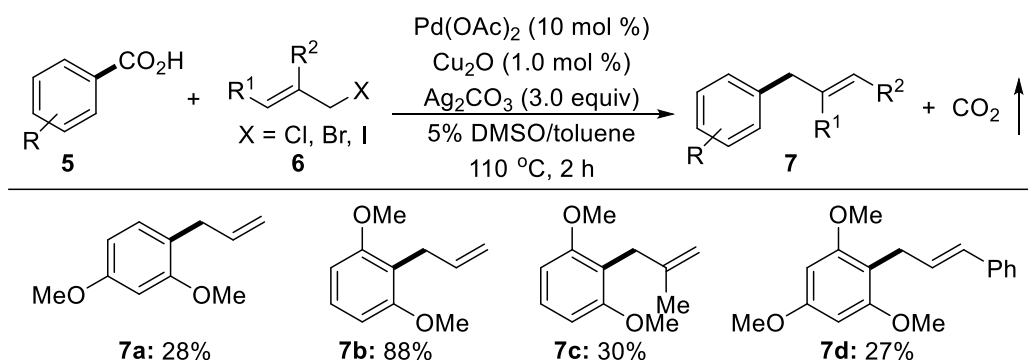
Scheme 6: Palladium-catalyzed intermolecular *sp²-sp³* decarboxylative allylation
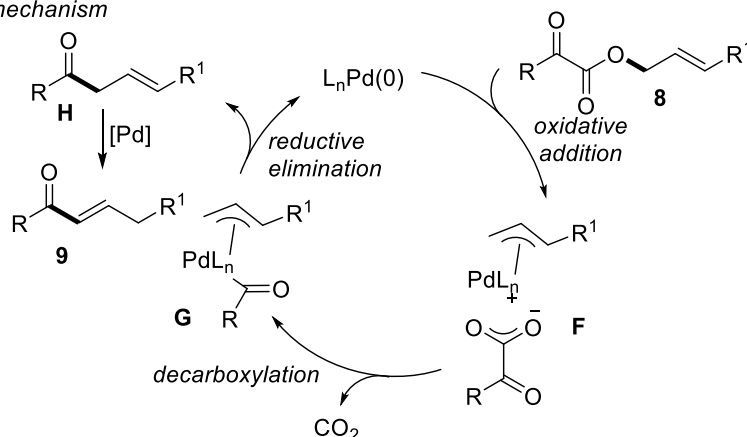
Scheme 7: Palladium-catalyzed decarboxylative allylation of *α*-oxocarboxylates

2.6. Palladium-catalyzed decarboxylative allylation of fluorinated benzoates

In 2014, Goossen's group showed a decarboxylative *sp²-sp³* allylation of arene benzoates with palladium catalysis (**Scheme 8**).[21] For this transformation no stoichiometric additive is required and the reaction proceeds under mild conditions. In the reaction only fluorinated

benzoates provided good to high yield of the desired allylation product with excellent linear selectivity. However, other electron deficient benzoates like allyl ester of nitrobenzoic acids did not provide any desired product.
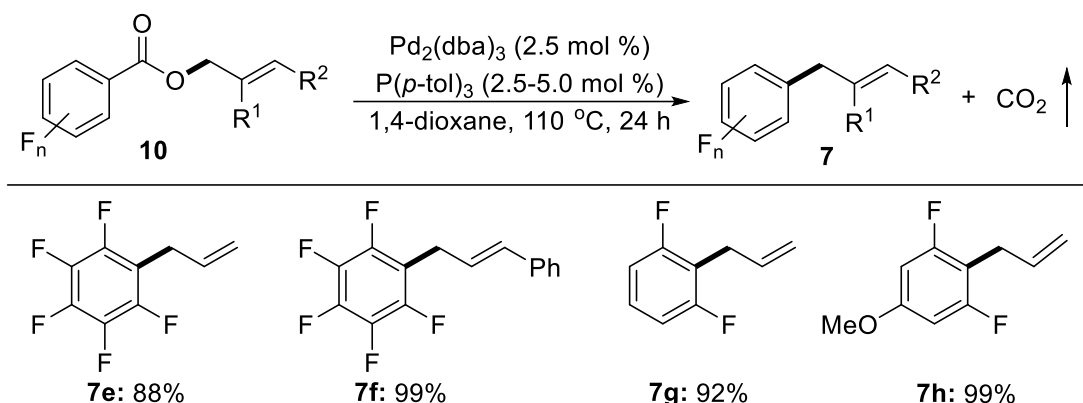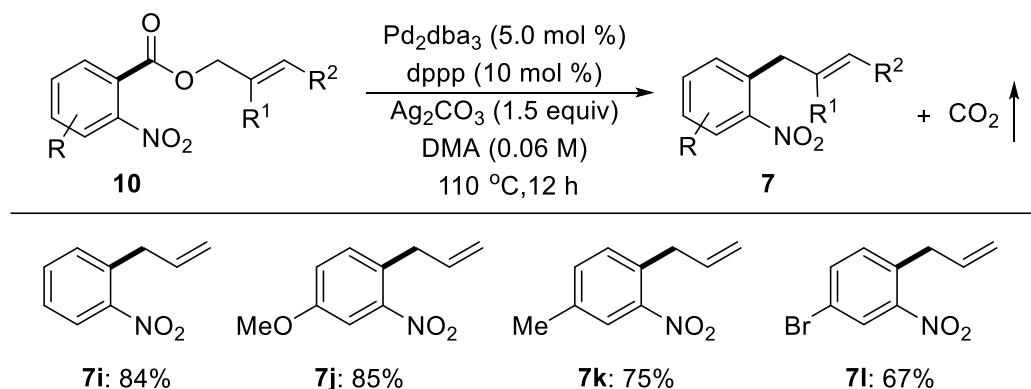

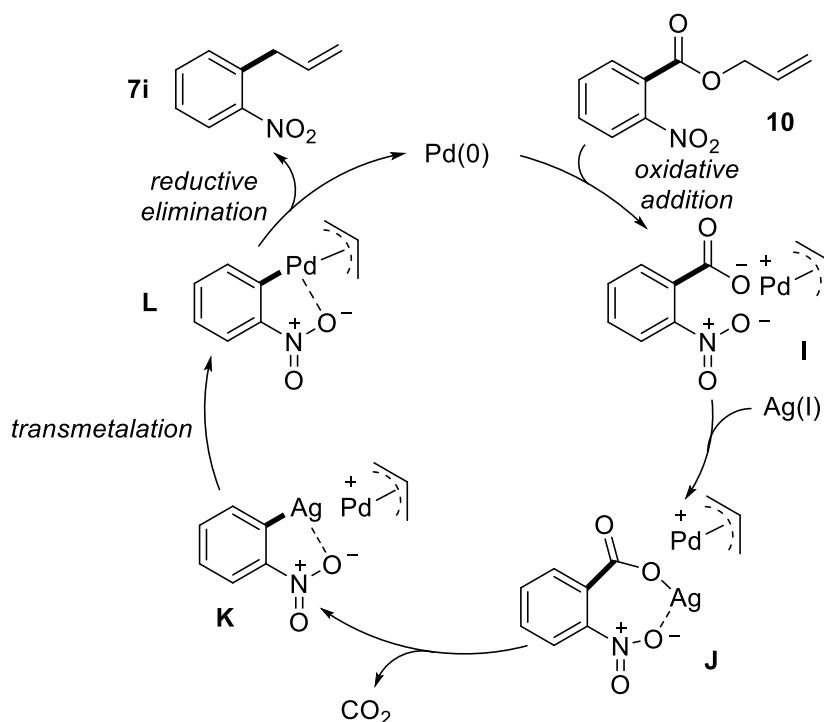**Scheme 8: Palladium-catalyzed decarboxylative allylation of fluorinated benzoates**

2.7. Palladium-catalyzed intramolecular decarboxylative allylation of *ortho* nitrobenzoic esters

Aromatic nitro compounds are beneficial intermediates for the synthesis of agrochemicals, pharmaceuticals, dyes, photo-reactive compounds, high energetic materials, radiopharmaceutical tracers, etc.[22] A facile reduction of the aromatic nitro groups to their corresponding anilines provides common starting materials for the syntheses of a plethora of *N*-heterocycles and natural products.[23] Despite their remarkable properties, access to *ortho*-substituted nitroarenes is restricted due to inherent incompatibility with some organometallic reagents.[24] Therefore, alternative routes to the synthesis of *ortho*-allylnitroarenes using inexpensive, air and moisture stable starting materials are in high demand. Recently, nitrobenzoic acid derivatives have been widely used in palladium-catalyzed decarboxylative cross-coupling reactions.[25] Therefore, synthesis of *ortho*-allylnitroarenes using *ortho* nitrobenzoic acids through novel decarboxylative allylation reaction will be attractive in view of practical applicability. In this vein, in 2014 the Jana group has successfully reported palladium-catalyzed intramolecular decarboxylative allylation of *ortho* nitrobenzoic esters using a combination of 5 mol % Pd_2dba_3, 10 mol % dppp with 1.5 equiv of Ag_2CO_3 in DMA at 110 °C provided *ortho*-allylnitroarenes in excellent yields (**Scheme 9**).[26]

Mechanistically, first palladium(0) undergoes an oxidative addition to the allyl ester **10** to form a π-allyl-Pd complex and *ortho*-nitrobenzoate anion (**I**). Subsequently, silver salt of the corresponding *ortho*-nitrobenzoic acid may form (**J**) and undergo Ag(I)-assisted decarboxylation to afford the corresponding aryl-Ag species **K**. A transmetalation between aryl-Ag and π-allyl-Pd complex generates an aryl-Pd species **L**. Finally, reductive elimination yields the desired allylated product and regenerated the Pd(0) catalyst to complete the catalytic turnover (**Scheme 9**).

Scheme 9: Palladium-catalyzed intramolecular decarboxylative allylation of *ortho* nitrobenzoic esters

To demonstrate the role of the nitro group in decarboxylative allylation, they synthesized diallyl ester **11** where both ester groups are at *ortho* to the nitro group and its corresponding regioisomer **12** where one allyl ester group at the *ortho* and other one at the *meta* position with respect to the nitro group. Under slightly modified reaction conditions, **11** afforded diallylation product in good yield via double decarboxylative allylations in regioselective manner. Whereas, **12** afforded the mono-allylation along with the decarboxylative protonation product at the *ortho* position leaving the *meta* allyl ester intact (**Scheme 10**).[26,] Similarly, *para*-nitro benzoic ester was inactive under the reaction conditions. Presumably, the nitro group at the *ortho* position has a dual role in decarboxylation. First, it can coordinate to either the Ag(I) or Pd(II) prior to and after decarboxylation. This is particularly important for "post-decarboxylation" acting as a C/O

bidentate ligand to form a relatively stable 5-membered palladacycle. Secondly, it imparts a strong inductive effect that stabilizes the incipient anion which leads to rapid decarboxylation followed by allylation.
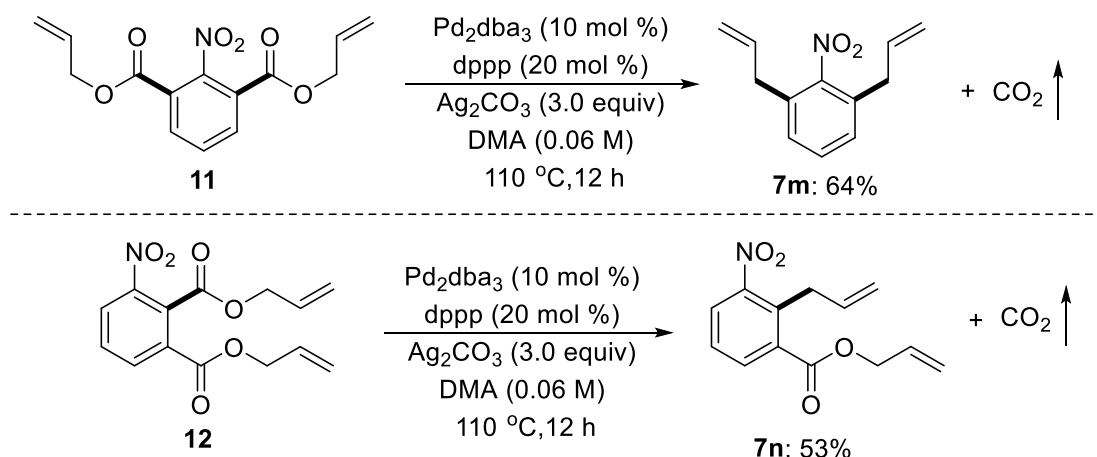
Scheme 10: Selective decarboxylative allylation of nitro benzoic esters[27]

Over the time, various decarboxylative allylation reactions have been reported by different research group under mild reaction conditions with excellent yields and broad substrate scopes.[28]

Conclusion:

Palladium-catalyzed decarboxylative allylation reactions represent a powerful and versatile approach for the proficient formation of carbon-carbon bonds. The ability to use readily available carboxylic acid derivatives and allyl electrophiles under mild conditions makes this reaction highly attractive for the synthesis of complex molecular frameworks. Mechanistic studies suggested that metal mediated decarboxylation occurred followed by the migration of the allyl group through reductive elimination pathway afforded the coupled allylated product. Although significant progress has been made in expanding the scope and improving the efficiency of these reactions, a major drawback of this protocol is that most of the reactions are substrate specific and activated carboxylic acid group in the substrate is essential and also high reaction temperature is required. Therefore, development of decarboxylative allylation reactions for generalised substrates under mild reaction conditions is highly demanded over the time.

References:

1.   (a) Trost, B. M.; Thiel, O. R.; Tsui, H.-C. *J. Am. Chem. Soc*. 2002, *124*, 11616-11617. (b) Yang, Y.; Buchwald, S. L. *J. Am. Chem. Soc*. 2013, *135*, 10642-10645. (c) Yang, Y.; Mustard, T. J. L.; Cheong, P. H-Y.; Buchwald, S. L. *Angew. Chem. Int. Ed*. 2013, *52*, 14098-14102.

2.   (a) Magano, J.; Dunetz, J. R. *Chem. Rev*. 2011, *111*, 2177. (b) Schmidt, A. W.; Reddy, K. R.; KnÖlker, H.-J. *Chem. Rev*. 2012, *112*, 3193-3328.

3. (a) Harrington-Frost, N.; Leuser, H.; Calaza, M. I.; Kneisel, F. F.; Knochel, P. *Org. Lett*. 2003, *5*, 2111-2114. (b) Evans, P. A.; Uraguchi, D. *J. Am. Chem. Soc*. 2003, *125*, 7158-7159. (c) Kacprzynski, M. A.; May, T. L.; Kazane, S. A.; Hoveyda, A. H. *Angew. Chem., Int. Ed*. 2007, *46*, 4554-4558. (d) Ohmiya, H.; Makida, Y.; Tanaka, T.; Sawamura, M. *J. Am. Chem. Soc*. 2008, *130*, 17276-17277. (e) Kiyotsuka, Y.; Acharya, H. P.; Katayama, Y.; Hyodo, T.; Kobayashi, Y. *Org. Lett*. 2008, *10*, 1719-1722. (f) Polet, D.; Rathgeb, X.; Falciola, C. A.; Langlois, J. B.; El Hajjaji, S.; Alexakis, A. *Chem. Eur. J*. 2009, *15*, 1205-1216.

4. (a) Kodomari, M.; Nawa, S.; Miyoshi, T. *J. Chem. Soc*., *Chem. Commun*. 1995, 1895-1896. (b) Niggemann, M.; Meel, M. J. *Angew. Chem., Int. Ed*. 2010, *49*, 3684-3687.

5. (a) Tsuji, J. *Tetrahedron* 1986, *42*, 4361-4609. (b) Trost, B. M.; Crawley, M. L. *Chem. Rev*. 2003, *103*, 2921-2944.

6. (a) Manikandan, R.; Madasamy, P.; Jeganmohan, M. *Chem. Eur. J*. 2015, *21*, 13934-13938. (b) Kumar, G. S.; Kapur, M. *Org. Lett*. 2016, *18*, 1112-1115. (c) Mishra, N. K.; Sharma, S.; Park, J.; Han, S.; Kim, I. S. *ACS Catal*. 2017, *7*, 2821-2847.

7. (a) Rayabarapu, D. K.; Tunge, J. A. *J. Am. Chem. Soc*. 2005, *127*, 13510-13511. (b) Waetzig, S. R.; Tunge, J. A. *J. Am. Chem. Soc*. 2007, *129*, 4138-4139. (c) Waetzig, S. R.; Tunge, J. A. *J. Am. Chem. Soc*. 2007, *129*, 14860-14861. (d) Enquist Jr, J. A.; Stoltz, B. M. *Nature*, 2008, *453*, 1228-1231.

8. Shimizu, I.; Yamada, T.; Tsuji, J. *Tetrahedron Lett*. 1980, *21*, 3199-3202.

9. Tsuda, T.; Chujo, Y.; Nishi, S.; Tawara, K.; Saegusa, T. *J. Am. Chem. Soc*. 1980, *102*, 6381-6384.

10. For recent reviews, see: (a) Trost, B. M.; Crawley, M. L. *Chem Rev*. 2003, *103*, 2921-2943. (b) Weaver, J. D.; Recio, III, A.; Grenning, A. J.; Tunge, J. A. *Chem. Rev*. 2011, *111*, 1846-1913. For allylic sp^3-sp^3 alkylations, see: (c) Nakamura, M.; Hajra, A.; Endo, K.; Nakamura, E. *Angew. Chem. Int. Ed*. 2005, *44*, 7248-7251. (d) You, S.-L.; Dai, L.-X. *Angew. Chem. Int. Ed*. 2006, *45*, 5246-5248. (e) Burger, E. C.; Tunge, J. A. *J. Am. Chem. Soc*. 2006, *128*, 10002-10003. (f) Waetzig, S. R.; Rayabarapu, D. K.; Weaver, J. D.; Tunge, J. A. *Angew. Chem. Int. Ed*. 2006, *45*, 4977-4980. (g) Waetzig, S. R.; Tunge, J. A. *J. Am. Chem. Soc*. 2007, *129*, 4138-4139. (h) Chattopadhyay, K.; Jana, R.; Day, V. W.; Douglas, J. T.; Tunge, J. A. *Org. Lett*. 2010, *12*, 3042-3045. (i) Behenna, D. C.; Liu, Y.; Yurino, T.; Kim, J.; White, D. E.; Virgil, S. C.; Stoltz, B. M. *Nat. Chem*. 2012, *4*, 130-133. (j) Trost, B. M.; Osipov, M. *Angew. Chem. Int. Ed*. 2013, *52*, 9176-9181. (k) Li, Z.; Zhang, S.; Wu, S.; Shen, X.; Zou, L.; Wang, F.; Li, X.; Peng, F.; Zhang, H.; Shao, Z. *Angew. Chem. Int. Ed*. 2013, *52*, 4117-4121. (l) Gartshore, C. J.; Lupton, D. W. *Angew. Chem. Int.*

Ed. 2013, *52*, 4113-4116. (m) Ghosh, S.; Bhunia, S.; Kakde, B. N.; De, S.; Bisai, A. *Chem. Commun.* 2014, *50*, 2434-2437.

11. (a) Tsuji, J.; Yamada, T.; Minami, I.; Yuhara, M.; Nisar, M.; Shimizu, I. *J. Org. Chem.* 2007, *52*, 2988-2995. (b) Grenning, A. J.; Tunge, J. A. *Org. Lett.* 2010, *12*, 740-742. (c) Schmitt, M.; Grenning, A. J.; Tunge, J. A. *Tetrahedron Lett.* 2012, *53*, 4494-4497.

12. Tsuda, T.; Chujo, Y.; Nishi, S.-i.; Tawara, K.; Saegusa, T. *J. Am. Chem. Soc.* 1980, *102*, 6381-6384.

13. Imao, D.; Itoi, A.; Yamazaki, A.; Shirakura, M.; Ohtoshi, R.; Ogata, K.; Ohmori, Y.; Ohta, T.; Ito, Y. *J. Org. Chem.* 2007, *72*, 1652-1658.

14. Recio III, A.; Tunge, J. A. *Org. Lett.* 2009, *11*, 5630-5633.

15. (a) Weaver, J. D.; Ka, B. J.; Morris, D. K.; Thompson, W.; Tunge, J. A. *J. Am. Chem. Soc.* 2010, *132*, 12179-12181. (b) Shibata, N.; Fukushi, K.; Furukawa, T.; Suzuki, S.; Tokunaga, E.; Cahard, D. *Org. Lett.* 2012, *14*, 5366-5369.

16. Jana, R.; Trivedi, R.; Tunge, J. A. *Org. Lett.* 2009, *11*, 3434-3436.

17. (a) Horton, D. A.; Bourne, G. T.; Smythe, M. L. *Chem. Rev.* 2003, *103*, 893. (b) Estevez-Craun, A.; Gonzalez, A. G. *Nat. Prod. Rep.* 1997, 465. (c) Ngameni, B.; Touaibia, M.; Patnam, R.; Belkaid, A.; Sonna, P.; Ngadjui, B. T.; Annabi, B.; Roy, R. *Phytochemistry* 2006, *67*, 2573. (d) Chun, K.; Park, S.-K.; Kim, H. M.; Choi, Y.; Kim, M.-H.; Park, C.-H.; Joe, B.-Y.; Chun, T. G.; Choi, H.-M.; Lee, H.-Y.; Hong, S. H.; Kim, M. S.; Nam, K.-Y.; Han, G. *Biorg. Med. Chem.* 2008, *16*, 530.

18. Jana, R.; Partridge, J. J.; Tunge, J. A. *Angew. Chem. Int. Ed.* 2011, *50*, 5157-5161.

19. Wang, J.; Cui, Z.; Zhang, Y.; Li, H.; Wua, L.-M.; Liu, Z. *Org. Biomol. Chem.* 2011, *9*, 663-666.

20. Rodríguez, N.; Manjolinho, F.; Grünberg, M. F.; Gooßen, L. J. *Chem. Eur. J.* 2011, *17*, 13688-13691.

21. Pfister, K. F.; Grünberg, M. F.; Gooßen, L. J. *Adv. Synth. Catal.* 2014, *356*, 3302-3306.

22. (a) *The Nitro Group in Organic Synthesis*; Ono, N., Ed.; Wiley-VCH: New York. 2001. (b) Hoogenraad, M.; ven der Linden, J. B.; Smith. A. A. *Org. Proc. Res. Dev.* 2004, *8*, 469-476.

23. For nitro reduction, see: (a) Tafesh, A.M.; Weiguny, J. *Chem. Rev.* 1996, *96*, 2035-2052. (b) Westerhaus, F. A.; Jagadeesh, R. V.; Wienhöfer, G.; Pohl, M.-M.; Radnik, J.; Surkus, A.-E.; Rabeah, J.; Junge, K.; Junge, H.; Nielsen, M.; Brückner, A.; Beller, M. *Nat. Chem.* 2013, *5*, 537-543. For *N*-heterocycle synthesis, see: (c) Quintero, L. M. A.; Palma, A.; Nogueras, M.; Cobo, J. *Synthesis*, 2012, *44*, 3765-3782. For natural product synthesis, see: (d) Fu, L. *J. Heterocycl. Chem.* 2010, *26*, 433-480.

24. (a) Severin, T. *Angew. Chem.* 1958, *70*, 164-165. (b) Bartoli, G.; Palmieri, G.; Bosco, M.; Dalpozzo, R. *Tetrahedron Lett*. 1989, *30*, 2129-2132. (c) Dobson, D. R.; Gilmore, J.; Long, D. A. *Synlett* 1992, 79-80. (d) Ricci, A.; Fochi, M. *Angew. Chem. Int. Ed*. 2003, *42*, 1444-1446.

25. For reviews, see: (a) Goossen, L. J.; Collet, F.; Goossen, C. *Israel J. Chem.* 2010, *50*, 617-629. (b) Rodríguez, N.; Goossen, L. J. *Chem. Soc. Rev*. 2011, *40*, 5030-5048. (c) Dzik, W. I.; Lange, P. P.; Gooßen, L. J. *Chem. Sci*, 2012, *3*, 2671-2678. For cross-couplings, see: (d) Gooßen, L. J.; Deng, G.; Levy, L. M. *Science*, 2006, *313*, 662-664. (e) Waetzig, S. R.; Tunge, J. A. *J. Am. Chem. Soc*. 2007, 129, 14860-14861. (f) Goossen, L. J. Rodríguez, N.; Melzer, B.; Linder, C.; Deng, G.; Levy, L. M. *J. Am. Chem. Soc*. 2007, *129*, 4824-4833. (g) Gooßen, L. J.; Zimmermann, B.; Knauber, T. *Angew. Chem. Int. Ed*. 2008, *47*, 7103-7106. (h) Goossen, L. J.; Rodríguez, N.; Linder, C. *J. Am. Chem. Soc.* 2008, *130*, 15248-15249. (i) Duan, Z.; Ranjit, S.; Zhang, P.; Liu, X. *Chem. Eur. J*. 2009, *15*, 3666-3669. (j) Wanga, Z.; Dinga, Q.; Hea, X.; Wua, J. *Tetrahedron*, 2009, 65, 4635-4638. (k) Gooßen, L. J.; Rodríguez, N.; Lange, P. P.; Linder, C. *Angew. Chem. Int. Ed.* 2010, *49*, 1111-1114. (l) Luo, J.; Lu, Y.; Liu, S.; Liu, J.; Deng, G.-J. *Adv. Synth. Catal*. 2011, *353*, 2604-2608. (m) Zhang, Y.; Patel, S.; Mainolfi, N. *Chem. Sci*. 2012, *3*, 3196-3199. (n) Zhou, J.; Wu, G.; Zhang, M.; Jie, X.; Su, W. *Chem. Eur. J*. 2012, 18, 8032-8036. (o) Hu, P.; Shang, Y.; Su, W. *Angew. Chem. Int. Ed*. 2012, *51*, 5945-5949. (p) Bhadra, S.; Dzik, W. I.; Goossen, L. J. *J. Am. Chem. Soc*. 2012, *134*, 9938-9941. (q) Song, B.; Knauber, T.; Gooßen, L. J. *Angew. Chem. Int*. *Ed*. 2013, *52*, 2954-2958. (r) Tang, J.; Gooßen, L. J. *Org. Lett*. 2014, *16*, 2664-2667. For decarboxylative Heck reactions, see: (s) Myers, A. G.; Tanaka, D.; Mannion, M. R. *J. Am. Chem. Soc*. 2002, *124*, 11250-11251. (t) Fu, Z.; Huang, S.; Su, W.; Hong, M. *Org. Lett.* 2010, *12*, 4992-4995.

26. Hossian, A.; Singha, S.; Jana, R. *Org. Lett*. 2014, *16*, 3934-3937.

27. Hossian, A. Development of Decarboxylative Cross-Coupling Reactions, *AcSIR*, *Ph.D. Thesis*, 2018.

28. (a) Ramirez, N. P.; Villarreal, T. L.; Gonzalez-Gomez, J. C. *EurJOC*. 2020, *10*, 1539-1550. (b) Geniller, L.; Kraim, H. B.; Clot, E.; Taillefer, M.; Jaroschik, F.; Prieto, A. *Chem. Eur. J.* 2024, *30*, e202401494.

A MACHINE LEARNING-AIDED FRAMEWORK FOR PREDICTING CRITICAL HEAT FLUX

Manisha Phukan

Department of Physics,

Lalit Chandra Bharali College, Maligaon, Guwahati

Corresponding author E-mail: mphukan09@gmail.com

Abstract:

The maximum limit of heat removal capacity before a sharp decline in efficiency or perhaps a catastrophic failure in thermal systems is known as the Critical Heat Flux (CHF). Conventional empirical correlations frequently don't transfer to different operating circumstances and geometries. This chapter introduces a *machine learning-aided* technique to use a *physics-informed* approach to categorize CHF into *Low*, *Medium*, and *High* levels. Three classes were created using a dataset of 1,865 experimental records from Zhao *et al.* (2020), and classifiers called *Random Forest* and *XGBoost* were trained, adjusted, and assessed. According to the results, *Random Forest* outperformed *Logistic Regression* and *XGBoost* under initial conditions, attaining an accuracy of 88.2% on the test set. The robustness of tree-based ensemble approaches was demonstrated by further *hyperparameter tuning*, which increased XGBoost to 86.86% test accuracy and produced a mean cross-validation accuracy of 88.61%. The potential of data-driven models for *predicting CHF* in a variety of thermal engineering applications is highlighted in this chapter.

Keywords: Critical Heat Flux, Machine Learning, Random Forest, XGBoost, Hyperparameter Tuning

Introduction:

Fundamental Physics of Critical Heat Flux (CHF)

The critical heat flux (CHF) is the highest amount of heat that a thermal system can remove before abruptly degrading heat transfer, which might result in catastrophic failures such as thermal runaway or component destruction (Sarbu, 2018). Boiling events, in particular nucleate and film boiling, are inherently tied to the mechanics behind CHF. Vapor bubble creation and departure promote heat transmission from a hot surface to a liquid under nucleate boiling conditions. These bubbles could, however, combine to create a vapor blanket over the heated surface as heat flux rises, significantly decreasing liquid-to-surface contact and resulting

in a precipitous decline in heat transfer efficiency. In convective heat transport, a fundamental heat flow connection is provided by:

$$q'' = h\Delta T, \tag{1}$$

where the convective heat transfer coefficient is represented by h, the heat flow by q'', and the temperature differential between the heated surface and the bulk fluid by ΔT. The issue is more complicated when boiling is involved. The correlation (Nikolayev, 2016) is a commonly used correlation to forecast CHF in pool boiling:

$$q''_{CHF} = C\, h_{fg}\, \rho_v\, [\sigma\, g\, (\rho_l - \rho_v)]^{1/4} \tag{2}$$

where σ is the surface tension, g is the gravitational acceleration, h_{fg} is the latent heat of vaporization, ρ_v and ρ_l are the vapor and liquid densities, and C is an empirical constant. Many conventional prediction models are based on this association, which highlights how CHF is influenced by fluid characteristics and operational circumstances.

Traditional Empirical and Semi-Empirical Models

In the past, empirical and semi-empirical correlations obtained from in-depth experimental research have dominated the assessment of CHF. Correlations between CHF and many operational and geometric characteristics have been postulated by researchers. A common empirical formulation, for instance, may be written as follows:

$$qCHF'' = K\, Gn, \tag{3}$$

where G is a collection of dimensionless factors that capture the impacts of fluid characteristics, mass flux, and flow geometry, and K and n are constants found by experimentation. The generalizability of such models is, however, constrained by the assumptions made during their derivation and the fact that they are frequently customized to certain ranges of operating circumstances and geometries (Kim, 2011).

Emergence of Machine Learning in Thermal Sciences

With the development of artificial intelligence (AI) and machine learning (ML), there are now strong substitutes for conventional CHF prediction techniques. When there are intricate, nonlinear relationships between several variables, machine learning approaches are especially wellsuited. Many machine learning models, from support vector machines and neural networks to ensemble techniques like Random Forest and XGBoost, have been used in thermal sciences to forecast CHF and other boiling events. The capacity to estimate interactions between variables like pressure, mass flow, hydraulic diameter, and exit quality without explicitly depending on pre-established physical correlations is a significant benefit of machine learning techniques. According to Mohanraj *et al.* (2015), machine learning algorithms have the ability to directly

discover complex patterns from experimental data, possibly surpassing traditional empirical correlations. Furthermore, ML offers a data-driven substitute that can adjust to various geometries and different operating situations.

Physics-Informed Machine Learning

The creation of physics-informed machine learning frameworks is a new trend in the fusion of machine learning and conventional physics. These methods improve model generalization and interpretability by integrating established physical rules and restrictions into the learning process. Adding a penalty element to an ML model's loss function to ensure conformity with physical principles is a common tactic:

$$L = Ldata + \lambda Lphysics, \qquad\qquad (4)$$

The usual data-driven loss (e.g., mean squared error) is represented by L_{data}, the departure from known physical laws is quantified by $L_{physics}$, and λ is a weighting factor that balances the two terms. These hybrid techniques, which draw on both empirical data and basic physics, have demonstrated potential in enhancing CHF predictions.

Comparative Studies and Recent Advances

The potential of ensemble learning techniques in CHF prediction has been brought to light by recent studies. In their exploration of neural network applications, Mohanraj *et al.* (2015) emphasized the need for exacting hyperparameter tweaking in order to fully capture the underlying physics. By including physics-informed features into the machine learning framework, Zhao *et al.* (2020) expanded on this work and achieved better prediction performance than conventional correlations. Because ensemble approaches like Random Forest and XGBoost are resilient in addressing non-linearities and lowering model variance, comparative studies repeatedly show that they produce superior outcomes.

Although conventional empirical correlations have historically improved our knowledge and capacity to predict CHF, their limited generalizability calls for the investigation of alternate approaches. Accurately predicting CHF under a variety of scenarios is made possible by machine learning, especially when combined with physics-based approaches. Building on previous developments, this chapter introduces a machine learning-assisted framework that uses the Random Forest and XGBoost algorithms to categorize CHF into three different groups: Low, Medium, and High. The methodology, experimental setup, model training, and evaluation are covered in depth in the parts that follow, highlighting the promise of data-driven approaches to improve thermal systems' efficiency and safety.

Literature Review

A number of academics have looked into using machine learning techniques to solve problems with heat transport and critical heat flux (CHF) prediction. Jalili and Mahmoudi (2025) early research on the classification of boiling heat transfer regimes using neural networks demonstrated both the models' capacity to learn intricate patterns from experimental data and the necessity of meticulous hyperparameter tuning for best results. Similar to this, Cuomo *et al.* (2022) presented a physics-informed machine learning methodology that incorporates domainspecific knowledge into the training process. This helps the model make predictions that are more physically realistic and improves its generalization across a range of operating conditions.

Ensemble learning techniques, including Random Forest and Gradient Boosted Decision Trees (XGBoost), have been the subject of numerous studies at the same time. Breiman (2001) showed how Random Forest can handle high-dimensional data with better accuracy and lower variance by combining the predictions of several decision trees to capture nonlinear relationships. Similarly, XGBoost, a technique that generates decision trees in a sequential fashion to reduce residual errors and improve prediction accuracy, was developed by Chen and Guestrin (2016). In the complicated and varied environment of CHF prediction, where interactions among multiple parameters greatly impact results, these ensemble strategies have proven especially useful.

The lack of defined benchmarks is still a major obstacle in spite of these encouraging advancements. Comparing the effectiveness of several machine learning models under various circumstances is challenging in the absence of uniform evaluation measures, cross-validation procedures, and methodical hyperparameter tuning. The current effort fills this gap by putting into practice a methodical approach intended to provide trustworthy and repeatable evaluation standards. This chapter attempts to offer a strong framework for evaluating and contrasting machine learning techniques in the prediction of CHF by combining consistent performance criteria, thorough hyperparameter tweaking, and rigorous cross-validation.

Materials and Methods:

Dataset Description

Zhao *et al.* (2020) assembled a dataset of 1,865 experimental records to investigate critical heat flux (CHF) phenomena. A number of crucial parameters that characterize the experimental setup's geometrical features and operational conditions are included in every record. These parameters are as follows: channel length (in mm), hydraulic diameter (D_h in mm), equivalent diameter (D_e in mm), exit quality (x_e_out), mass flux (in kg/m^2-s), operating

pressure (in MPa), and the measured CHF (in MW/m^2). When combined, these characteristics offer a thorough understanding of the fluid and thermal dynamic environment affecting CHF.

Since the main goal of this study is to categorize CHF into three different groups—Low, Medium, and High—quantile-based binning was used to discretize the continuous CHF variable (chf_exp in MW/m^2). Effective training and evaluation of machine learning models depend on a fairly balanced distribution of records across the three classes, which is ensured by this method. A selection of representative records from the dataset are shown in the table below, which highlights the diversity and variety of the main characteristics.

Table 1: Example Records from the CHF Dataset

Record ID	Pressure (MPa)	Mass Flux (kg/m^2-s)	x_e_out	D$_e$ (mm)	D$_h$ (mm)	CHF (MW/m^2)
1	0.39	5600	-0.1041	3.0	3.0	11.3
2	0.31	6700	-0.0596	3.0	3.0	10.6
3	0.33	4300	-0.0395	3.0	3.0	7.3
4	0.62	6400	-0.1460	3.0	3.0	12.8
5	0.64	4700	-0.0849	3.0	3.0	11.0

Machine Learning Models

Based on experimental data, three distinct machine learning models were used in this study to forecast and categorize critical heat flux (CHF). The first model, Logistic Regression (LR), is a baseline linear technique that uses a linear combination of characteristics to represent the connection between the input features and the probability of each class. Notwithstanding its ease of use and interpretability, logistic regression offers a helpful standard by which more sophisticated techniques can be evaluated, even though it might not be able to capture intricate nonlinear connections.

The class that represents the mode of the classes predicted by individual trees is produced by the second model, Random Forest (RF), an ensemble learning technique that builds a large number of decision trees during training. Because of this averaging procedure, which lowers overall variance and lessens overfitting, Random Forest is especially capable of managing highdimensional data and identifying nonlinear feature correlations.

The gradient boosting approach used in the third model, XGBoost (XGB), creates decision trees in a sequential fashion, with each new tree attempting to fix the mistakes of its predecessors. XGBoost can provide great prediction performance and scalability on big datasets

by using gradient descent to optimize a particular loss function. Its efficacy in challenging classification tasks is further increased by the methods it incorporates to deal with missing information and avoid overfitting.

Data Splitting and Preprocessing

The dataset was split 80/20 between training and testing sets to ensure dependable model training and evaluation. This method guarantees that a sizable amount of the data is utilized to uncover the underlying patterns, with a different test set set aside for an objective assessment of the model's functionality.

Data preprocessing entails a number of crucial stages. In order to ensure that every feature contributes equally to the model, StandardScaler has been used to standardize the numerical variables because Logistic Regression is sensitive to the scale of input data. Tree-based techniques, such as Random Forest and XGBoost, on the other hand, can function well with unscaled data and are intrinsically invariant to scaling. Additionally, LabelEncoder was used to translate categorical data like geometry and author into numerical representations. In order to ensure a balanced distribution across classes for efficient classification, the target variable, which represents CHF, was further discretized into three classes (Low, Medium, and High) based on quantile criteria.

Hyperparameter Tuning

Careful hyperparameter tweaking is necessary to maximize the performance of machine learning models, and in this study, GridSearchCV was used to methodically examine the parameter space. The number of trees (n_estimators), the maximum depth of each tree (max_depth), and the minimum number of samples needed to divide an internal node (min_samples_split) were among the important hyperparameters that were changed for the Random Forest. These parameters are essential for managing model complexity and striking a balance between variance and bias.

Likewise, hyperparameter tuning for the XGBoost model concentrated mainly on max_depth, n_estimators, and learning rate (learning_rate), which establishes the step size in the optimization process. A 5-fold cross-validation technique was incorporated into the grid search procedure to further guarantee the dependability of the chosen parameters. In addition to reducing overfitting, this cross-validation ensures that the adjusted hyperparameters work well when applied to new data by offering a reliable assessment of model performance across various data subsets.

Results and Discussion:

A detailed analysis of the data was the first step in the evaluation of the critical heat flux (CHF) prediction models. Expressed in MW/m^2, the experimental CHF values show a wide range, which is indicative of the intrinsic unpredictability in the operating conditions. This wide dispersion, as shown in Figure 1, emphasizes how difficult it is to effectively model CHF because the models need to be resilient enough to handle a variety of situations.
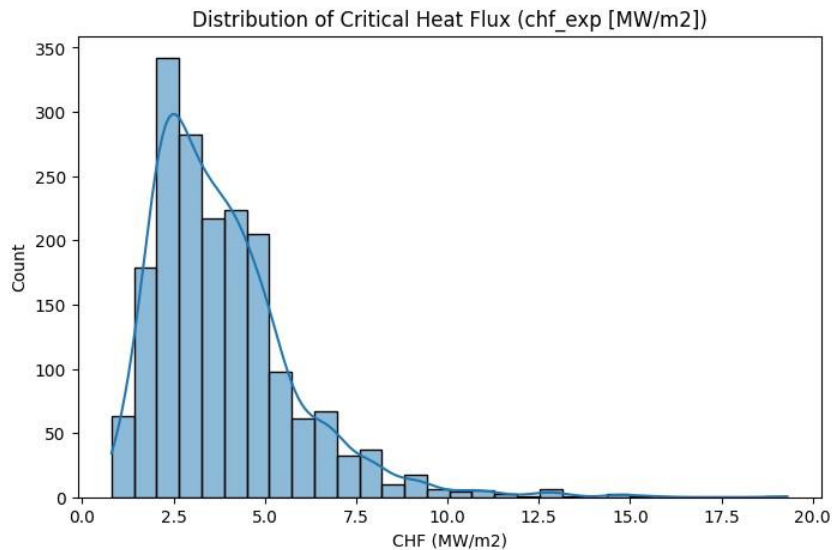

Figure 1: Distribution of Critical Heat Flux (CHF) in MW/m²

Quantile-based binning was used to discretize the continuous target into three classes (Low, Medium, and High) after the raw CHF values were analyzed. The number of samples in each CHF class is displayed in Figure 2, which displays a very balanced distribution. For objective model training and precise classification performance, this balanced class distribution is essential.
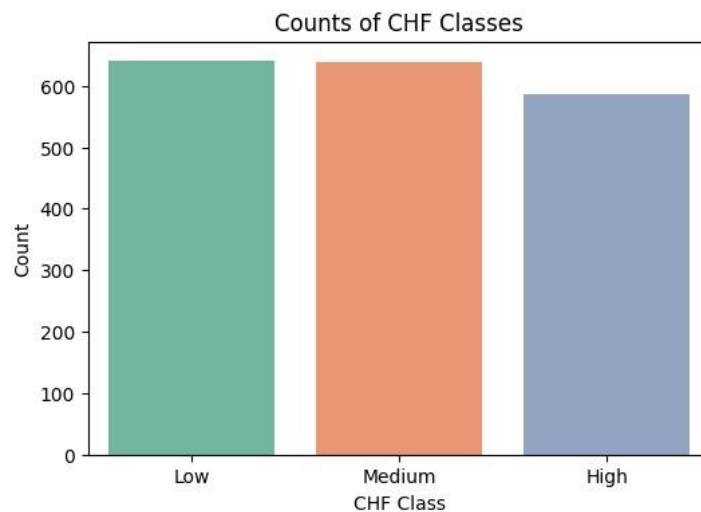

Figure 2: Counts of CHF Classes (Low, Medium, High)

The performance of various machine learning models on the dataset was then assessed. The accuracies of the original, untuned models were as follows: XGBoost obtained 87.94%, Random Forest obtained 88.20%, and Logistic Regression obtained 77.48%. A bar chart summarizing these accuracy results is shown in Figure 3, which makes it evident that the ensemble approaches (Random Forest and XGBoost) perform better than the baseline linear model.
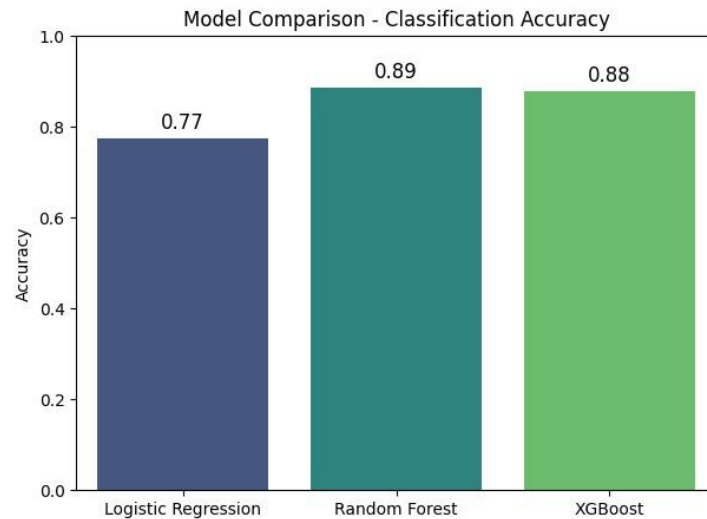

**Figure 3: Model Comparison - Classification Accuracy (Untuned Models).**

Confusion matrices were created in order to obtain a better understanding of the models' categorization behaviors. Moderate misclassifications are found in the Logistic Regression confusion matrix (Figure 4), especially between the Medium and High classes. While the Medium class still presents certain difficulties, the Random Forest confusion matrix (Figure 5) shows better performance for the Low and good classes with good recall and precision. In a similar vein, the confusion matrix for XGBoost (Figure 6) performs similarly to Random Forest, with occasionally somewhat better differentiation.
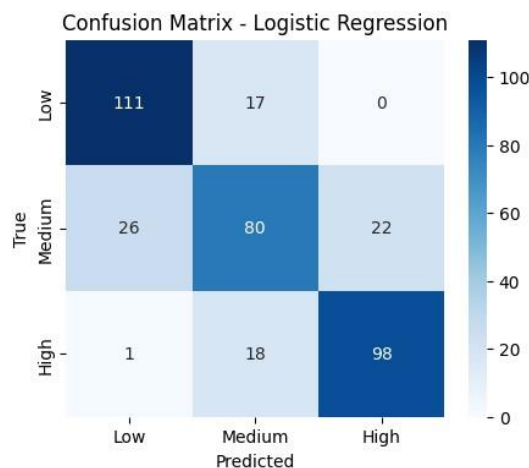
**Figure 4: Confusion Matrix - Logistic Regression.**
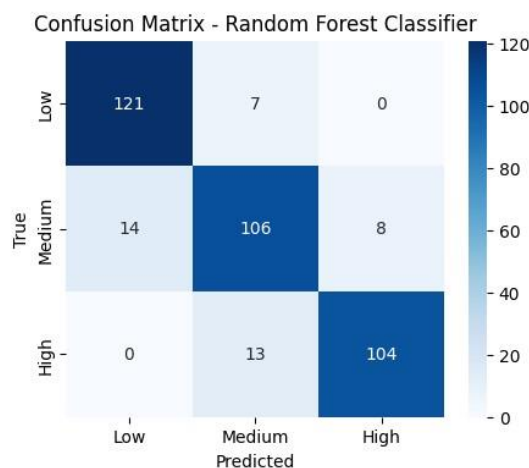
**Figure 5: Confusion Matrix - Random Forest.**
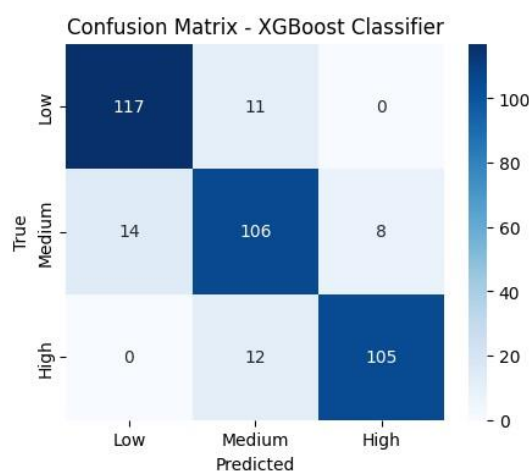
Figure 6: Confusion Matrix - XGBoost.

In order to improve the performance of the ensemble approaches, GridSearchCV was used to do hyperparameter tuning after the initial model assessments. With the n_estimators=50, max_depth=None, and min_samples_split=2, the optimized Random Forest model produced a mean cross-validation accuracy of 89.08% and a test accuracy of 88.20%. Similarly, the tweaked XGBoost model achieved a mean cross-validation accuracy of 88.61% and a test accuracy of 86.86% with a learning_rate of 0.1, max_depth of 5, and n_estimators of 200. A 5-fold cross-validation was conducted to visualize the stability of these modified models, and Figure 7 displays the boxplot that was produced. This plot's small interquartile range suggests that both models perform consistently across various data splits.

Figure 8 provides a summary of the cross-validation results for the untuned models for comparison. While the ensemble approaches (Random Forest and XGBoost) exhibit greater median accuracies and less variability, the boxplot displays a wider range of accuracy ratings for Logistic Regression. The appropriateness of ensemble approaches for simulating CHF is supported by this consistency.
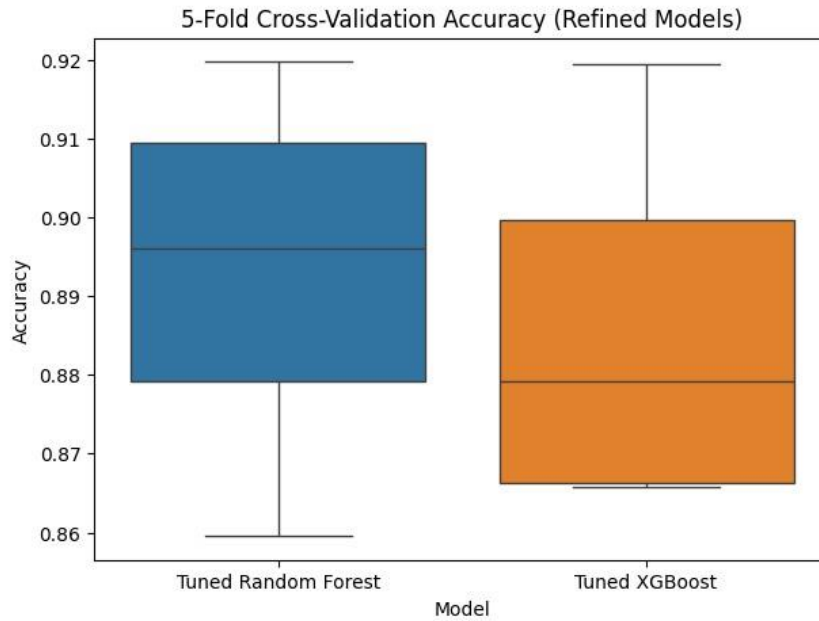
Figure 7: 5-Fold Cross-Validation Accuracy Scores for Tuned Models.
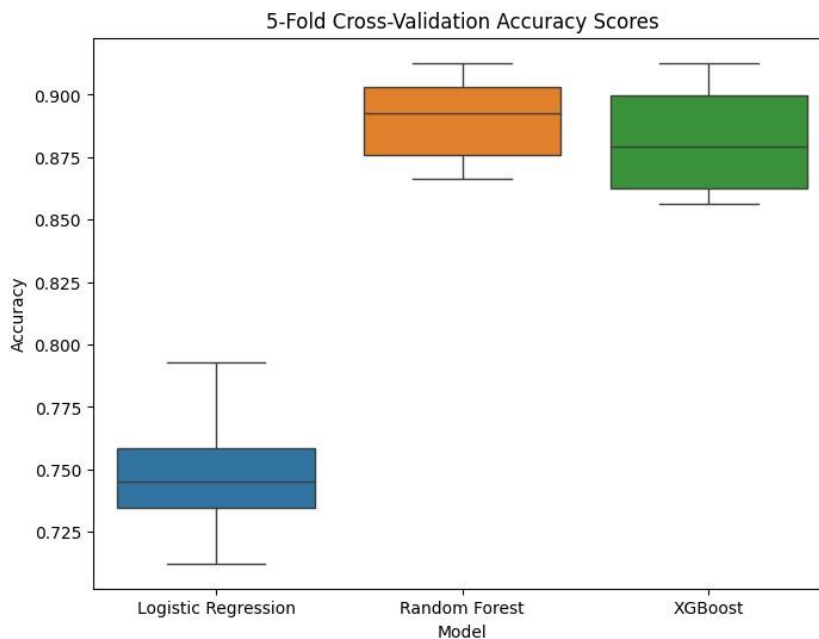
Figure 8: 5-Fold Cross-Validation Accuracy Scores for Untuned Models.

A thorough examination of the data shows that ensemble techniques—Random Forest and XGBoost in particular—are quite successful at dividing CHF into Low, Medium, and High categories. Untuned ensemble models perform better than logistic regression, according to the preliminary evaluations, and their performance was further enhanced by additional hyperparameter tuning. The models' ability to differentiate between classes is demonstrated by the confusion matrices, which also show some difficulties with the Medium class, especially for Low and High CHF values. The robustness of these models is confirmed by the boxplots, which show consistent performance in cross-validation.

Conclusion:

Using a sizable experimental dataset, this chapter illustrated the effectiveness of Random Forest and XGBoost in classifying critical heat flux (CHF) (Zhao *et al.* 2020). The findings show that XGBoost performed similarly to Random Forest, which reached a test accuracy of up to 88.20%. In order to improve model robustness and guarantee consistent predictive performance, thorough cross-validation and rigorous hyperparameter adjustment have proven crucial. These results highlight how ensemble machine learning techniques can effectively represent the intricate, nonlinear relationships seen in CHF data, providing a viable substitute for conventional empirical correlations.

In the future, adding sophisticated feature engineering methods, including integrating dimensionless factors like Reynolds and Prandtl numbers, could lead to even greater gains in model performance. The ideal parameters for ensemble models may be further refined by extending the search over larger parameter grids. Furthermore, using explainability tools like SHAP or LIME would increase transparency and confidence in the model's predictions by offering insightful information about how it makes decisions. More precise control of safety margins in thermal systems may potentially be possible by investigating regression techniques to forecast precise CHF values. All things considered, these results demonstrate that machine learning provides accurate and broadly applicable CHF predictions, minimizing the need for strict empirical techniques and opening the door to better thermal system design and optimization.

References:

1. Sarbu, I., & Dorca, A. (2018). Review on heat transfer analysis in thermal energy storage using latent heat storage systems and phase change materials. *International Journal of Energy Research*, 43(1), 29–64. https://doi.org/10.1002/er.4196

2. Nikolayev, V., & Beysens, D. (2016). Boiling crisis and non-equilibrium drying transition. *ArXiv*. https://doi.org/10.1209/epl/i1999-00395-x

3. Kim, H. (2011). Enhancement of critical heat flux in nucleate boiling of nanofluids: a stateof-art review. *Nanoscale Research Letters*, 6(1), 415. ://doi.org/10.1186/1556-276X-6-415

4. Mohanraj, M., Jayaraj, S., & Muraleedharan, C. (2015). Applications of artificial neural networks for thermal analysis of heat exchangers – A review. *International Journal of Thermal Sciences*, 90, 150–172. https://doi.org/10.1016/j.ijthermalsci.2014.11.030

5. Zhao, X. (2020). Data for: On the prediction of critical heat flux using a physics-informed machine learning-aided framework. *Mendeley Data*, 1. https://doi.org/10.17632/5p5h37tyv7.1

6. Jalili, D., & Mahmoudi, Y. (2025). Physics-informed neural networks for two-phase film boiling heat transfer. *International Journal of Heat and Mass Transfer*, 241, 126680. https://doi.org/10.1016/j.ijheatmasstransfer.2025.126680

7. Cuomo, S., di Cola, V. S., Giampaolo, F., Rozza, G., Raissi, M., & Piccialli, F. (2022). Scientific Machine Learning through Physics-Informed Neural Networks: Where we are and What's next. *ArXiv:2201.05624 [Physics]*. https://arxiv.org/abs/2201.05624

8. Breiman, L. (2001). Random Forests. *Machine Learning*, 45(1), 5–32. https://doi.org/10.1023/a:1010933404324

9. Chen, T., & Guestrin, C. (2016). XGBoost: a Scalable Tree Boosting System. In *Proceedings of the 22nd ACM SIGKDD International Conference on Knowledge Discovery and Data Mining - KDD '16* (pp. 785–794). https://doi.org/10.1145/2939672.2939785

THE KINETICS OF THE REACTION BETWEEN DIACETONE ALCOHOL AND IODINE IN ACIDIC MEDIUM BY IODIMETRY

Chandanapriya K H M, Bhavana B S, Sindhu H K, Greeshma K and Ramesh T N*

Department of Studies and Research in Chemistry,

University College of Science, Tumkur University, Tumkur-572103, India

*Corresponding author E-mail: adityaramesh77@yahoo.com

Abstract:

The reaction between diacetone alcohol (DAA) and iodine in an acidic environment yields 1-iodo-diacetone alcohol and hydrogen iodide. This study investigates the reaction kinetics using a volumetric method. The reaction proceeds through a two-step mechanism, with the first step being the rate-determining step. The reaction exhibits first-order kinetics with respect to both DAA and sulphuric acid concentrations, as doubling their concentrations doubles the reaction rate. The reaction rate remains unaffected by changes in iodine concentration. Consequently, the overall reaction order is determined to be two.

Introduction:

The kinetic studies of acetone and iodine in acidic media has been extensively studied to understand their interactions and mechanisms [1-8]. A prominent reaction involves the formation of halo ketones and carboxylic acids, catalyzed by the acid which enhances the electrophilicity of iodine [6]. In acidic solutions, iodine can be protonated to form the iodonium ion (I_3^+), further increasing its electrophilicity: $2I_2 + H^+ \rightleftharpoons I_3^+ + HI$. This iodonium ion reacts with carbonyl carbon of acetone, forming a tetrahedral intermediate which subsequently dissociates, yielding iodoacetone: $CH_3COCH_3 + I_2 + H^+ \rightarrow CH_3C(I)CH_3 + HI$

Acids like HCl or H_2SO_4 enhance electrophilicity of iodine, facilitating the reaction [9,10].

Diacetone alcohol (DAA), a versatile organic compound, finds applications as a solvent, in pharmaceutical production, and as a synthetic building block [11-13]. DAA participates in reactions with aldehydes and ketones in the presence of iodine, yielding aldol condensation products [14]. It reacts with iodine under basic conditions to form 2-iodo-1,3-propanediol [15]. Kinetic studies of DAA with iodine are crucial for determining reaction rates and identifying influencing factors like concentration, temperature, and catalysts (e.g., acids) [16,17]. Oxidation of DAA by iodine can lead to products like diacetoxyacetone, diacetone dicarboxylic acid, or 1-acetyl-1-methylhydantoin (AMH) [18]. The reaction mechanism in which iodine reacts with this

protonated DAA species, leads to halogenation and other transformations, producing iodoacetone or other halogenated compounds. In acidic conditions, molecular iodine (I_2) may be the reactive species, facilitating alcohol halogenation. This study focuses on the reaction involving DAA (4-hydroxy-4-methylpentan-2-one) with iodine in an acidic medium to predict the rate of reaction under different conditions. The reaction kinetics are investigated with respect to DAA and sulphuric acid concentrations. The rate of reaction and order with respect to each reactant was determined by the initial rate method and integrated rate method under different conditions (varying concentrations of reactants). The rate of the reaction has been determined by monitoring the change in concentration of iodine over time using iodimetric titration. This study provides valuable insights into the reaction mechanism and the factors governing its rate.

Experimental Section:

All the reagents were procured from SD Fine Chemicals private limited, India and used as received.

The following solutions were prepared: 2 M/1 M diacetone alcohol, 2 M/1 M sulphuric acid and 0.05/0.025 M iodine solution. Iodination of diacetone alcohol was monitored by iodimetric titration for the reaction mixtures I to IV given in Table 1 are as follows:

From the reaction mixture-I, 20 mL was removed at 5 minutes interval and transferred into conical flask containing 1 M sodium acetate. The residual iodine was in presence of starch indicator forms deep blue colour and on titrating it with sodium thiosulphate (0.005/0.0025 M) results in discharge of colour. The total volume of the reaction mixture was maintained constant and the details about the concentrations of diacetone alcohol, sulphuric acid and iodine are given in Table 1. Experiments were repeated for the reaction mixtures-II, III and IV, the data was recorded for the reaction mixtures III to IV.

Table 1: Details of the different reaction mixtures taken (concentrations/volumes)

Reaction mixture	DAA		H_2SO_4		Iodine in 10% KI solution		Water
	2 M	1 M	1 M	0.5 M	0.05 M	0.025 M	
I	20 mL		10 mL	-	20 mL	-	150 mL
II	-	20 mL	10 mL	-	20 mL	-	150 mL
III	20 mL	-	-	10	20 mL	-	150 mL
IV	20 mL	-	10 mL	-	-	20 mL	150 mL

The rate of iodination depends on the reactant concentrations: rate = $k[DAA]^a[I_2]^b[H_2SO_4]^c$, where a, b, and c represents the reaction order with respect to DAA, iodine, and H_2SO_4, respectively.

Using initial rate method the value of rate constants 'k' for the reaction mixtures I to IV were calculated by varying the concentration of one reactant at a time. Also by using integrated rate equation, the rate constant 'k' values were calculated for the reaction mixtures I to IV. From the rate constant values, the order of the reaction with respect to diacetone alcohol and H_2SO_4 were determined.

Results and Discussion:

Figure 1(a) shows the changes in the titre values of sodium thiosulphate (equivalent of iodine) with variation in the DAA concentrations (sulphuric acid and iodine concentrations maintained constant) during the reaction for the reaction mixtures I and II. The titre values ($Na_2S_2O_3$) decrease linearly with time. Figure 1(b) shows the changes titre values of sodium thiosulphate (equivalent of iodine) during reaction between DAA and iodine with variation in the concentrations of sulphuric acid (diacetone alcohol and iodine concentrations maintained constant) for the reaction mixtures 1 and 3 respectively. Figure 1(c) shows the changes titre values of sodium thiosulphate (equivalent of iodine) during reaction between DAA and iodine with variation in the concentrations of iodine (diacetone alcohol and sulphuric acid concentrations maintained constant) for the reaction mixtures 1 and 4 respectively. In all the cases, the titre values decreases linearly with time. The linear fit was performed for the data obtained for the reaction mixtures I to IV and from the slope, the rate constants for the reaction mixtures I to IV were calculated and is given in Table 2. Also first order integrated rate equation was used to calculate the rate constant 'k' for the reaction mixtures I to IV and the values are given in Table 2. From the rate constant values (both experimental and graphical methods) we observe that the rate of the reaction doubles with increase in the concentration of diacetone alcohol or sulphuric acid (refer to Table 2).

Table 2: Rate constant values obtained for different reaction mixtures from integrated rate equation

Reaction mixture	I	II	III
Rate constant: k, sec^{-1} (Substitution method in integrated rate equation (Experimental)	8.39×10^{-3}	3.431×10^{-3}	3.813×10^{-3}
Rate constant:k, sec^{-1} Substitution method in integrated rate equation (graph)	8.196×10^{-3}	2.763×10^{-3}	3.109×10^{-3}

Table 3: Comparison of the order of the reactions for the reaction mixtures obtained by initial rate method and integrated rate method

Order of the reaction	Initial rate method (15 minutes differrence)	Substitution method in integrated rate equation
Diacetone alcohol	1.24	1.1 (1.5)
Sulphuric acid	1.3	1.29 (1.39)
Iodine	1.1	-

On comparing the rate constants between the reaction mixtures I and II, [concentrations of diacetone alcohol are 0.667 M and 0.33M] the order of the reaction is found to be one. While for the reaction mixtures I and III [concentrations of sulphuric acid are 0.667 M and 0.33M] the order of the reaction is one. In the reaction mixtures I and IV, concentrations of iodine [I_2] are 0.05 M and 0.025 M and the order could not be calculated due to lower concentrations. Therefore, rate of the reaction is dependent on the concentration of the diacetone alcohol and sulphuric acid with a two fold increase in their values. The experimental data matches well with the results obtained for the acetone-iodine/diacetone alcohol-iodine using colorimetric method [19].
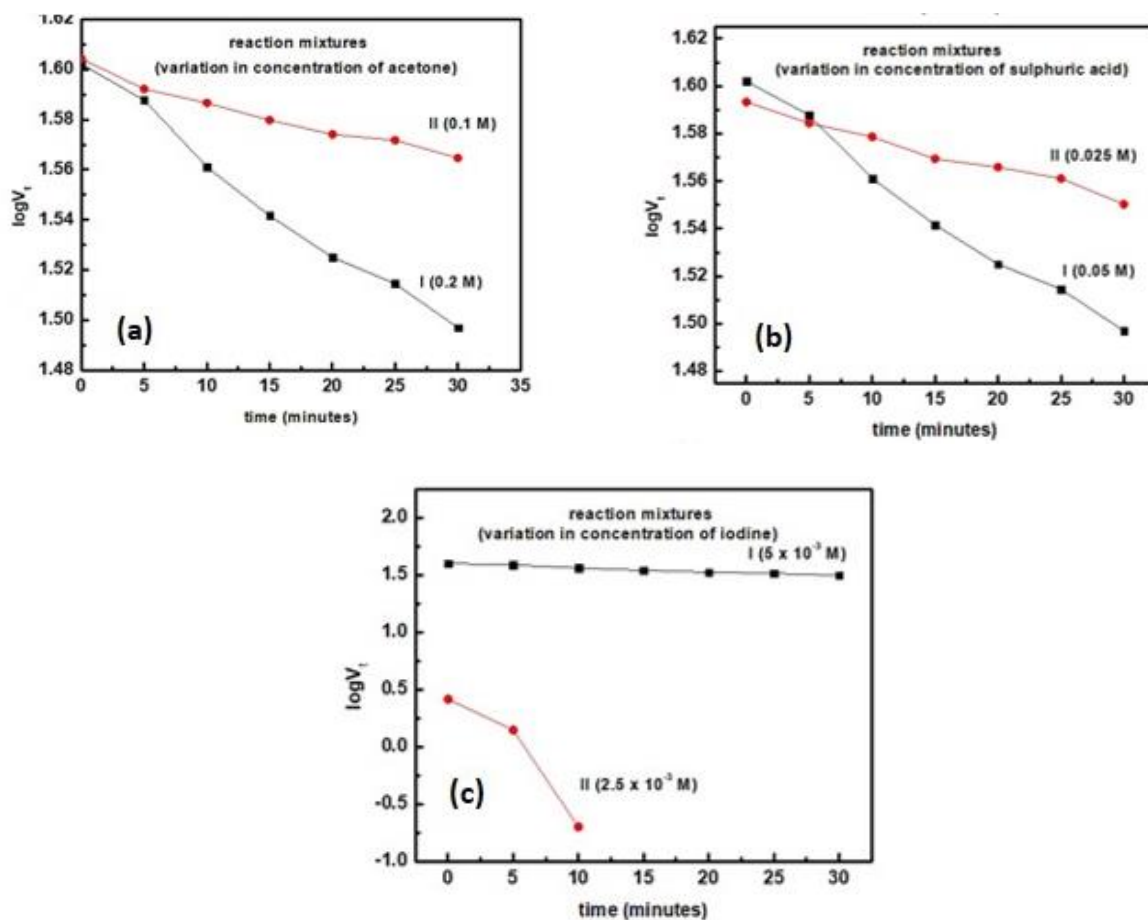
Figure 1: Variation in the concentrations of

a) diacetone alcohol, b) sulphuric acid and c) iodine

Conclusion:

The reactions between DAA and iodine in acidic media were studied. The reaction rate doubles with increasing DAA concentration. Doubling the concentrations of DAA or sulphuric acid doubles the rate, indicating first-order kinetics with respect to each. The iodine concentration has no effect on the rate. Therefore, the overall reaction order is two. These studies provide insights into organic oxidation reactions and their kinetics. Further studies are needed to determine the precise mechanism and identify any intermediates involved.

Acknowledgement:

Authors gratefully thank Tumkur University for the support.

References:

1. King, L. C., & Hlavacek, R. J. (1950). The reaction of ketones with iodine and thiourea. *Journal of the American Chemical Society, 72*(8), 3722–3725.

2. Seelye, R. N., & Turney, T. A. (1959). The iodoform reaction. *Journal of Chemical Education, 36*(11), 572.

3. Meyer, E. N. (2010). Rate and activation energy of the iodination of acetone. *Lab Report*, 1-5.

4. Gantz, G. M., & Walters, W. D. (1941). The thermal decomposition of acetone catalyzed by iodine. *Journal of the American Chemical Society, 63*(12), 3412–3419.

5. Bell, R. P., & Longuet-Higgins, H. C. (1946). Kinetics of the halogenation of acetone in alkaline solutions. *Journal of the Chemical Society*, 636-638.

6. Jones, J. L. (1939). Kinetic studies on iodine derivatives. I. The thermal decomposition of acetyl iodide. *Journal of the American Chemical Society, 61*(12), 3284–3288.

7. Tapuhi, E., & Jencks, W. P. (1982). Base-catalyzed halogenation of acetone. *Journal of the American Chemical Society, 104*(21), 5758–5765.

8. Abeywickrema, A. N., & Beckwith, A. L. J. (1987). Mechanistic and kinetic studies on the iododediazoniation reaction. *The Journal of Organic Chemistry, 52*(12), 2568–2571.

9. Levi, A. G., & Scorrano, M. G. (1974). Protonation equilibriums of ketones in aqueous sulfuric acid. *Journal of the American Chemical Society, 96*(21), 6585–6588.

10. Kulkarni, S., & Shukla, S. T. (2015). Kinetics of iodination of acetone, catalyzed by HCl and H_2SO_4: A colorimetric investigation of relative strength. *Journal of Chemical and Pharmaceutical Research, 7*, 226-229.

11. Walton, D. C., Kehr, E. F., & Loevenhart, A. S. (1928). A comparison of the pharmacological action of diacetone alcohol and acetone. *The Journal of Pharmacology and Experimental Therapeutics, 33*, 175-183.

12. Åkerlöf, G. (1926). Decomposition of diacetone alcohol in alkali hydroxide-alkali salt solutions. *Journal of the American Chemical Society, 48*(12), 3046–3063.

13. Rios, D., Schoendorff, G., Van Stipdonk, M. J., Gordon, M. S., Windus, T. L., Gibson, J. K., & de Jong, W. A. (2012). Roles of acetone and diacetone alcohol in coordination and dissociation reactions of uranyl complexes. *Inorganic Chemistry, 51*(23), 12768–12775.

14. Kulkarni, P., & Totre, G. (2019). Synthesis of dibenzylidene acetone via aldol condensation of diacetone alcohol with substituted benzaldehydes. *Orbital: The Electronic Journal of Chemistry, 11*(5), 292-296.

15. French, C. C. (1929). Basic catalysis in the decomposition of diacetone alcohol. *Journal of the American Chemical Society, 51*(11), 3215–3225.

16. Pollack, R. M., & Ritterstein, S. (1972). Primary amine catalysis in the dealdolization of diacetone alcohol. *Journal of the American Chemical Society, 94*(14), 5064–5069.

17. Åkerlöf, G. (1928). Decomposition of diacetone alcohol by sodium hydroxide in water mixtures of organic solvents. *Journal of the American Chemical Society, 50*(5), 1272–1275.

18. McAllister, S. H., Bailey, W. A., Jr., & Bouton, C. M. (1940). The catalyzed cleavage of diacetone alcohol and other ketols and unsaturated ketones. *Journal of the American Chemical Society, 62*(11), 3210–3215.

19. Bhavana, B. S., Chandanapriya, K. H. M., & Ramesh, T. N. (2023). Comparative studies on the kinetics of iodination of propanone and 4-hydroxy-4-methyl-2-pentanone in acidic medium by colorimetric method. *Conference Proceedings of National Conference on "Emerging Trends in Chemical Science Research"*, Tumkur University Publication (1st ed.), 29-36.

THERAPEUTIC POTENTIAL OF FLAVONO-ISOXAZOLE DERIVATIVES: A MEDICINAL CHEMISTRY PERSPECTIVE

Pravin S. Bhale

Department of Chemistry,

Yeshwantrao Chavan Mahavidyalaya, Tuljapur, Dist-Dharashiv-413601, Maharashtra, India

Corresponding author E-mail: bhale.ps@gmail.com

Abstract:

Flavono-isoxazole derivatives, combining the bioactive properties of flavonoids and isoxazole rings, represent a promising class of compounds in medicinal chemistry. These hybrids exhibit diverse therapeutic activities, including antimicrobial, anticancer, anti-inflammatory, and neuroprotective effects. Recent advancements have highlighted their potential in addressing global health challenges such as drug-resistant infections, cancer, diabetes, and neurodegenerative disorders. This review explores biological activities, and structure-activity relationships (SAR), emphasizing their mechanisms of action and challenges in clinical translation. By summarizing current progress, this work underscores the potential of flavono-isoxazole derivatives as versatile candidates for novel drug development.

**Keywords:** Flavonoid, Isoxazole, Natural Products, Structure-Activity Relationships

Introduction:

Flavonoids are a diverse group of natural compounds widely distributed in plants, known for their vibrant pigmentation and significant biological activities. Flavonoids are polyphenolic compounds characterized by a 15-carbon skeleton arranged in a C6-C3-C6 framework. This structure comprises two aromatic rings (A and B) connected by a three-carbon bridge forming a heterocyclic pyran or pyrone ring (C-ring). Variations in the hydroxylation, methylation, glycosylation, and other substitutions on these rings give rise to different subclasses, such as flavones, flavonols, flavanones, anthocyanins, and isoflavones (Figure 1). These polyphenolic compounds play crucial roles in plant growth, defense, and reproduction. In human health, flavonoids are recognized for their broad pharmacological properties, including antioxidant, anti-inflammatory, anti-cancer, and cardiovascular-protective effects. Their ability to modulate cellular signaling pathways and neutralize reactive oxygen species (ROS) has made them a focus of extensive research in nutraceuticals and drug development. With their multifaceted benefits and natural abundance, flavonoids continue to inspire the discovery of novel therapeutic agents [1-2].
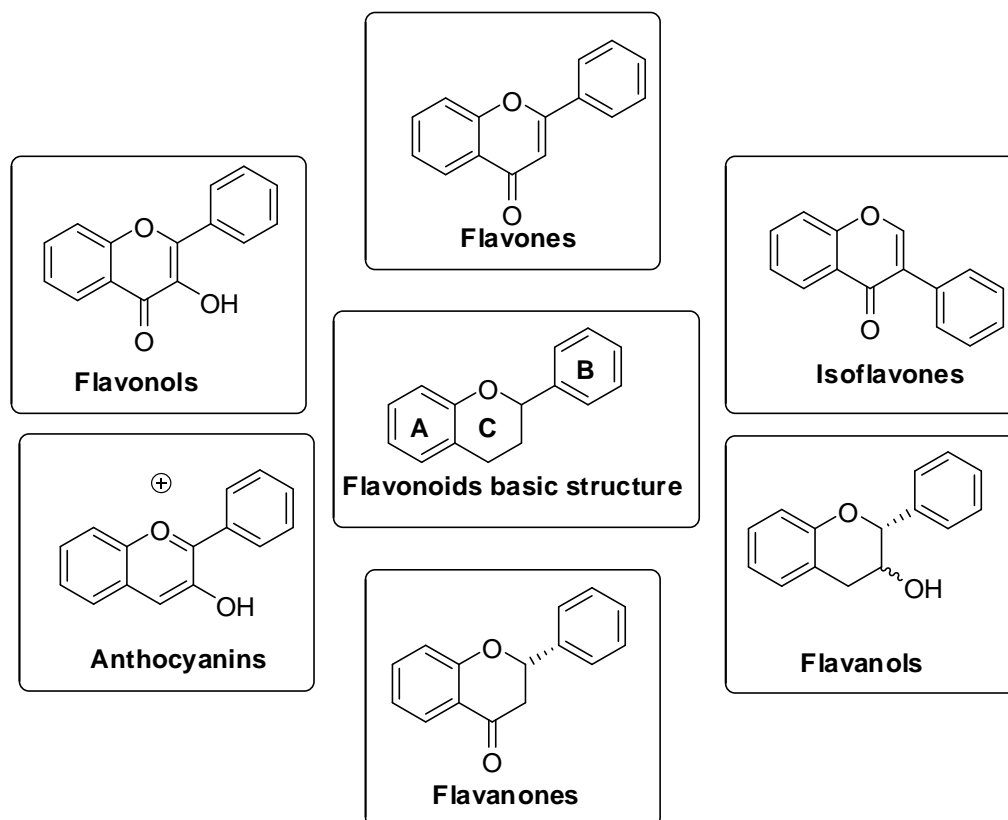
Fig. 1: Structures of flavonoid subgroups

Isoxazole is a five-membered heterocyclic aromatic compound consisting of three carbon atoms, one nitrogen atom, and one oxygen atom, arranged in a 1,2-oxazole configuration (Figure 2). It exhibits aromaticity due to the delocalization of π-electrons across the ring structure, contributing to its chemical stability and unique reactivity. Isoxazole and its derivatives have garnered significant attention in both academic research and industrial applications due to their versatile chemical properties and wide-ranging biological activities [3].
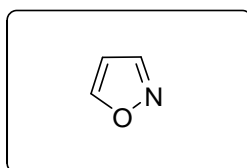

Fig. 2: Structures of Isoxazole

In medicinal chemistry, isoxazole serves as a valuable scaffold in the design and development of therapeutic agents. Many isoxazole derivatives display potent pharmacological activities, including antimicrobial, anti-inflammatory, anticancer, antiviral, and analgesic properties. These attributes make them essential components in drug discovery and development programs targeting various diseases. Isoxazole-containing drugs, such as leflunomide (used for rheumatoid arthritis) and valdecoxib (a COX-2 inhibitor), highlight the compound's therapeutic relevance. Beyond pharmaceuticals, isoxazole plays a vital role in organic synthesis, serving as a

precursor or intermediate in constructing more complex molecules. Its functional groups offer opportunities for diverse chemical transformations, including nucleophilic and electrophilic substitution reactions. Additionally, isoxazole derivatives find applications in material sciences, where their thermal stability and electronic properties are utilized in developing polymers, liquid crystals, and advanced materials. Overall, isoxazole is a cornerstone in modern chemistry, with its unique structural features and multifaceted applications making it indispensable in advancing both scientific understanding and practical innovations [4-6]. Currently, numerous drugs containing isoxazole fragments are available in the market. These medications play a crucial role in alleviating and addressing the symptoms of various diseases, thereby helping to protect and improve human health (Figure 3).
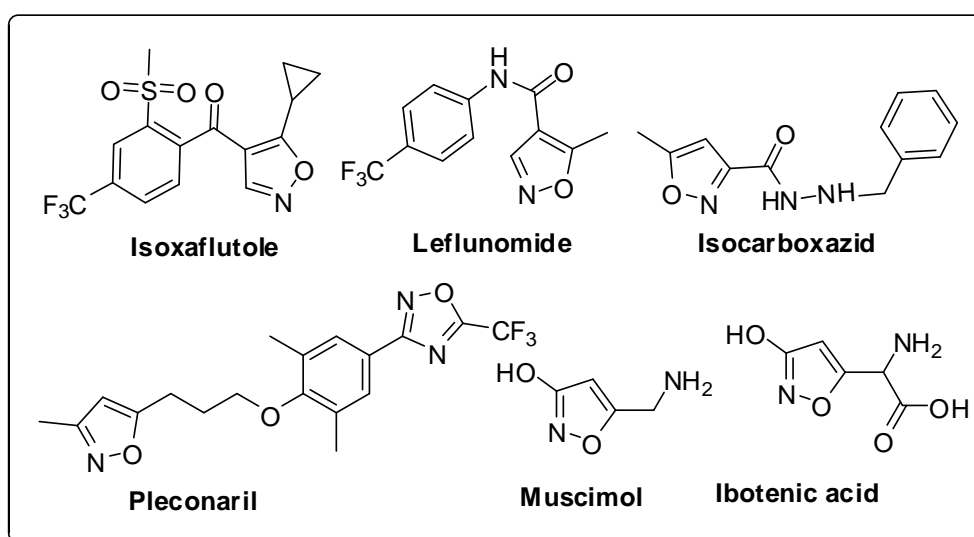
Fig. 3: Some isoxazole-based commercially available drugs.

Flavono-isoxazole derivatives are an emerging class of hybrid compounds that merge the structural and functional attributes of flavonoids and isoxazole rings. Flavonoids, widely found in plants, are renowned for their diverse biological activities, including antioxidant, anti-inflammatory, and anticancer properties. These natural compounds have been extensively studied for their health benefits and pharmacological potential. On the other hand, isoxazoles, five-membered heterocyclic compounds containing nitrogen and oxygen atoms, have gained significant attention in medicinal chemistry due to their versatile biological activities, such as antimicrobial, antiviral, anti-tumor, and neuroprotective effects. The combination of flavonoids and isoxazole moieties into a single molecular framework creates flavono-isoxazole derivatives, which are designed to enhance the pharmacological properties of each component while mitigating their individual limitations. This structural hybridization leverages the complementary

bioactivities of both flavonoids and isoxazoles, offering a promising strategy for developing novel therapeutic agents [7].

Flavono-isoxazole derivatives have shown potential in addressing a wide range of medical challenges, including antibiotic resistance, chronic inflammation, metabolic disorders, and cancer. Their ability to modulate key biological pathways, coupled with favorable pharmacokinetic profiles, positions them as attractive candidates for drug discovery and development. This book chapter explores the latest medicinal applications and structure-activity relationships of flavono-isoxazole derivatives.

Therapeutic potential of flavono-isoxazole derivatives:

Rao *et al.* conducted a comprehensive study in which they designed and synthesized a series of heterocyclic flavono-isoxazole compounds to evaluate their biological activities. The antiproliferative potential of these compounds was assessed using the sulforhodamine B (SRB) assay and turbidimetry to determine their efficacy against MCF-7 breast cancer cells. Among the synthesized compounds, Compound **1** (Figure 4) demonstrated a significant inhibitory effect on MCF-7 cells, with an IC_{50} value of 34.2 μM, indicating its potential as an anticancer agent. In addition to its antiproliferative activity, Compound **1** was evaluated for its antibacterial properties. At a concentration of 30 μM, the compound exhibited moderate antibacterial activity, achieving an inhibitory rate of 41.7%. These findings highlight the dual biological activity of Compound **1**, making it a promising candidate for further development in cancer and antibacterial therapies [8].

The enhanced activity is believed to stem from the presence of a methyl, amine, and sulfur-substituted pyrimidine moiety.

3-O-[(E)-4-(4-cyanophenyl)-2-oxobut-3-en-1-yl] kaempferol has been identified as a lead compound with notable anti-diabetic and anti-obesity properties. Building upon this foundation, Nie *et al.* developed a novel isoxazole derivative, Compound **2**, designed to enhance these therapeutic effects. The compound was specifically engineered to improve glucose consumption in insulin-resistant (IR) HepG-2 cells, exhibiting remarkable potency with an EC_{50} value of 0.8 nM, demonstrating its effectiveness at the nanomolar level. To synthesize this derivative, kaempferol was first methylated using dimethyl sulfate, a process that protected specific hydroxyl groups. The subsequent demethylation step was carried out under controlled conditions using anhydrous aluminum bromide in acetonitrile, resulting in the formation of 3-hydroxyflavone. Compound **2** (Figure 4) was then synthesized through a nucleophilic substitution reaction, followed by cyclization with chloro-benzaldoxime, ultimately yielding the desired isoxazole derivative [9].

Biological evaluation of Compound **2** revealed its significant ability to modulate key metabolic pathways. In HepG-2 cells, it substantially increased the phosphorylation levels of AMP-activated protein kinase (AMPK), a crucial regulator of cellular energy homeostasis. Concurrently, the expression levels of phosphoenolpyruvate carboxykinase (PEPCK) and glucose-6-phosphatase (G6Pase), enzymes involved in gluconeogenesis, were markedly reduced. This dual effect suggests that Compound **2** exerts its anti-diabetic activity through activation of the AMPK pathway and subsequent inhibition of PEPCK and G6Pase, which play pivotal roles in glucose metabolism. These findings underscore the therapeutic potential of Compound **2** as a novel agent for managing diabetes and obesity through targeted modulation of the AMPK/PEPCK/G6Pase pathway. Further studies could provide deeper insights into its molecular mechanisms and efficacy in clinical settings.
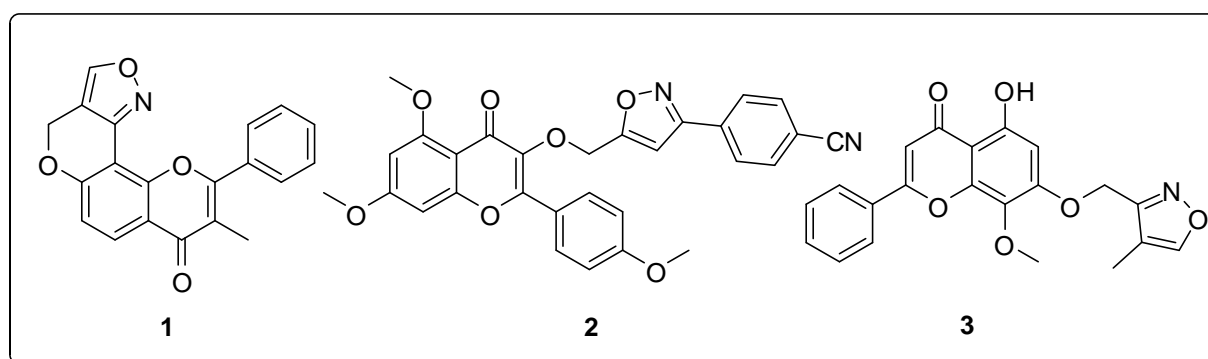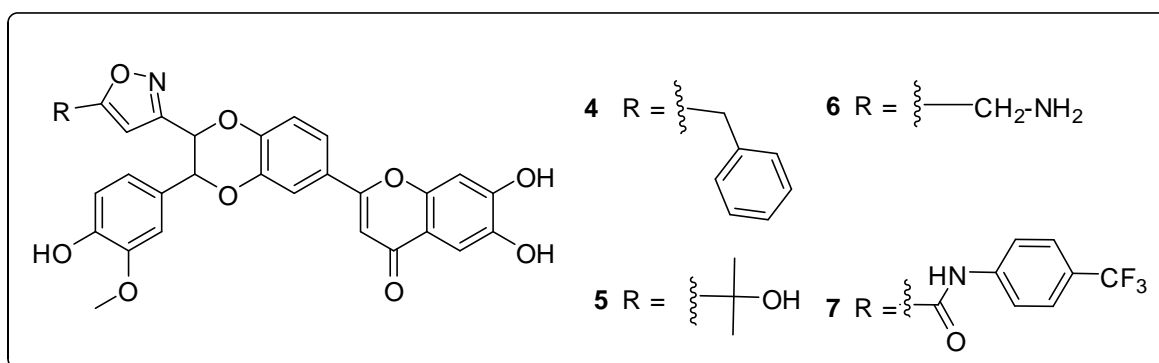

Fig. 4: Flavono-isoxazole derivatives 1-3

Wogonin, chemically known as 5,7-dihydroxy-8-methoxy-flavonoid, is a natural compound with well-documented anticancer properties. Extensive research has demonstrated its potent anti-tumor activity in both *in vitro* and *in vivo* models [10]. Recognizing the therapeutic potential of wogonin, Bian *et al.* aimed to enhance its anticancer efficacy by modifying its structure. In their study, an isoxazole moiety was introduced at position 7 of the wogonin molecule, resulting in a novel derivative referred to as Compound **3**. The structural modification was designed to explore how the incorporation of the isoxazole group might influence the compound's biological activity. The anti-tumor potential of Compound **3** was evaluated using HepG-2 hepatocellular carcinoma cells [11].

Compound **3** (Figure 4) demonstrated some inhibitory activity against HepG-2 cells, with an IC_{50} value of 21.66 μM. While this result indicated anticancer potential, the activity was slightly lower compared to the parent compound, wogonin, which had an IC_{50} value of 19.0 μM. Furthermore, the efficacy of Compound **3** was also less than that of the reference chemotherapeutic agent, 5-fluorouracil, which exhibited an IC_{50} value of 17.2 μM under the same conditions. The study suggests that while the structural modification to include an

isoxazole group did not enhance the anticancer activity of wogonin, it provides valuable insights into the structure-activity relationship of wogonin derivatives. These findings could guide future efforts to optimize the anticancer potential of wogonin and its analogs.

The flavonoid hydnocarpin, extracted from the seeds of *Hydnocarpus wightiana* Blume, has drawn interest for its potential biological activities. Arya *et al.* sought to enhance its therapeutic potential by chemically linking it to an isoxazole moiety, resulting in a series of novel hydnocarpin-isoxazole derivatives. These derivatives were synthesized and evaluated for their anti-proliferative activities against three cell lines: A375 (human melanoma), A549 (human lung carcinoma), and WI-38 (normal lung fibroblasts). The synthetic modification of hydnocarpin began with the targeted transformation of the primary hydroxyl group at the C-9′ position into its corresponding aldehyde. This conversion was achieved using Moffatt oxidation, a method that facilitates selective oxidation of alcohols to aldehydes under mild conditions. Following this step, the researchers utilized a one-pot [3 + 2] cycloaddition reaction to construct the isoxazole ring, yielding the desired hydnocarpin-isoxazole derivatives.

The resulting compounds, labeled as **4-7** (Figure 5), were subjected to biological evaluation for their anti-proliferative effects. Notably, these derivatives exhibited significant inhibitory activity against A375 and A549 cancer cells, with IC_{50} values ranging from 0.65 to 7.5 μM. The observed activity highlights the potential of these modified derivatives as effective agents for targeting specific cancer cell types. This study underscores the value of structural modifications, such as the incorporation of isoxazole groups, in enhancing the biological properties of natural products like hydnocarpin. The findings also provide a foundation for further exploration of hydnocarpin-isoxazole derivatives in the development of anticancer therapies [12].
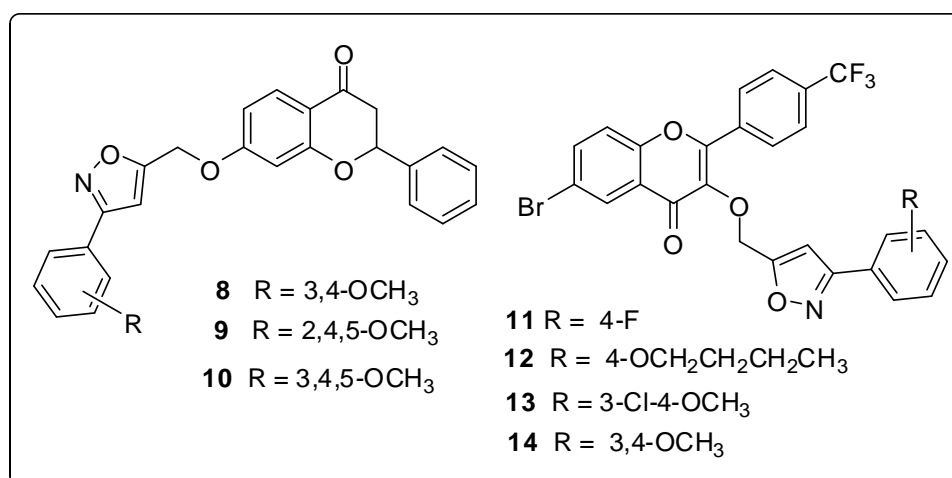

Fig. 5: Flavono-isoxazole derivatives 4-7

Asha Bhanu *et al.* conducted a detailed study focused on the design and synthesis of 7-hydroxyflavone derivatives to evaluate their antibacterial properties. The study aimed to explore how structural modifications to the flavone core could enhance antimicrobial efficacy. Through a

systematic synthetic approach, the researchers developed a series of novel derivatives. These compounds were subsequently tested for their antibacterial activity against selected bacterial strains. Among the synthesized derivatives, Compounds **8-10** (Figure 6) stood out for their potent antibacterial effects.

The antibacterial activity of these compounds was compared to that of standard antibiotics, including Streptomycin and Cycloheximide. Notably, Compounds **8-10** demonstrated strong inhibitory activity, with effects that either exceeded or closely approached the efficacy of the reference drugs. This level of activity highlights the potential of these 7-hydroxyflavone derivatives as promising candidates for the development of new antibacterial agents. The findings of this study underscore the importance of chemical modifications in optimizing the pharmacological properties of flavonoid-based compounds. Additionally, the results provide valuable insights into the structure-activity relationships of 7-hydroxyflavone derivatives, paving the way for further research and potential therapeutic applications [13].

Inhibiting α-amylase is a recognized therapeutic strategy for managing glucose absorption disorders, as it can help regulate postprandial blood glucose levels. Among the various classes of compounds studied for this purpose, flavonoids, isoxazoles, and their halogenated derivatives have garnered significant attention in pharmaceutical chemistry due to their potent biological activity. In a study conducted by Saidi *et al.* a series of novel halogenated flavonoid-isoxazole derivatives were designed, synthesized, and evaluated for their potential to inhibit α-amylase activity. The in vitro assays revealed that compound **11** (Figure 6) exhibited the highest α-amylase inhibitory activity, with an IC_{50} value of 16.2 μM, which is comparable to the standard inhibitor acarbose, known for its IC_{50} value of 15.7 Mm

Fig. 6: Flavono-isoxazole derivatives 8-14

Compounds **12**, **13**, and **14** (Figure 6) while slightly less potent than compound **11**, also demonstrated significant α-amylase inhibition, with IC_{50} values of 17.33 μM, 17.58 μM, and 18.36 μM, respectively. The results suggest that structural modifications, particularly the introduction of electron-withdrawing substituents at the para-position of the benzene ring, enhance inhibitory activity. This structural feature likely increases the compounds' affinity for the enzyme, thereby improving their efficacy as α-amylase inhibitors. Overall, the findings from this study highlight the promising potential of halogenated flavonoid-isoxazole derivatives as therapeutic agents for glucose absorption disorders, with compound **11** standing out as the most effective candidate in this series [14].

Gu *et al.* conducted a comprehensive study to design, synthesize, and evaluate the anti-psychotic potential of a series of dihydroflavone derivatives using both *in vitro* and *in vivo* models. Initially, they synthesized dihydroflavones featuring various chemical substitutions. These synthesized intermediates were further processed to obtain the target compounds through a three-step nucleophilic substitution reaction. The anti-psychotic activity of the synthesized compounds was assessed by evaluating their ability to inhibit the activity of dopamine D2 receptors in a cellular model. Specifically, compounds **15-17** (Figure 7) were tested on HEK293 cells cotransfected with the D2 receptor and G protein α16a. These compounds demonstrated significant inhibitory activity, with half-maximal inhibitory concentration (IC_{50}) values ranging from 0.0513 to 0.116 μM. Furthermore, compounds **15-17** exhibited notable anti-inflammatory effects.

15 n = 4, R = OCH_3
16 n = 4, R = F
17 n = 3, R = OCH_3
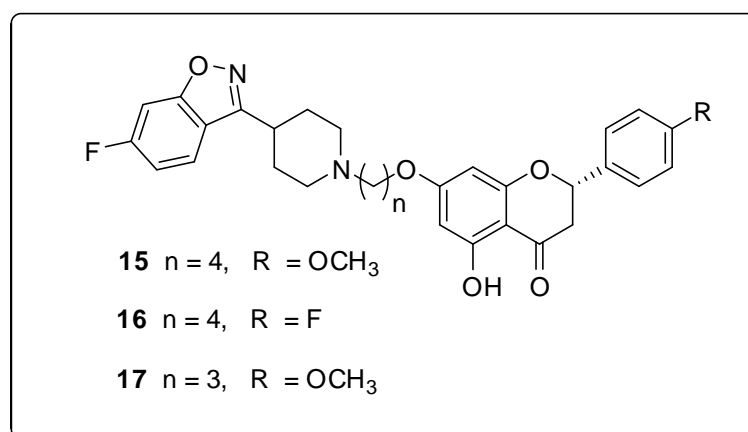
Fig. 7: Flavono-isoxazole derivatives 15-17

They effectively suppressed the overproduction of nitric oxide induced by lipopolysaccharide (LPS) and interferon-gamma in BV-2 microglial cells, indicating their potential to mitigate neuroinflammation. *In vivo*, the anti-psychotic properties of compounds **15-17** were further validated using animal models. These compounds reversed the hyperactivity in

mice induced by MK-801, an N-methyl-D-aspartate (NMDA) receptor antagonist, when administered via oral gavage. Additionally, they reduced the excessive climbing behavior triggered by apomorphine, a dopamine receptor agonist, suggesting their ability to regulate dopaminergic overactivity. Overall, the study highlights the therapeutic potential of compounds **15-17** as promising candidates for anti-psychotic drug development, owing to their dual action in modulating dopaminergic activity and attenuating neuroinflammatory responses [15].

Qiu *et al.* carried out an investigation into the design, synthesis, and evaluation of a series of isoflavone analogs for their potential lipid-lowering effects. These compounds were tested for their ability to reduce lipid accumulation in 3T3-L1 adipocytes, a well-established model for studying adipogenesis. The results indicated that most of the synthesized compounds significantly reduced lipid accumulation in these adipocytes, demonstrating promising lipid-lowering activities. Among these compounds, four of them specifically compounds **18** through **19** (Figure 8) showed stronger inhibitory effects on lipid accumulation compared to GW4064, a known FXR agonist, suggesting that these analogs may offer superior activity in reducing lipid levels. Of particular interest, compound **19** exhibited potent agonistic activity against the farnesoid X receptor (FXR), as demonstrated in cell-based luciferase reporter assays. FXR is a key nuclear receptor involved in regulating bile acid synthesis and lipid metabolism, making it a crucial target in lipid-lowering research.

Further analysis revealed that compound **19** not only activated FXR, but also led to the upregulation of several genes involved in lipid metabolism. Specifically, it enhanced the expression of FXR, small heterodimer partner (SHP), and bile salt export pump (BSEP) genes, all of which are important in maintaining lipid homeostasis and bile acid metabolism. In addition, compound **19** significantly downregulated the mRNA expression of SREBP-1c, a key transcription factor involved in lipogenesis, suggesting that compound **19** may reduce lipid accumulation by inhibiting the lipogenic pathway. Moreover, the safety profile of compound **19** was also assessed through a HepG-2 cytotoxicity test, and it was found to be safer than GW4064, further supporting it's potential as a therapeutic agent for lipid-related disorders. These findings highlight compound **19** as a promising candidate for further development in the context of lipid-lowering therapy [16].

Nifantev *et al.* conducted a study where they synthesized a series of dihydroquercetin aryl derivatives and evaluated their cytotoxic effects on two cell lines: HeLa cells (a human cervical cancer cell line) and murine fibroblasts (a type of connective tissue cell). The aim of the study was to assess the potential anticancer activity of these compounds by determining their ability to reduce cell viability. Among the derivatives synthesized, compound **20** (Figure 9), which

contained an isoxazole group, was of particular interest. The researchers tested the cytotoxicity of this compound by exposing HeLa cells and murine fibroblasts to a concentration of 100 μM. The results revealed that compound **20** exhibited weak cytotoxic effects on HeLa cells, as evidenced by a survival rate of 50% at the tested concentration. This indicated that compound **20** was able to reduce the viability of cancer cells, although the effect was not as pronounced as that of more potent cytotoxic agents.
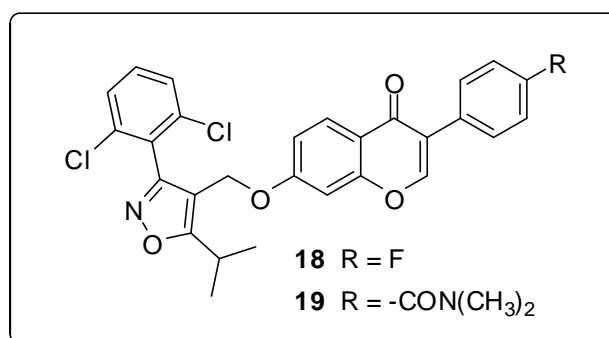
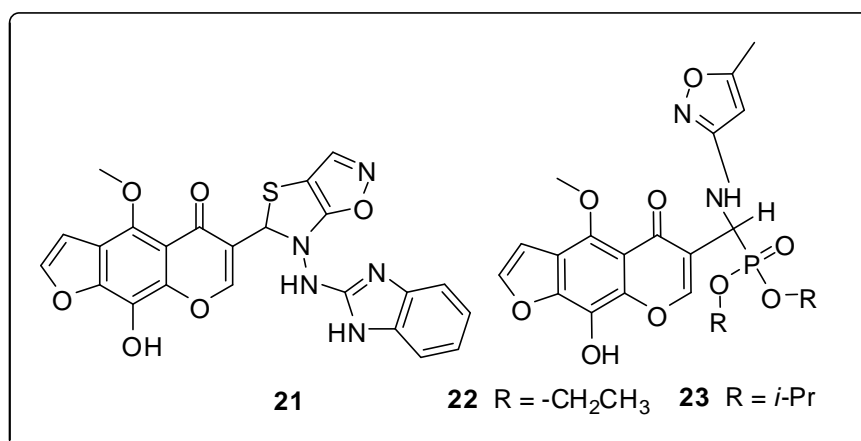**Fig. 8: Flavono-isoxazole derivatives 18-19**

In contrast, compound **20** showed significantly lower toxicity to murine fibroblasts. At the same concentration of 100 μM, the survival rate of the fibroblasts was 83%, suggesting that the compound was relatively less harmful to normal cells. These findings indicate that compound **20** may exhibit some degree of selective toxicity, potentially targeting cancer cells more effectively than normal cells, though its cytotoxicity remains modest. Overall, the study by Nifantev *et al.* provides valuable insights into the cytotoxic properties of dihydroquercetin aryl derivatives, with compound **20** showing a potential for further development as a less toxic anticancer agent [17].
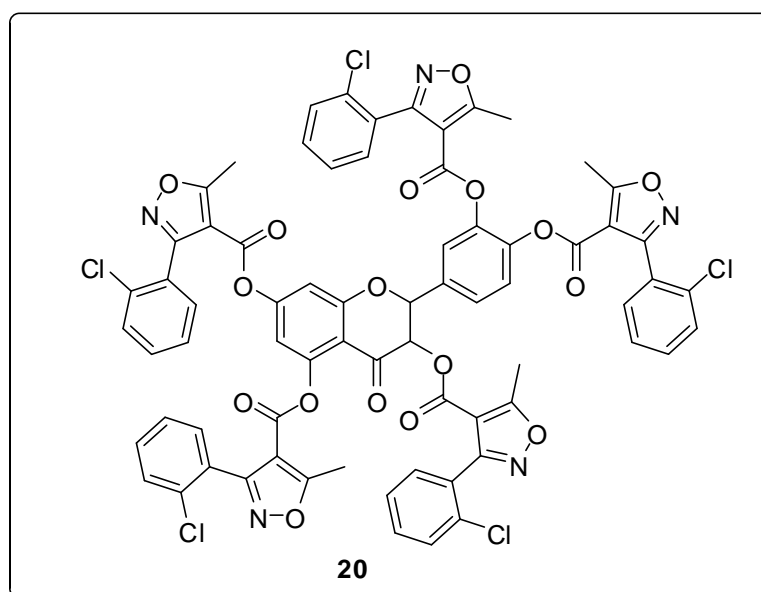
Fig. 9: Flavono-isoxazole derivatives 20

Abu-Bakr *et al.* synthesized a series of furo[3,2-g]chromone derivatives and evaluated their anticancer activity by testing their inhibitory effects on three human cancer cell lines: HCT-116 (colon carcinoma), MCF-7 (breast cancer), and HepG-2 (hepatocellular carcinoma). The study focused on determining the compounds' ability to inhibit cell growth by measuring their IC_{50} values, which indicate the concentration of a compound required to reduce cell viability by 50%. Among the synthesized compounds, compound **21** (Figure 10) exhibited a potent inhibitory effect on the HepG-2 cell line, with an IC_{50} value of 7.9μg/mL. This suggests that compound **21** is particularly effective in inhibiting the growth of liver cancer cells. Meanwhile, compounds **22** and **23** (Figure 10) demonstrated strong inhibitory effects on the HCT-116 cell line, with IC_{50} values of 4.7 μg/mL and 7.8 μg/mL, respectively. These results indicate that both compounds **22** and **23** are effective against colon cancer cells, with compound **22** showing slightly higher potency compared to compound **23**. Overall, the study highlights the potential of furo[3,2-g]chromone derivatives as promising candidates for the development of novel anticancer agents, specifically for liver and colon cancer treatment [18].


Fig. 10: Flavono-isoxazole derivatives 21-23

Badadhe *et al.* focused on designing and synthesizing a new series of isoxazol pigment compounds with the aim of evaluating their antibacterial properties. The study was motivated by the need to explore novel compounds with potential antibacterial activity, particularly those that could target Gram-positive bacteria, which are known to be resistant to certain antibiotics. Pharmacological testing was carried out to assess the antibacterial activities of the synthesized isoxazol pigment compounds. The results revealed that compounds **24, 25** and **26** (Figure 11) exhibited moderate antibacterial activity against Gram-positive bacterial strains. While these compounds did not show extremely high levels of activity, their moderate effectiveness suggests that they have potential as lead candidates for further development. These findings imply that isoxazol pigment compounds could serve as valuable scaffolds for the development of new

antibacterial agents. Further investigations are likely needed to optimize the structure of these compounds and improve their antibacterial potency, especially in the context of combating resistant bacterial strains [19].

Diabetic retinopathy (DR) is a significant cause of vision loss and blindness, particularly among individuals with diabetes. One of the potential therapeutic targets for treating DR is Rho-associated coiled-coil containing serine/threonine protein kinases (ROCKs), which play a crucial role in regulating various cellular processes, including those involved in the pathogenesis of DR. In light of this, Zhao *et al.* focused on designing and synthesizing a novel class of ROCK inhibitors, specifically a 4H-chromen-4-one derivative, to explore their potential for DR therapy. Among the synthesized compounds, compound **27** (Figure 11), which incorporates an isoxazole group, demonstrated remarkable inhibitory effects on both ROCK I and ROCK II isoforms. The compound exhibited very low IC_{50} values, indicating potent inhibition. Specifically, compound **27** was able to reduce ROCK I activity with an IC_{50} value of 0.068 μM and ROCK II activity with an even lower IC_{50} value of 0.005 μM. These findings suggest that compound **27** is highly effective in inhibiting the activity of both ROCK I and ROCK II, making it a promising candidate for further development as a therapeutic agent for diabetic retinopathy. The study by Zhao *et al.* highlights the potential of 4H-chromen-4-one derivatives as effective ROCK inhibitors, offering a new direction for the treatment of DR and possibly other diseases where ROCKs play a critical role [20].
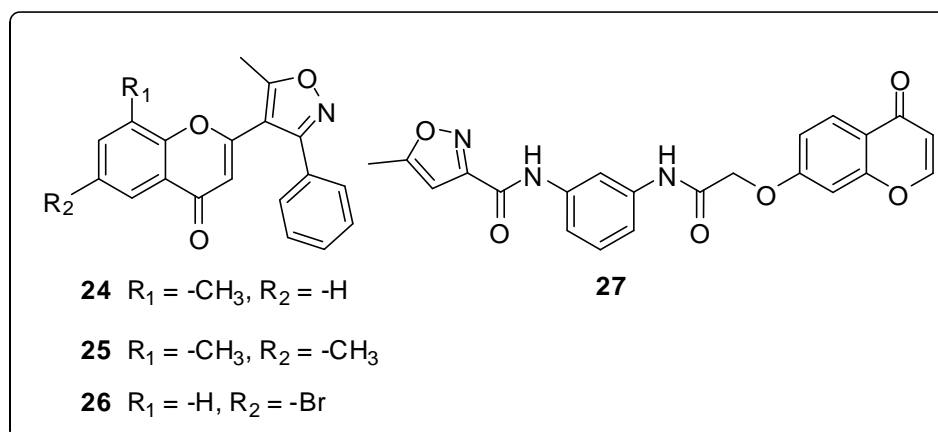
Fig. 11: Chromone-isoxazole derivatives 24-27

Kaushik *et al.* designed and synthesized a series of isoxazolylchromone derivatives with the goal of exploring their potential as anticancer agents, particularly targeting estrogen receptor-positive (ER+) breast cancer cells. Among the synthesized compounds, compound **28** (Figure 12) was found to exhibit significant cytotoxicity in MCF-7 cells, a human breast cancer cell line. The compound showed an IC_{50} value of 31.25 μg/mL, indicating its effective ability to inhibit cell

proliferation. The study further explored the mechanism of action of compound **28** by confirming its selectivity for the estrogen receptor alpha (ERα). This was achieved through ERα silencing experiments, which demonstrated that the deactivation of compound **28** led to a decrease in ERα luciferase reporter gene expression. Additionally, treatment with compound **28** resulted in the induction of ERβGFP (green fluorescent protein), confirming its interaction with the estrogen receptors.

A detailed examination of the cell cycle revealed that treatment with compound **28** led to an increase in the sub-G0/G1 phase population, suggesting that the compound promotes cell death by causing cell cycle arrest. Further investigations showed that compound **28** induced cell death primarily through apoptosis, a process of programmed cell death. Similar to the action of tamoxifen, a well-known anti-estrogen therapy, compound **28** induced cell death through an increase in reactive oxygen species (ROS) levels. However, while tamoxifen treatment is known to trigger autophagy in cells, compound **28** exhibited a different mechanism. It induced the loss of mitochondrial transmembrane potential and activated caspases, key enzymes in the apoptotic pathway, without signs of autophagy. In summary, Kaushik *et al.* demonstrated that compound **28** is a potent cytotoxic agent against MCF-7 breast cancer cells, acting through apoptosis induction mediated by ROS. The compound also shows specificity for the ERα receptor and has a distinct mechanism of action compared to tamoxifen, highlighting its potential as a novel therapeutic agent in breast cancer treatment [21].

Awadallah *et al.* synthesized a series of isoxazole-containing pigment compounds and investigated their cytotoxic activities against two cancer cell lines, MCF-7 (breast cancer) and A-549 (lung cancer). In addition to assessing their anticancer properties, the researchers also evaluated the compounds' ability to inhibit carbonic anhydrases (CAs), a family of enzymes involved in various physiological processes, including tumor progression. The results showed that compounds **29-31** (Figure 12) exhibited weak inhibitory activity against the cytoplasmic, off-target carbonic anhydrase isoforms hCA I and hCA II, which are generally not associated with cancer progression. However, the compounds displayed significant inhibitory effects against tumor-associated isoforms, namely hCA IX and hCA XII. These two isoforms are commonly overexpressed in tumor tissues and are known to contribute to the acidification of the tumor microenvironment, facilitating cancer cell survival and metastasis.

Among the synthesized compounds, compound **29** demonstrated the most potent cytotoxic effects. It exhibited high inhibitory activity against both MCF-7 and A-549 cell lines, with IC$_{50}$ values of 25.80 μM and 57.23 μM, respectively. These values indicate that compound **29** is effective in reducing cell viability in both breast and lung cancer cell lines, making it a

promising candidate for further anticancer development. In summary, the study by Awadallah *et al.* highlighted the potential of isoxazole-containing pigment compounds as dual-action agents, capable of inhibiting tumor-associated carbonic anhydrase isoforms and exhibiting significant cytotoxicity in cancer cells. Compound **29**, in particular, showed strong activity against MCF-7 and A-549 cells, warranting further investigation for its therapeutic potential in cancer treatment [22].
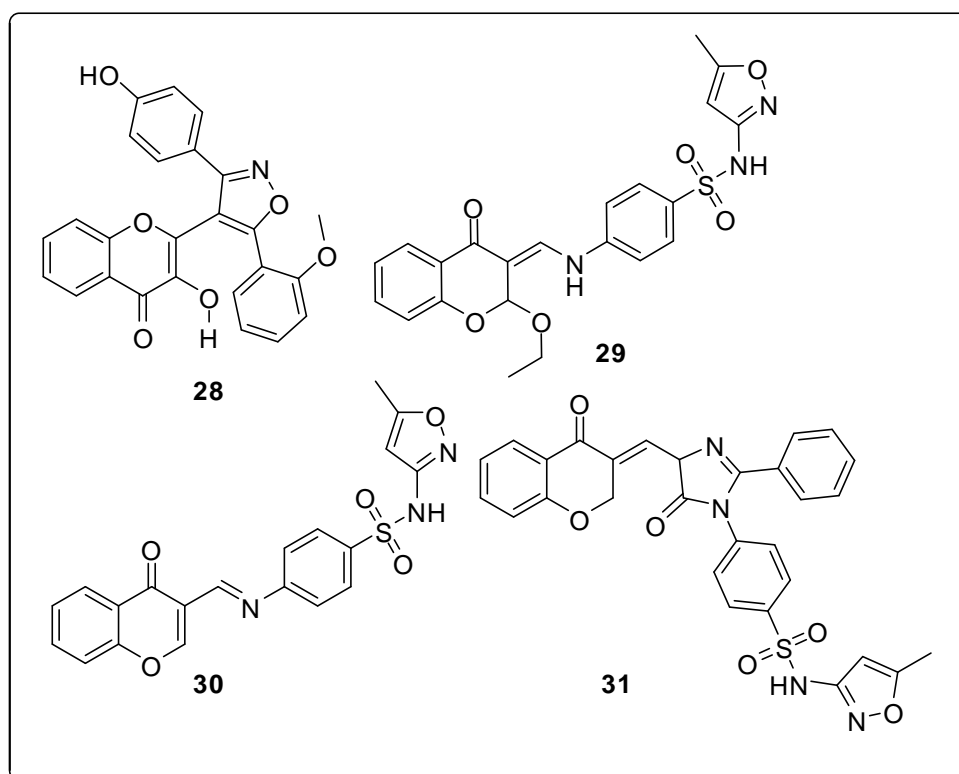
Fig. 12: Flavono-isoxazole derivatives 28-31

Dengale *et al.* designed and synthesized a novel series of 2-(4,5,6,7-tetrahydrobenzo[c]isoxazol-3-yl)-4H-chromen-4-ones with the aim of evaluating their anti-inflammatory and antioxidant properties. These compounds were compared to two well-known standard drugs: diclofenac sodium, an anti-inflammatory agent, and ascorbic acid, a potent antioxidant. The study revealed that compounds **32-34** (Figure 13) exhibited moderate anti-inflammatory activity when compared to diclofenac sodium. Although they were not as potent as the standard drug, their anti-inflammatory effects were significant and suggest that these compounds could be explored further as potential anti-inflammatory agents. In addition, the compounds demonstrated antioxidant activity that was comparable to that of ascorbic acid, indicating their ability to scavenge free radicals and reduce oxidative stress.
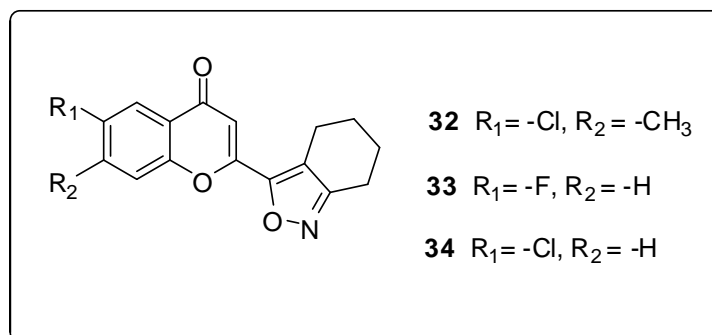
Fig. 13: Chromone-isoxazole derivatives 32-34

A preliminary structure–activity relationship (SAR) analysis was conducted to understand the factors influencing the biological activities of these compounds. The SAR findings revealed that the presence of an electron-withdrawing group (R1) on the molecular structure enhanced the anti-inflammatory activity of the compounds. In contrast, the incorporation of an electron-donating group (R2) was found to be detrimental to this activity. This insight suggests that modulating the electronic properties of the substituent groups could lead to the optimization of the compounds for better anti-inflammatory effects [23]. Overall, Dengale *et al.*'s research highlights the potential of 2-(4,5,6,7-tetrahydrobenzo[c]isoxazol-3-yl)-4H-chromen-4-one derivatives as both anti-inflammatory and antioxidant agents. The study also provides valuable information for the future design of more potent derivatives by manipulating the substituent groups to enhance the desired biological activities.

Conclusion:

Flavone-isoxazole hybrid natural products exhibit anti-tumor, anti-psychotic, lipid-lowering activities, and potential for treating diabetic retinopathy. Compound **2** shows promise as an anti-diabetic drug, while compounds **15-17** may be useful for schizophrenia treatment due to their antipsychotic effects. Most hybrid isoxazole derivatives did not show significant improvements in anti-tumor activity, but hydnocarpin derivatives **4-7** displayed enhanced anti-tumor effects. The isoxazole structure plays a key role in this activity. Among them, compound 5 exhibited the strongest anti-tumor activity against A375 cells, with an IC_{50} of 0.65 μM, making it a valuable candidate for further study.

References:

1. Wenzel, U., Flavonoids as drugs at the small intestinal level, *Current Opinion in Pharmacology*, 2013, 13(6), 864-868.

2. Liga, S., Paul, C., Péter, F., Flavonoids: Overview of Biosynthesis, Biological Activity, and Current Extraction Techniques, *Plants*, 2023, 12(14), 2732.

3. Jani, T., Shastri, A., Prajapati, D., Vinodkumar, P.C., Limbachiya, C., Vinodkumar, M., Structural, spectroscopic and electron collisional studies of isoxazole, *Chemical Physics*, 2022, 553, 111379.

4. Stiefvater, O.L., Nösberger, P., Sheridan, J., Microwave spectrum and structure of isoxazole, *Chemical Physics*, 1975, 9(3), 435-444.

5. Agrawal, N., Mishra, P., The synthetic and therapeutic expedition of isoxazole and its analogs, *Med Chem Res*., 2018, 27(5), 1309-1344.

6. Huang, X., Deng, H., Shen, Q.K., Quan, Z.S., Tanshinone IIA: pharmacology, total synthesis, and progress in structure-modifications, *Curr. Med. Chem.*, 2022, 29, 1959-1989.

7. Wang, J., Dong-Bo Wang, Li-Li Sui, Luan, T., Natural products-isoxazole hybrids: A review of developments in medicinal chemistry, *Arabian Journal of Chemistry*, 2024, 17, 105794.

8. Rao, Y.J., Sowjanya, T., Thirupathi, G., Murthy, N.Y.S., Kotapalli, S.S., Synthesis and biological evaluation of novel flavone/triazole/benzimidazole hybrids and flavone/isoxazole-annulated heterocycles as antiproliferative and antimycobacterial agents. *Mol. Diversity*, 2018, 22, 803–814.

9. Nie, J.P., Qu, Z.N., Chen, Y., Chen, J.H., Jiang, Y., Jin, M.N., Yu, Y., Niu, W.Y., Duan, H. Q., Qin, N., Discovery and anti-diabetic effects of novel isoxazole based flavonoid derivatives, *Fitoterapia,* 2020, 142, 104499.

10. Polier, G., Ding, J., Konkimalla, B.V., Eick, D., Ribeiro, N., K¨ohler, R., Giaisi, M., Efferth, T., Desaubry, L., Krammer, P.H., Li-Weber, M., Wogonin and related natural flavones are inhibitors of CDK9 that induce apoptosis in cancer cells by transcriptional suppression of Mcl-1, *Cell Death Dis*., 2011, 2, 182.

11. Bian, J., Li, T., Weng, T., Wang, J., Chen, Y., Li, Z., Synthesis, evaluation and quantitative structure-activity relationship (QSAR) analysis of Wogonin derivatives as cytotoxic agents, *Bioorg. Med. Chem. Lett*., 2017, 27, 1012–1016.

12. Arya, J.S., Joseph, M.M., Sherin, D.R., Nair, J.B., Manojkumar, T.K., Maiti, K.K., Exploring mitochondria-mediated intrinsic apoptosis by new phytochemical entities: an explicit observation of cytochrome c dynamics on lung and melanoma cancer cells, *J. Med. Chem.*, 2019, 62, 8311–8329.

13. Asha Bhanu, P., China Raju, B., Jayavardhana Rao, Y., Narasimha, G., Kesava Rao, B., Facile synthesis and docking studies of 7-hydroxyflavanone isoxazoles and acrylates as potential anti-microbial agents, *Med. Chem. Res*., 2020, 29, 217–228.

14. Saidi, I., Manachou, M., Znati, M., Bouajila, J., Ben Jannet, H., Synthesis of new halogenated flavonoid-based isoxazoles: in vitro and in silico evaluation of α-amylase inhibitory potential, a SAR analysis and DFT studies, *J. Mol. Struct.*, 2020, 1247, 131379.

15. Gu, H.S., Chen, X., Zhang, J.W., Zhang, L., Li, L., Synthesis and biological evaluation of novel flavanone derivatives as potential antipsychotic agents, *Chem. Biol. Drug Des.*, 2017, 89, 353–364.

16. Qiu, R., Luo, G., Cai, X., Liu, L., Chen, M., Chen, D., You, Q., Xiang, H., Structure guided design and synthesis of isoflavone analogs of GW4064 with potent lipid accumulation inhibitory activities, *Bioorg. Med. Chem. Lett.*, 2018, 28, 3726–3730.

17. Nifantev, E.E., Koroteev, A.M., Pozdeev, A.O., Koroteev, M.P., Vasyanina, L.K., Kaziev, G. Z., Rogovskii, V.S., Knyazev, V.V., Shirokikh, K.E., Semeikin, A.V., Fedotcheva, T.A., Matyushin, A.I., Shimanovskii, N.L., Synthesis and cytotoxic activity of dihydroquercetin aryl derivatives, *Pharm. Chem. J.*, 2015, 49, 78–81.

18. Abu-Bakr, S.M., Khidre, M.D., Omar, M.A., Swelam, S.A., Awad, H.M., Synthesis of furo[3,2-g]chromones under microwave irradiation and their antitumor activity evaluation, *J. Heterocycl. Chem.*, 2019, 57, 731–743.

19. Badadhe, P.V., Patil, L.R., Bhagat, S.S., Chate, A.V., Shinde, D.W., Nikam, M.D., Gill, C. H., Synthesis and antimicrobial screening of some novel chromones and pyrazoles with incorporated isoxazole moieties, *J. Heterocycl. Chem.*, 2013, 50, 999–1004.

20. Zhao, L., Li, Y., Wang, Y., Qiao, Z., Miao, Z., Yang, J., Huang, L., Tian, C., Li, L., Chen, D., Yang, S., Discovery of 4H-chromen-4-one derivatives as a new class of selective rho kinase (ROCK) inhibitors, which showed potent activity in ex vivo diabetic retinopathy models, *J. Med. Chem.*, 2019, 62, 10691–10710.

21. Kaushik, S., Sanawar, R., Lekshmi, A., Chandrasekhar, L., Nair, M., Bhatnagar, S., Santhoshkumar, T.R., ER alpha selective chromone, isoxazolylchromones, induces ROS-mediated cell death without autophagy, *Chem. Biol. Drug Des.*, 2019, 94, 1352–1367.

22. Awadallah, F.M., El-Waei, T.A., Hanna, M.M., Abbas, S.E., Ceruso, M., Oz, B.E., Guler, O. O., Supuran, C.T., Synthesis, carbonic anhydrase inhibition and cytotoxic activity of novel chromone-based sulfonamide derivatives, *Eur. J. Med. Chem.*, 2015, 96, 425–435.

23. Dengale, S.G., Akolkar, H.N., Darekar, N.R., Shaikh, M.H., Deshmukh, K.K., Mhaske, S. D., Karale, B.K., Raut, D.N., Khedkar, V.M., Synthesis and biological evaluation of 2-(4,5,6,7-tetrahydrobenzo[c]Isoxazol-3-yl)-4H-chromen-4-ones, *Polycyclic Aromat. Compd.*, 2022, 42, 6337–6351.

Research Trends in Chemical and Material Science
ISBN: 978-93-48620-44-6

About Editors

Dr. Neeraj Mohan Gupta, Assistant Professor in the Department of Chemistry at Govt. Postgraduate College, Guna, MP, holds a Ph.D. from CSIR-CDRI, Lucknow. He has qualified multiple national-level exams, including NET (JRF) and GATE, and also cleared the MPPSC exam. With over three years of teaching experience at UG and PG levels, he specializes in fluorescent organic chemistry and nanomaterial chemistry. Dr. Gupta has published nine research articles in reputed international journals like ACS, EJOC, Elsevier, MDPI, and the Indian Journal of Chemistry. His expertise extends to using advanced analytical instruments and software such as Fluorescence Spectrophotometry, TGA, Cyclic Voltammetry, IR, Flash Chromatography, and DFT analysis. His research focuses on designing and synthesizing heterocyclic organic fluorescent chemosensors, donor-acceptor-based fluorescent dyes, and nanomaterials for heavy metal detection and biomedical applications. Actively participating in national and international conferences, he remains dedicated to advancing research in nanomaterials and catalysis.

Dr. Shailendra Bhalchandra Kolhe is an Associate Professor at Shivaji Arts, Commerce, and Science College, Kannad, Chhatrapati Sambhajinagar. He earned his M.Sc. from North Maharashtra University, Jalgaon (1995), and his Ph.D. from Dr. Babasaheb Ambedkar Marathwada University, Chhatrapati Sambhajinagar (2010). With 25 years of teaching experience, he has made significant contributions to physics education and research. Dr. Kolhe has published 26 research papers in esteemed national and international journals and conference proceedings. Additionally, he holds one patent, reflecting his innovative research contributions. He is an active member of the scientific community, being a life member of both the Indian Association of Physics Teachers and the Indian Physics Association. His dedication to academia and research continues to inspire students and colleagues alike.

Dr. Prasenjit Talukdar is working as an Associate Professor and Head of the Department of Petroleum Engineering, Dibrugarh University Institute of Engineering and Technology (DUIET), Dibrugarh University, Assam, India. He did his Ph.D from the Department of Petroleum Technology, Dibrugarh University in the area of Non Damaging Drilling Fluid. His current research focuses on advanced EOR techniques, rheology of complex fluids, flow assurance of waxy crude oil, CCUS, and nano-based drilling fluids for challenging environments. He has finished three significant research projects. In his role, he has authored more than fifteen numbers of book chapters, fifty-three numbers of international journal articles, two numbers of granted patents and sixty-seven conference papers.

Dr. Gaurav B. Pethe (M.Sc., M.Phil., Ph.D.) is working as Associate Professor, Department of Chemistry, Narayanrao Kale Smruti Model College, Karanja Ghadge, Dist.-Wardha affiliated to RTM Nagpur University, Nagpur, M.H., He has more than 14 years of teaching and 19 years of research experience. His research area includes Coordination Complexes, Physical Chemistry and Catalysis. He has published more than 55 research paper in various National and International journals of repute with 275 citations, h-index 10 and i10 index 10. He published three book to his credit. He has presented his work in many National and International conferences.